論文 / 著書情報
Article / Book Information

題目(和文)	タイ王国パーム油製造プロセスにおけるパーム核殻活性炭を用いた吸着による排水の処理
Title(English)	Effluent Treatment by Adsorption Using Activated Carbon Produced from Palm Kernel Shell in Palm Oil Mill Process in Thailand
著者(和文)	ｳｨｰﾀﾗ ﾌﾞﾝﾀﾑ
Author(English)	Weetara Boontham
出典(和文)	学位:博士（工学）, 学位授与機関:東京工業大学, 報告番号:甲第11973号, 授与年月日:2021年3月26日, 学位の種別:課程博士, 審査員:江頭 竜一,中﨑 清彦,高橋 史武,森 伸介,吉村 千洋,はばき 広顕
Citation(English)	Degree:Doctor (Engineering), Conferring organization: Tokyo Institute of Technology, Report number:甲第11973号, Conferred date:2021/3/26, Degree Type:Course doctor, Examiner:,,,,,
学位種別(和文)	博士論文
Type(English)	Doctoral Thesis

EFFLUENT TREATMENT BY ADSORPTION
USING ACTIVATED CARBON
PRODUCED FROM PALM KERNEL SHELL
IN PALM OIL MILL PROCESS IN THAILAND

DEPARTMENT OF TRANSDISCIPLINARY SCIENCE AND ENGINEERING

BOONTHAM WEETARA

EFFLUENT TREATMENT BY ADSORPTION USING ACTIVATED CARBON PRODUCED FROM PALM KERNEL SHELL IN PALM OIL MILL PROCESS IN THAILAND

BOONTHAM WEETARA

THESIS SUBMITTED FOR THE DEGREE OF
DOCTOR OF ENGINEERING

TOKYO INSTITUTE OF TECHNOLOGY
DEPARTMENT OF TRANSDISCIPLINARY SCIENCE AND ENGINEERING
GRADUATE SCHOOL OF ENVIRONMENT AND SOCIETY

2021

ABSTRACT

The palm oil mill industry is considered one of the important agro-industries contributing to Thailand's economy over the past decades. Currently, Thailand is the third biggest global palm oil producer. With the growth in the palm oil mill industry, environmental concerns due to the waste generated by the industry is also increasing in Thailand. The objective of this thesis is to treat the effluent by adsorption using activated carbon produced from palm kernel shell in palm oil mill process in Thailand. Firstly, the current palm oil mill process and the actual problem from the industry was investigated. During the palm oil production process, large amounts of solid byproducts and liquid waste are generated. The solid byproducts can still be further utilized for added value. In contrast, the liquid waste, namely palm oil mill effluent, leads to serious environment issues due to its characteristic, and improper treatment method. Secondly, palm kernel shell, one of the byproducts of the palm oil mill industry, was characterized by proximate, ultimate, and thermogravimetric analyses in order to understand physical and thermal properties of palm kernel shell. The high carbon and low ash contents in the palm kernel shell indicated that palm kernel shell is a promising precursor for producing activated carbon. The presence of chemical activating reagent, orthophosphoric acid, in palm kernel shell could hinder thermal decomposition in the high temperature, showing the potential to produce a high yield of activated carbon. Next, the palm kernel shell which was chemically treated with orthophosphoric acid in chapter 2 was pyrolyzed to produce palm kernel shell activated carbon and other products (off-gas and condensable liquid). The pyrolysis was performed under various operating conditions which varied in chemical treatment concentration, pyrolysis temperature, and pyrolysis time. The effects of operating conditions on yields and characterization of PKSAC and other products were discussed. The elemental balance among pyrolysis products was also performed. Chemical treatment with orthophosphoric acid could improve the yield of palm kernel shell activated carbon. The effect of pyrolysis temperature greatly affected the yield of palm kernel shell activated carbon whereas the effects of orthophosphoric acid concentration and pyrolysis time were insignificant. Produced palm kernel shell activated carbon had a relatively high micropore volume and specific surface area. The surface functional groups of palm kernel shell activated carbon also changed by chemical treatment. The off-gas contained flammable and non-flammable gases and an hour of pyrolysis time was sufficient to obtain almost all of the off-gas. The condensable liquid contained chemical components such as acetic acid and methanol. The carbon content mainly remained in PKSAC while the oxygen content remained in off-gas and condensable liquid. After that, the produced palm kernel shell activated carbon was used as an adsorbent to remove unfavorable compounds, namely, phenolic compounds and lignin in model palm oil mill effluent. Palm kernel shell activated carbons produced from various operating conditions could successfully adsorb and remove unfavorable compounds in batch equilibrium adsorptions. The adsorption performances were correlated with the characteristics of the palm kernel shell activated carbon. Lastly, based on the experimental results, the proposed process of using palm kernel shell activated carbon to treat palm oil mill effluent was introduced into the current palm oil mill process in Thailand. The products obtained from pyrolysis could be applied into the current process in three ways. Palm kernel shell activated carbon is used as the adsorbent to treat unfavorable compounds in palm oil mill effluent. Off-gas could be used as an energy source for additional operations in the process. The compounds contained in condensable liquid, such as, acetic acid, methanol, etc., could be raw materials for other chemical processes.

TABLE OF CONTENTS

CHAPTER 1

INTRODUCTION

1.1 BACKGROUD

1.1.1 OIL PALM TREE

a) General information

Oil palm (*Elaeis guineensis*), an African tree in the *Arecaceae* palm family, is cultivated as a source of oil. This tree originated from West Africa and became a beneficial tree for local peoples, cultures and economies in African region. However, oil plam has grown extensively in Southeast Asia especially in Malaysia, Indonesia, and Thailand since the late 20th century due to soil and climate suitability for growing oil palm tree. **Figure 1.1** shows the dense oil palm cultivation in Krabi province, Thailand. The oil palm has a single stem and can reach 20 metres in height when it is mature. The tree consists of many tiny flowers crowded on short branches that develop into a dense cluster of oval fruits some 0.04 metres long as shown in **Figure 1.2**. The weight of the ripe bunch is between 5 to 30 kg depending on the age of the palm tree (Wikipedia). The palm fruits are brown with a red base. The cross section of the oil palm fruit is represented in **Figure 1.3**. Each fruit comprises of an oily, fleshy outer layer (pericarp), with a oil-rich seed or kernel (endosperm). Both of the palm fruit and seed can be used for the oil extraction. The crude palm oil (CPO) and palm kernel oil (PKO) are extracted from the outer mesocarp and endosperm, respectively.

In general, oil palm tree can be classified into three varieties by shell thickness which are *dura*, *pisifera* and *tenera*. *Tenera* is a preferred variety for plantation throughout Southeast Asia. *Tenera* is a hybrid between *dura* and *pisifera* as shown in **Figure 1.4**. *Dura* has thick shell while *pisifera* is shell-less. These two types are planted for seed production and they are not suitable for oil extraction due to their fruit characteristics. On the other hand, *Tenera* is planted commercially for oil production because it contains more oil and crude palm oil which can be separated easily.

Figure 1.1 Dense oil palm cultivation

Figure 1.2 Palm fruit (left) and fresh fruit bunch (right)

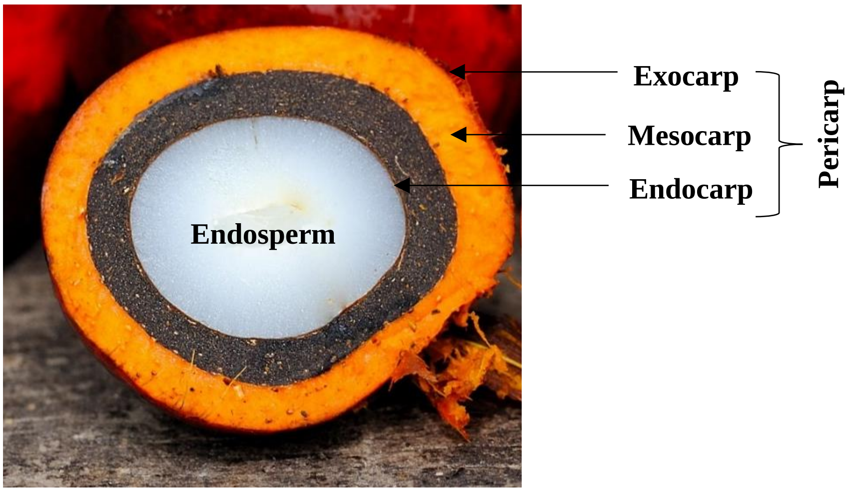

Figure 1.3 Cross section of oil palm fruit

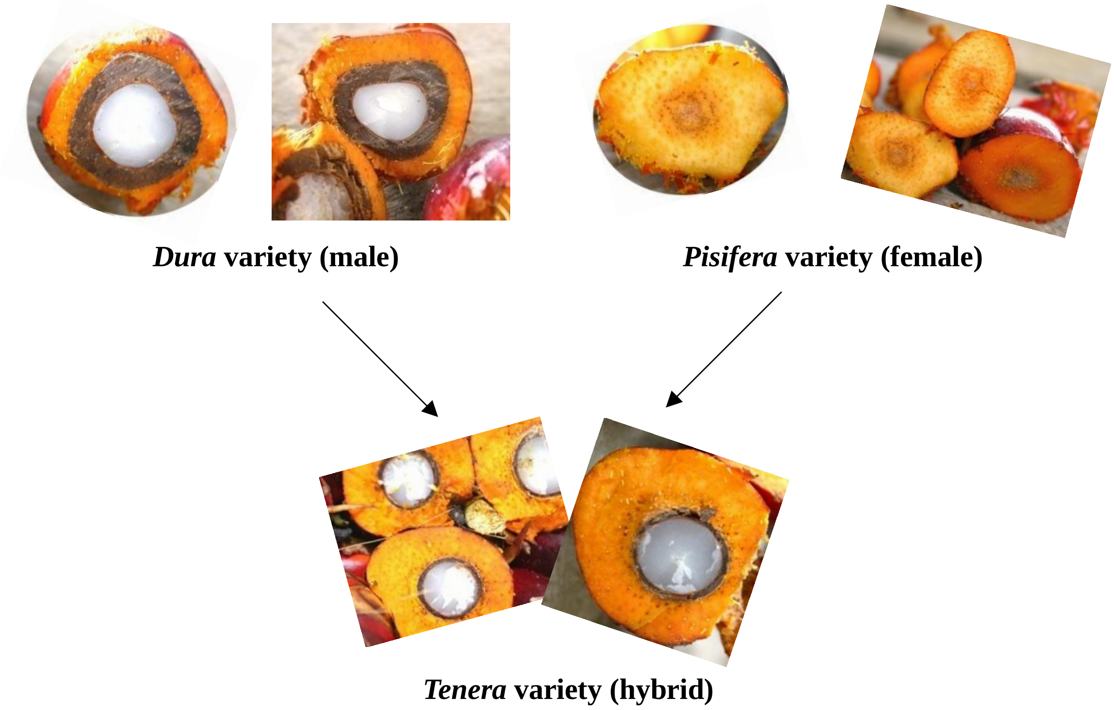

Figure 1.4 Palm oil varieties *dura*, *pisifera* and *tenera*

Oil palm tree is very effective crop to produce oil compared to other major oil crops. **Table 1.1** shows the comparison between the yield production of palm oil and other major oil crops. From the table it appears that oil palm tree has the highest oil yield among any other leading oil crop (Sheil *et al*., 2009). Apart from the yield production, the area requires to produce 1 metric ton of oil palm is only 0.27 ha while in the case of rapeseed, sunflower, and soybean requires 1.49, 2.08, and 2.69 ha, respectively. Due to the high yield and less land usage of oil palm cultivation, the global production and demand for palm oil are increasing rapidly.

Table 1.1 Oil production of palm and other major oil crops (Sheil *et al.*, 2009**)**

Oil type	**Oil yield [kg ha^{-1}]**
Palm	4000–5000
Rapeseed	1000
Groundnut	890
Sunflower	800
Soya bean	375
Coconut	395
Cotton seed	173
Sesame seed	159

b) World distribution of oil palm cultivation

The total global oil palm cultivation area is shown in **Figure 1.5**. The cultivation of oil palm is gaining popularity across the continents of Latin America, Africa, and Asia. Two major oil palm-producing countries currently are Indonesia and Malaysia, accounting for over 80 percent of the global share (Vijay *et al.*, 2016). In the third place is Thailand, accounting for 3 percent of the global share. Indonesia is the more important country of the two, producing 36.0 million tons annually, while Malaysia produces 18.9 million tons a year. They are also major exporters as they produce more than 90% of the palm oil in international markets.

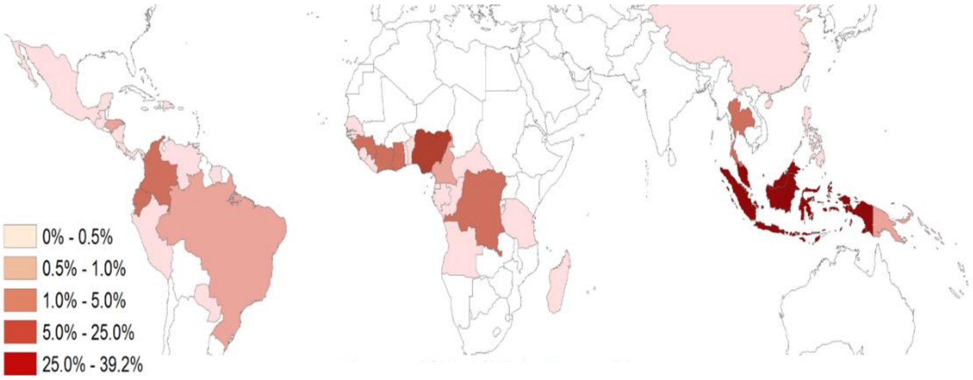

Figure 1.5 Total global oil palm cultivation area in 2013 (Vijay *et al.*, 2016**)**

c) Use of palm tree

As mentioned above that oil palm tree is cultivated as oil source. However, only 10 percent is used for palm oil production, while the remaining 90 percent is biomass residue (Abnisa *et al.*, 2013). Oil Palm tree can be divided into three main components which are trunk, frond, and fruit bunch. The usage of each component from oil palm tree is summarized in **Figure 1.6.** The frond and trunk are the major byproducts obtained from the cultivation. Oil palm trunk can be an important source for furniture and particle board industries, as well as the feedstuff for animal, and energy source. Oil palm frond, high-fiber and low-protein material, is able to be good feeding for many classes of herbivore livestock. Palm fruit bunch, the main product from oil palm tree cultivation, is used for palm oil production in palm oil mill industry.

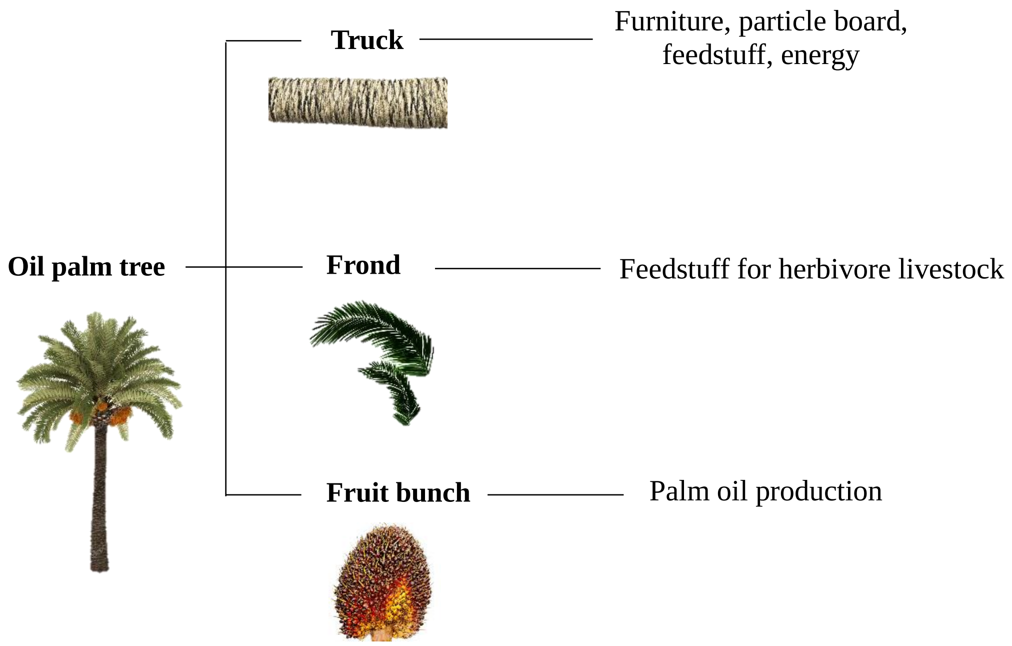

Figure 1.6 Use of palm tree

1.1.2 PALM OIL MILL INDUSTRY IN THAILAND

Thailand sits in the third place of palm oil global production with the cultivated area of 930,000 ha in 2018. Oil palm tree was first cultivated in 1969 by Univanich Palm Oil PCL, a pioneer of the palm oil industry in Thailand. The trend of oil palms cultivation area in Thailand is shown in **Figure 1.7**. The total area of oil palm cultivation has rapidly risen in the past decade. Khomphetet *et al.*, 2018, reported that oil palm cultivation is expected to reach 1.6 million ha by 2029 owing to the promotion by the Thai national government. **Figure 1.8** represents the palm oil production based on Thailand's regions. The majority of oil palm production area in Thailand approximately 91 percent is in the southern peninsular region, particularly in Krabi, Chumphon, Phang-nga and Surat Thani provinces. The remaining 9 percent are produced in the center, the north and the north east of the country (Sowcharoensuk, 2020). More than 95 percent of the palm oil produced in Thailand is used locally, and a small portion is for export.

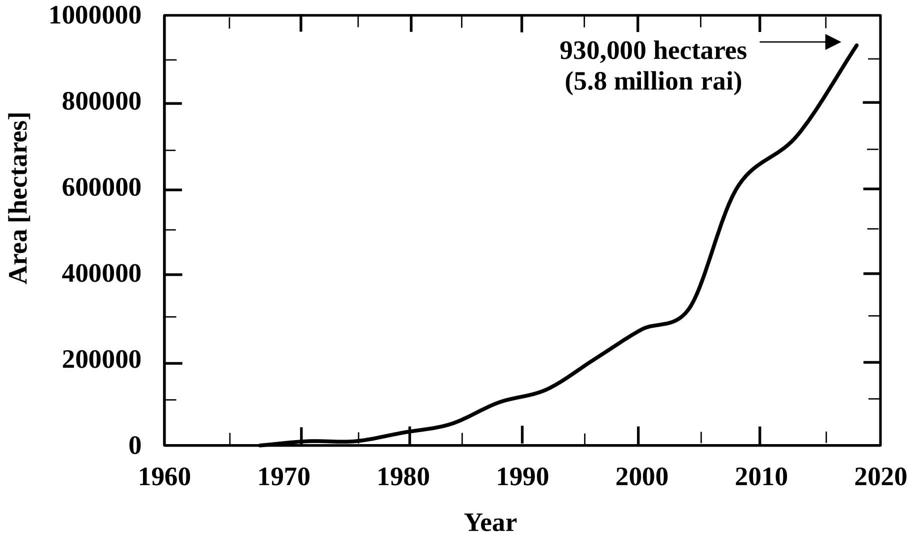

Figure 1.7 Cultivation area of oil palms in Thailand

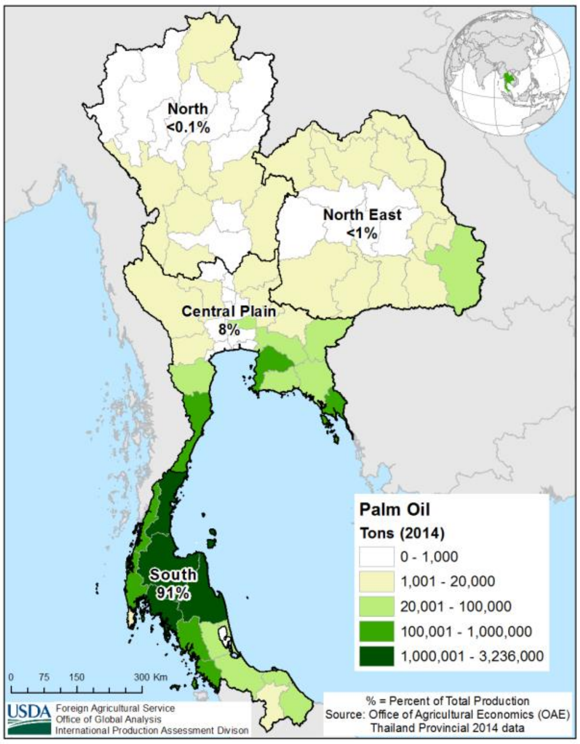

% = Percent of Total Production
Source: Office of Agricultural Economics (OAE)
Thailand Provincial 2014 data

Figure 1.8 Palm oil production based on Thailand's regions

a) Palm oil production process and material flow

The principle of palm oil production process is to extract the oil from palm fruit using steam and pressing machine. A schematic flow diagram of the standard palm oil mill process and material balance is shown in **Figure 1.9**.

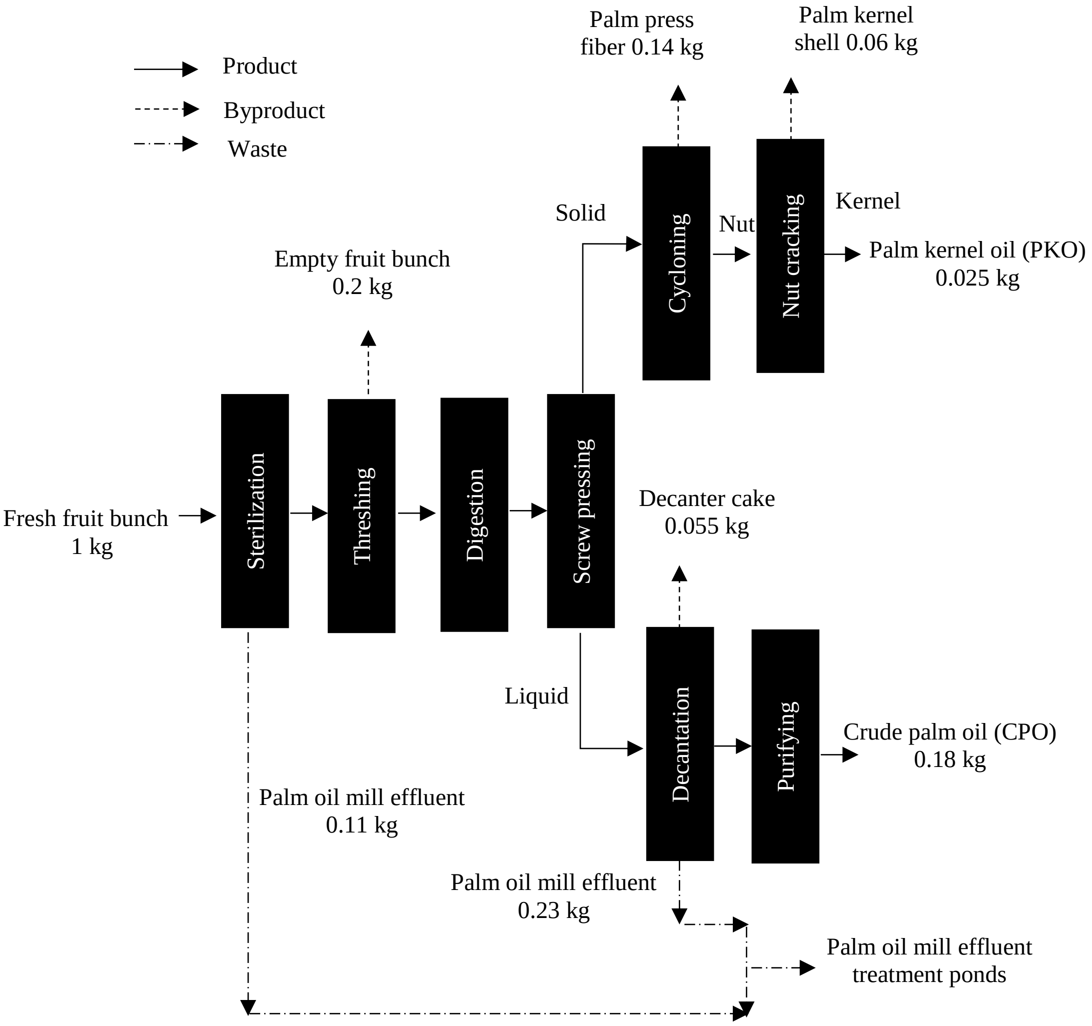

Figure 1.9 Palm oil mill process and material balance (Kerdsuwan *et al.*, 2011; Sampattagul *et al.*, 2011)

Details of main processes in palm oil mill industry are described below:

Arrival and storage of fresh fruit bunches (FFB)

Fresh fruit bunches from oil palm field should be transported to the palm oil mill company within 3 days in order to avoid an excessive production of free fatty acids from a natural enzymatic process in the mesocarp. In general, ripe oil palm fruit contains about 1 percent of free fatty acids. The content of free fatty acids in oil palm fruit can urge the maturation of the fruits and thus, could affect the value of the oil. **Figure 1.10** shows the arrival process of FFB

Figure 1.10 Arrival process of fresh fruit bunch

Sterilization

The extraction of palm oil starts with the sterilization of fresh fruit bunch (FFB) in the sterilizer. The objective of this process is to inactivate the natural enzymatic activity and loosen the fruit, as well as to soften the mesocarp, resulting in easier extraction of oil. The autoclaves can load 20-30 tons of FFB, with the application of hot steam, at temperature 403 K and pressure of 3.1 bars. This process takes 1.5 hours to complete. **Figure 1.11** shows the conventional sterilizer for palm fruit sterilization.

Figure 1.11 Conventional sterilizer

Threshing

The sterilized FFB are transported to rotary drum threshers to separate the sterilized fruits from the bunch stalks. The sterilized fruits are then pressed for its oil while empty fruit bunches (EFB), residues from this process are separated and further utilized into the biomass. **Figure 1.12** shows the appearance of EFB from the threshing process.

Figure 1.12 Appearance of empty fruit bunch from threshing process

Digestion

The separated fruits from threshing process are discharged into vertical steam-jacketed drums (digesters) and treated mechanically to convert them into a homogeneous oily mash. Hot water is added to the digester to facilitate homogenization. This mash is subsequently put into the oil extraction press in screw press process.

Screw pressing

Screw pressing is a process to extract palm oil from mash. The extracted oil phase is collected and discharged to the purification section to remove impurities and improve crude palm oil quality while the solid parts comprising fiber and nuts are separated by physical means. The solids are transferred to palm kernel oil processing unit to extract palm kernel oil.

Further details of other processes can be found elsewhere (Department of Industry Works, 2006)

The appearance of crude palm oil (CPO) and palm kernel oil (PKO) is shown in **Figure 1.13**. CPO is orange-red in color. CPO is used for making soaps, detergents, candles, cosmetic and etc. PKO is a white to yellowish oil. PKO is commonly used as an ingredient in commercial food such edible products as chocolate confections, margarine, ice cream, cookies, and bread, as well as many pharmaceuticals.

Figure 1.13. Appearance of crude palm oil (left) and palm kernel oil (right)

b) Byproducts from palm oil mill industry

According to the standard process of palm oil mills shows in **Figure 1.9**, the major solid byproducts of the palm oil mill industry include empty fruit bunch (EFB), palm kernel shell (PKS), palm fiber (PFP), and decanter cake (DC). The picture of byproducts generated from palm oil mill industry is shown in **Figure 1.14**.The utilization of these byproducts could reduce the waste disposal costs incurred by the industry and, at the same time, minimize their impact on the receiving environment. The way in which each solid byproduct can be utilized has been explained below.

EFB can serve as an organic fertilizer and soil conditioner as it is capable of maintaining the humidity of the soil. Local farmers can purchase it and use it as a substrate for mushroom cultivation. Currently, some mills have introduced EFB pressing techniques as a way to obtain lower moisture content in the EFB, which can then be used as biomass fuel in boiler systems producing steam or electricity.

Almost all the PFP generated by mills is used as fuel in the boiler for the generation of steam and electricity. The amount of fiber palm oil mills generate can sufficiently satisfy all steam and electricity requirements for crude palm oil (CPO) production. Any excess fiber generated can be sold as biomass fuel to other industries, including power and cement plants.

PKS functions as a fuel much like PFP. However, the amount of PFP generated is a sufficient energy source for an individual oil mill. A majority of the shells generated is sold to other industries (i.e., power and cement plants) as fuel or for activated carbon (AC) production.

DC, which is created during the oil separation process, is either dumped as solid waste or sold to farmers. They are often used as fertilizers or added to animal feed.

Figure 1.14 Byproducts generated from palm oil mill industry

c) Waste from palm oil mill industry

The major waste generates in this industry is a liquid waste namely palm oil mill effluent (POME). POME is a highly polluted wastewater which mainly from sterilization, condensation, and hydrocycloning process (Ohimain and Izah, 2017). Raw POME is hot, acidic, brownish, and contains high organic and inorganic materials, which are harmful and still being released into environment without undergoing proper treatment. (Iskandar *et al.*, 2018: Rupani *et al.*, 2010). Even the POME is treated, the color still remains. Most of the palm oil mills employ conventional biological treatment systems to treat POME. Nevertheless, some mills are unable to treat their POME to meet the effluent standards (Phonepaseuth *et al.*, 2019). **Figure 1.15** shows the picture of raw POME taken from fieldwork.

Figure 1.15 Raw palm oil mill effluent

d) Problem from palm oil mill industry

The problem from this industry mostly comes from the production process. One of the problem that have been discussed in several studies is POME. POME is a brownish and acidic wastewater with high organic content, high biological oxygen demand, hazardous compounds, oil, grease, etc. (Rana *et al.*, 2017: Phonepaseuth *et al.*, 2019: Kaman *et al.*, 2017). Some hazardous compounds present in POME include phenolic compounds, phenolic acids and heavy metals (Kietkwanboot *et al.*, 2020: Prasertsan and Binmaeil, 2018). Apart from these, POME's brownish colour comes from the presence of lignin and tannins. It is estimated that about 0.87 m^3 of POME is generated from every tonne of fresh fruit bunch in Thailand palm oil mills (Prasertsan and Binmaeil, 2018). The huge amount of POME discharged daily by palm oil mill industry can lead to serious environment issues which severely threatens natural environment. **Table 1.2** shows the typical characteristics of the raw POME and treated POME. POME typically contains oil and greases, total solids, suspended solids, heavy metal, lignin, and phenolic compounds. The concentration of unfavorable compounds in raw POME is reduced after several effluent treatment methods.

Table 1.2 Typical characteristics of the raw POME and treated POME

Parameter	**Raw POME (Bello *et al.*, 2013)**	**Treated POME (Khongkhaem *et al.*, 2016)**
pH	3.5	8
Temperature [K]	360	300
Oil and grease [mg L^{-1}]	130–18000	-
BOD [mg L^{-1}]	10250–43750	160
COD [mg L^{-1}]	15000–100000	850
Total solids [mg L^{-1}]	11500–79000	560
Suspended solids [mg L^{-1}]	5000–54000	-
Copper [mg L^{-1}]	0.89	-
Iron [mg L^{-1}]	103.3	-
Zinc [mg L^{-1}]	7.5	-
Lignin [mg L^{-1}]	4700	215
Phenolic compounds [mg L^{-1}]	5800	26

Most palm oil mills employ a conventional ponding system to treat POME owing to its low cost and ease of operation (Baharuddin, 2010). POME is generally treated using conventional biological treatment systems including anaerobic and facultative ponds in series, facultative ponds in series, and anaerobic and aerobic lagoons in series. Some mills use a series of shallow ponds to reduce the impact of POME on the environment. Nonetheless, ponding systems require a large open area and longer hydraulic retention time. Furthermore, some reports indicated that the treated POME in some mills did not meet the meet effluent standards (Phonepaseuth *et al.*, 2019). Additionally, the rainy season, overflow from POME treatment plants causes heavy water pollution in nearby water bodies. Communities located near oil mills also complain about the strong odor caused by inappropriate POME treatment systems. Therefore, it can be concluded that the treatment of POME is a major concern of palm oil mills. The concern has gained interest from many researchers to investigate the more appropriate POME treatment methods. **Figure 1.16** shows the picture of conventional palm oil mill effluent treatment taken from fieldwork.

Figure 1.16 Conventional palm oil mill effluent treatment

1.2 PREVIOUS STUDIES

1.2.1 Adsorption

Adsorption is a mass transfer process by which a substance is transferred from the liquid phase to the surface of a solid, and becomes bound by physical and/or chemical interactions. The substance being absorbed is called an adsorbate and the solid on which the process occurs is called adsorbent. Activated alumina, activated carbon, polymeric, and zeolite are the major adsorbents used in the industry. Most of them are manufactured and a few such as some zeolites that occur naturally. **Table 1.3** summarizes the ability of adsorbents to treat pollutants. The adsorbents listed in Table 1.3 including activated carbon prepared from the industrial byproduct have potential to treat several organic compounds, showing the feasibility to treat wastewater.

Table 1.3 The ability of adsorbents to treat pollutants

Adsorbent	**Pollutants to be treated**
Activated alumina	phenol (Roostaei and Tezel, 2004)
Activated carbon	*commercial activated carbon* phenol, *p*-nitrophenol (Mohamed *et al.*, 2011) *industrial byproduct activated carbon* palm kernel shell activated carbon: phenol (Boontham *et al.*, 2020), bisphenol (Soni and Padmaja, 2014), chlorophenol, nitrophenols, dinitrophenol sawdust activated carbon: phenol (Othaman *et al.*, 2008) bagasse activated carbon: phenol (Mohtashami *et al.*, 2018)
Polymeric	phenol, *p*-cresol, *p*-chlorophenol, *p*-nitrophenol (Li *et al.*, 2004)
Zeolite	Phenol (Chaouati*et al.*, 2013), 4-chlorophenol (Kuleyin, 2006), o-chlorophenol (Baker and Ghanem, 2009)

1.2.2 Activated carbon

Activated carbon (AC) is a highly porous carbonaceous material which widely used as an adsorbent in environmental applications. AC has been used since 3750 B.C. by the Egyptians for smelting ores to create bronze. Later, it was developed and applied in other fields such as medical, manufacturing processes, and chemical industry. The successful discovery of using AC was from English sugar refinery in 1794. The study found that AC can be used as a decoloring agent. Also in 1862, Frederick Lipscombe discovered that AC was able to purify potable water. Commercial AC was first produced in an industrial scale by Chemische Werke plant at the beginning of the 20th century and became widely used since then. Today, the uses of AC continue to grow. It can be found virtually everywhere and used on almost a daily basis. It is used in a variety of industries, including corn and cane sugar refining, liquid and gas adsorption, pharmaceuticals, odor removal, food and beverage manufacturing, and much more.

a) Classification

Due to the complexity of the material, AC is difficult to classify using general fundamentals such as AC behavior and surface characteristics. The AC classification based on size is the most widely used in research. The three main AC types using this criterion are as follows: powdered AC (PAC), granular AC (GAC), and extruded AC (EAC). **Figure 1.18** shows the picture of AC classification based on AC size.

Powdered activated carbon (PAC)

PAC is a powder form or fine granules less than 1.0 mm in size with an average diameter 0.15–0.25 mm. PAC is mostly made up of crushed or ground carbon particles, 95–100% of which passes through a designated mesh sieve. According to the American Society for Testing and Materials (ASTM), particles passing through an 80-mesh sieve (0.177 mm) and smaller can be considered as PAC. PAC can be used for air, water, and chemical purification and catalysts, food and beverage, and pharmaceuticals.

Granular activated carbon (GAC)

GAC is larger in size in comparison with PAC. The size ranges from 0.2–5 mm. GAC has been used in air and chemical purification and catalysts, automotive emission control, mining, and pharmaceuticals.

Extruded activated carbon (EAC)

EAC combines PAC with a binder. They are fused together and extruded into a cylindrical AC block with diameters ranging from 0.8–4 mm. This AC are mainly used for gas phase applications such as automotive emission control due to their low pressure drop, low dust content, and high mechanical strength. EAC is also marketed as CTO (chlorine, taste, odor) filter.

Figure 1.17 Activated carbon classification

b) Activated carbon production

AC can be produced using two methods, namely physical or chemical activation. The difference between these two methods is in the production process. **Figure 1.18** illustrates the process flow for activated carbon production. Physical activation is a two-step process that starts with pyrolysis of the precursor, followed by activation of the resulting char at a temperature above 873 K in the presence of suitable oxidizing gases such as carbon dioxide, oxygen, and steam, whereas chemical activation is a one-step process that uses chemical reagents such as zinc chloride ($ZnCl_2$), phosphoric acid (H_3PO_4), sodium hydroxide (NaOH) and potassium hydroxide (KOH) to treat with a precursor, which is then pyrolyzed at a moderate temperature of 673−873 K. **Table 1.4** summarizes advantages and disadvantages of physical and chemical activation. From Table 1.4, it is noted that the chemical activation has a fewer preparatory step, requires lower production temperature, and provides high production yield as well as high porosity development. As a result, chemical activation is favored in a commercial application.

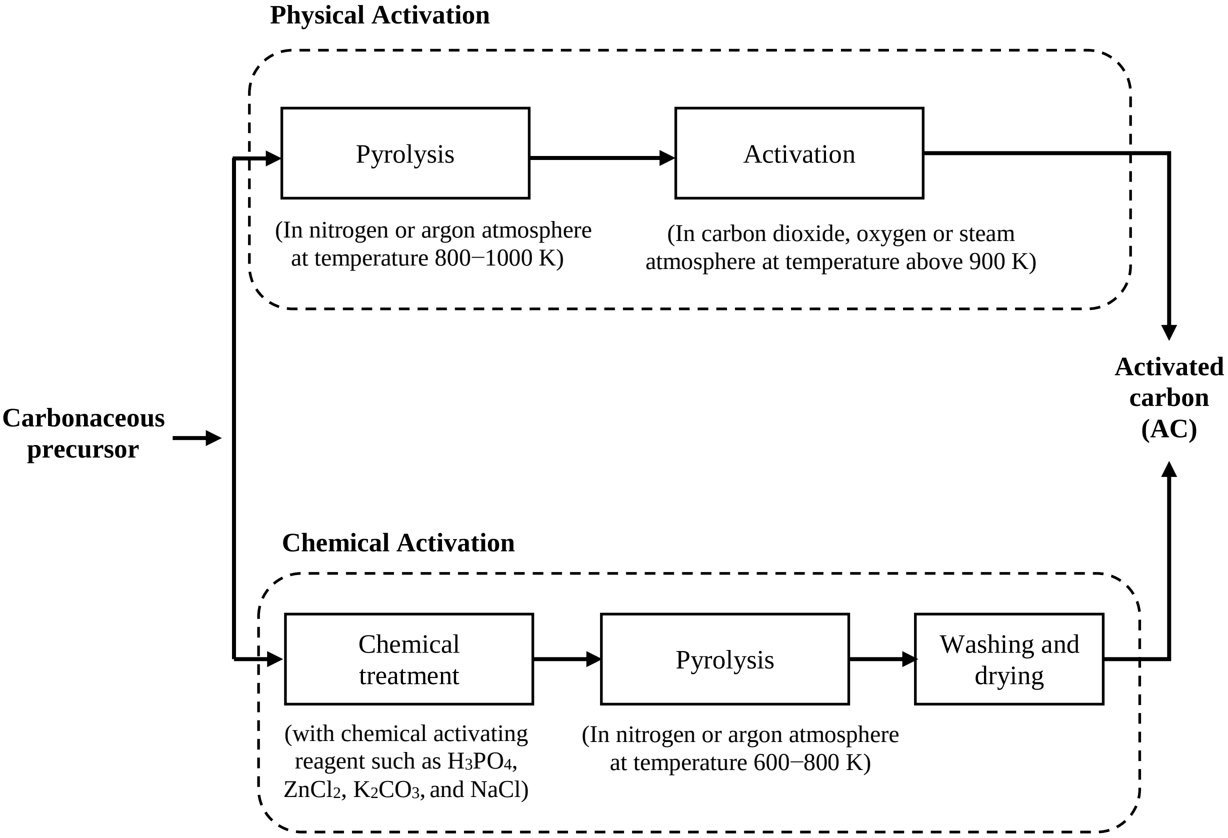

Figure 1.18 Process flow for activated carbon production (adapted from Bedia *et al.*, 2020)

Table 1.4 Advantages and disadvantages of physical and chemical activation (Hernández-Montoya et al., 2012)

Physical Activation	**Chemical Activation**
Advantages -Environmental friendly of activation reagent - No incorporation of impurities coming from the activating reagent	Advantages - Short production time - Low production temperature - High product yield - High porosity development
Disadvantages - High production temperature - Long production time - Low product yield - High energy cost	Disadvantages - Incorporation of impurities coming from the chemical activating reagent - Cost of the chemical activating reagent - Washing step is required

1.3 OBJECTIVE AND STRUCTURE OF THESIS

1.3.1 Objective

The objective of this thesis is to treat the effluent by adsorption using activated carbon produced from palm kernel shell in palm oil mill process in Thailand. In order to achieve this main objective, several studies were conducted in the following ways:

1. Study on the current palm oil mill process and identification of major problem from palm oil mill industry
2. Characterization of palm kernel shell
3. Pyrolysis of palm kernel shell to produce palm kernel shell activated carbon and other products under various operating conditions
4. Study on the performance of palm kernel shell activated carbon as adsorbent for treating the unfavorable compounds in model palm oil mill effluent
5. Application of effluent treatment using palm kernel shell activated carbon in Thailand’s palm oil mill process

1.3.2 Structure

Figure 1.19 shows the structure of this thesis. This thesis consists of six chapters. The chapters are prepared in order to achieve the objectives listed above. In chapter 2–5, an introduction of the chapter is provided to guide the readers briefly understand the contents and the objective of the chapter.

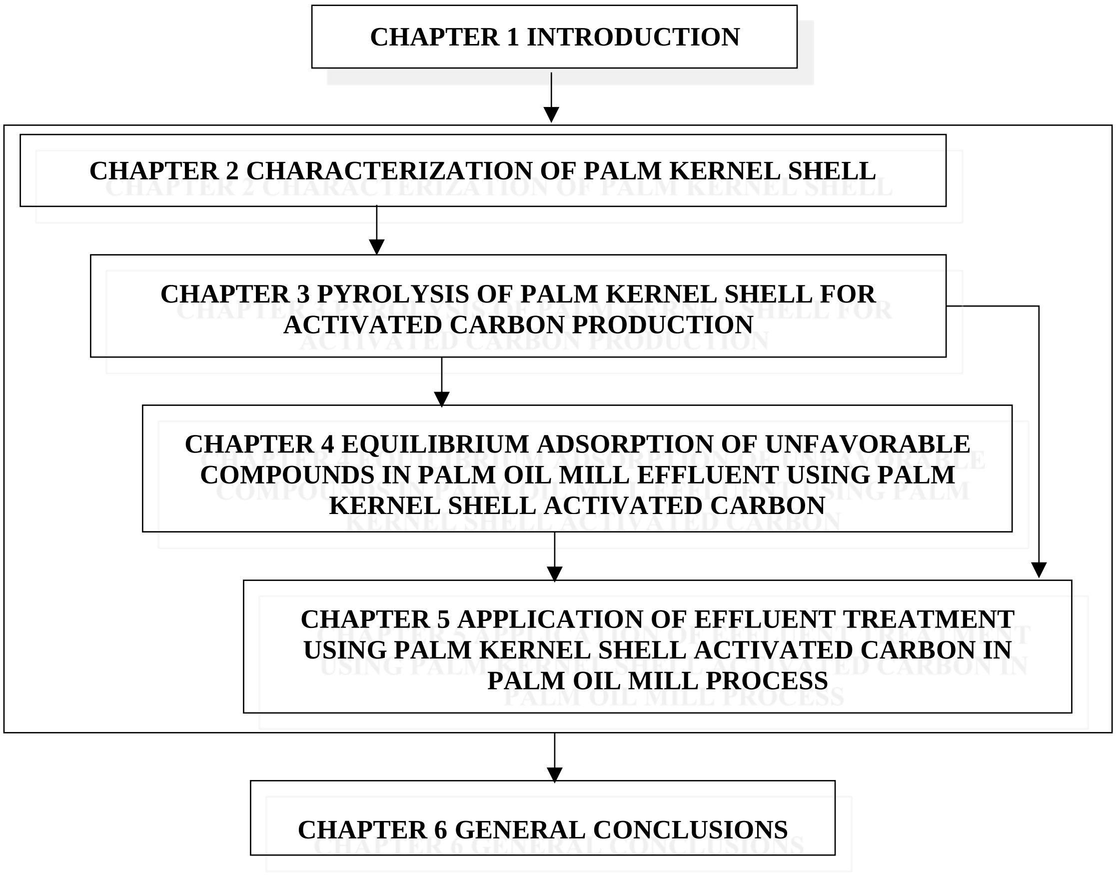

Figure 1.19 Thesis structure

CHAPTER 2

CHARACTERIZATION OF PALM KERNEL SHELL

2.1 INTRODUCTION

This chapter presents the characterization of palm kernel shell which was obtained from Thailand. Several analyses were carried out in order to understand physical and thermal properties of palm kernel shell. The analyses included proximate, ultimate, and thermogravimetric analyses. The results of proximate and ultimate analyses of palm kernel shell were compared with other plant-based biomasses. The thermogravimetric analysis of palm kernel shell without and with chemical treatment was performed in order to evaluate the potential of chemical activating reagent for further palm kernel shell activated carbon production.

2.2 EXPERIMENTAL

2.2.1 Material and sample preparation

a) Palm kernel shell

The raw palm kernel shell (PKS) was obtained from a private company in Krabi province, Thailand.

b) Sample preparation

The raw PKS was washed thoroughly with deionized water (Millipore Milli-Q System: Millipore, USA) to remove any impurities, dried at 383 K for 12 h, and ground by blender (Wonder Blender, WB-1, Osaka Chemical Co., Ltd.). The ground sample was further sieved with a commercial sieve having an aperture of 0.425×10^{-3} m (Tokyo Screen Co.), and part of the sample passing through the sieve was used for the were used for the characterization and pyrolysis of PKS. **Figure 2.1** shows the appearance of raw PKS and sieved PKS. Palm shell is dark brown and hard. The size and thickness of palm shell are varied.

Figure 2.1 Appearance of palm kernel shell (left: raw palm kernel shell right: sieved palm kernel shell)

c) Chemical treatment of palm kernel shell

Chemical treatment of PKS was employed using orthophosphoric acid (H_3PO_4, Wako Pure Chemical Industries, Ltd.) before pyrolysis. The purpose of chemical treatment is to help in developing the porosity of palm kernel shell activated carbon (PKSAC) during the pyrolysis. By employing the chemical treatment method, the pore structure should be enhanced during the pyrolysis and a high yield of PKSAC is expected. The experimental conditions were referred from a previous study (Yorgun and Yıldız, 2015), and the details are provided in **Table 2.1**. The PKS was contacted with a solution having a specific H_3PO_4 concentration, c_p, on a hot plate (HSH-6D, AS ONE CORP) with a magnetic stirrer for a specified duration. After contacting, the PKS was filtered from the chemical treatment solution and dried at 383 K in an electric oven (OF-450B-R, AS ONE CORP) for 24 h to obtain chemically treated PKS. **Figure 2.2** shows the appearance of chemically treated PKS. The chemically treated PKS changed into black color after drying.

Table 2.1 Experimental conditions for chemical treatment of palm kernel shell

Feed	PKS
Mass of feed [kg]	1.5×10^{-2}
Chemical activating reagent	H_3PO_4
Volume of aqueous solution of chemical activating reagent [m^3]	1.0×10^{-4}
H_3PO_4 concentration, c_P [kmol m^{-3}]	1−8
Temperature [K]	358
Time [h]	6
Stirring speed [h^{-1}]	1.8×10^{4}

Figure 2.2 Palm kernel shell (left) and chemically treated palm kernel shell (right) prior pyrolysis

2.2.2 Method

a) Proximate and ultimate analyses

Proximate analysis of the PKS were carried out using Shimadzu DTG-60 fitted with a FC-60A flow rate controller and TA-60WS thermal analyzer. The working conditions for proximate and thermogravimetric analyses are shown in **Table 2.2**. Approximately 1.0×10^{-5} kg of PKS was heated from 313 K to 1273 K at heating rate 1.8×10^{-5} K h^{-1} under N_2 atmosphere with a constant flow rate of 0.009 m^3 h^{-1}, and kept at 379 K for 5 min; the N_2 flow was then switched to air with a constant flow rate of 0.003 m^3 h^{-1}, and the sample was further heated from 379 to 1100 K. The volatile matter, the fixed carbon and the ash of each sample were determined following the American Society for Testing and Materials (ASTM) D3172 standard. **Figure 2.3** shows the picture of instrument for proximate analysis.

Figure 2.3 Instrument for proximate analysis

Table 2.2 Working conditions for proximate analysis

Detector type	DTG-60H
Atmospheric gas	N_2 and O_2
Gas flow [$m^3\ h^{-1}$]	0.009 and 0.003
Sample weight [kg]	1.0×10^{-5}
Initial temperature [K]	313
Temperature rate [$K\ h^{-1}$]	1.8×10^{-5}
Holding temperature [K]	1100
Holding time [h]	1100

The ultimate analysis of PKS was performed using CHN elemental analyzer (J-Science JM10) at Center for Advanced Materials Analysis, Tokyo Institute of Technology. The Carbon (C), Hydrogen (H), Nitrogen (N), and Sulphur (S) contents of PKS were determined using the analyzer and oxygen (O) was determined by the difference. **Figure 2.4** illustrates the elemental analyzer at the center. The machine is using a mixture of helium and oxygen for combustion and a dual piston pump for detection. The detection limit is 0.5−400 μg for H, 3−2600 μg for C and 1−1000 μg for N.

Figure 2.4 Elemental analyzer (J-Science JM10) for ultimate analysis

b) Thermogravimetric analysis

Thermogravimetric analysis of PKS without and with chemical treatment was carried out using Shimadzu DTG-60 fitted with a FC-60A flow rate controller and TA-60WS thermal analyzer. The working conditions were same as described in **Table 2.2** but the analysis was carried out in air atmosphere.

2.3 RESULTS AND DISCUSSION

2.3.1 Composition of palm kernel shell

The results of the proximate and elemental analyses of the PKS compared with previous studies and other plant-based biomasses are shown in **Table 2.3**. The PKS has high volatile matter, carbon, and oxygen contents but low ash and sulfur contents, which is similar to other PKS and plant-based biomasses reported in the previous studies (Guo and Lau, 2003; Hamza *et al.*, 2016). The contents of particular composition in each biomass depend on the type of plant-based biomasses and origin or geographical region in which it is formed. The high carbon and low ash contents in PKS were considered as a positive factor for the production of palm kernel shell activated carbon with a high specific surface area since these two factors promoted the formation of porous structure and enrichment of carbon in the precursor (Canales Flores *et al.*, 2017).

Table 2.3 Compositions of palm kernel shell compared with other plant-based biomasses (in mass fraction)

	PKS	PKS from previous studied	Corn cob	Coconut shell	Eucalyptus leaf
Proximate analysis					
Ash	0.04	(0.03 a))	0.019	0.076	0.11
Volatile matter	0.77	(0.77 a))	0.76	0.69	0.79
Fixed carbon	0.19	(0.20 a))	0.23	0.17	0.10
Ultimate analysis					
C	0.52	(0.47 b))	0.45	0.48	0.47
H	0.06	(0.06 b))	0.065	0.061	0.062
N	0.004	(0.009 b))	0.003	0.002	0.012
S	0.001	(0.0003 b))	0.001	0.001	0.008
O	0.41	(0.45 b))	0.46	0.46	0.45

a) Guo and Lua (2003)
b) Hamza *et al.* (2016)

2.3.2 Thermal property of palm kernel shell

Figure 2.5 shows the results of the thermogravimetric analysis of the PKS without and with chemical treatment, where the mass ratio of the remaining sample relative to the initial value is plotted against temperature. The mass ratio of PKS decreased with increase in temperature, and it took place in roughly three stages. In the first stage, the reduction occurred in the temperature range below 420 K due to the desorption of water from the PKS (Li *et al.*, 2008). Thereafter, the mass ratio decreased significantly to approximately 0.36 in the temperature range of 420−650 K. This was due to the decomposition of hemicellulose and cellulose (Ma *et al.*, 2015). The massive loss of mass ratio in this range indicates that PKS should be pyrolyzed at temperature above 500 K. Subsequently, the mass ratio decreased by about 0.15 in the temperature range of 650−870 K due to the decomposition of lignin and cellulose. From this point (above 870 K) onward, the mass ratio was almost constant, and there was scope for further thermal decomposition of PKS (Hamza *et al.*, 2016).

In comparison with the mass ratio of PKS, the mass ratio of chemically treated PKS decreased gradually with increase in temperature. However, in this case, it was difficult to determine the stages of the TGA profile. Similar results were also reported by Pereira *et al.*, 2014; Kumar and Jena, 2016. The chemical activating reagent, H_3PO_4, enhanced the dehydration of hemicellulose and cellulose in PKS. H_3PO_4 promoted the cleavage of linkages in hemicellulose and cellulose at sub-pyrolysis temperature, which was followed by a crosslinking reaction that hindered the thermal decomposition at a relatively high temperature. As a result, the mass ratio in chemically treated PKS was greater than that in PKS even at high temperatures (Guo and Lau, 2003).

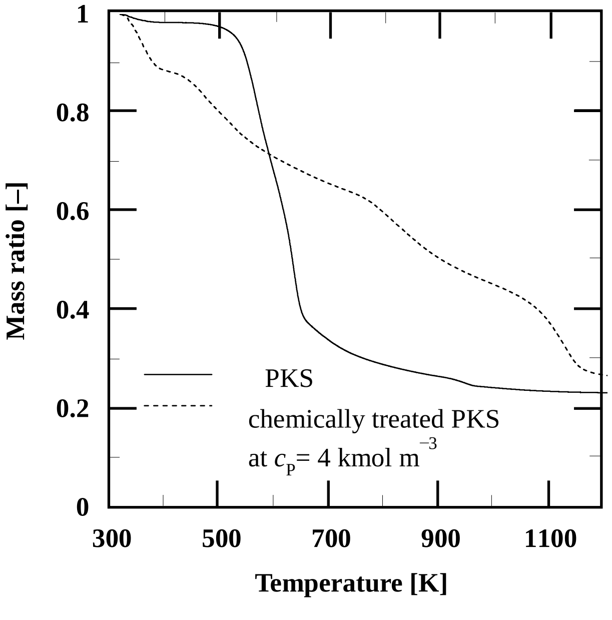

Figure 2.5 Thermogravimetric analysis of the palm kernel shell without and with chemical treatment

2.4 CONCLUSIONS

Palm kernel shell from Thailand was characterized by proximate, ultimate, and thermogravimetric analyses. The high carbon and low ash contents in palm kernel shell indicated that palm kernel shell is a favorable precursor to prepare palm kernel shell activated carbon. The pyrolysis of palm kernel shell should be done at temperature above 500 K. The presence of chemical activating reagent, orthophosphoric acid, could hinder thermal decomposition in palm kernel shell in the high temperature, indicating the potential to produce a high yield of palm kernel shell activated carbon.

CHAPTER 3

PYROLYSIS OF PALM KERNEL SHELL FOR ACTIVATED CARBON PRODUCTION

3.1 INTRODUCTION

The prepared palm kernel shell with chemical treatment in chapter 2 was pyrolyzed to produce palm kernel shell activated carbon and other products. The effects of chemical concentration and pyrolysis operating conditions were studied to determine the parameters that affect the yields of palm kernel shell activated carbon and other products. The characterization of palm kernel shell activated carbon and other products were discussed accordingly to investigate their further utilization. Elemental balance among pyrolysis products was performed to determine the elemental composition in pyrolysis products.

3.2 EXPERIMENTAL

3.2.1 Material

The material used in this chapter was PKS with chemical treatment by orthophosphoric acid prepared in chapter 2.

3.2.2 Apparatus and procedure

a) Pyrolysis of palm kernel shell

The schematic diagram and the appearance of the apparatus of the pyrolysis are shown in **Figure 3.1** and **3.2**, respectively. The main component of this device was a tubular reactor inserted horizontally into an electrically heated furnace (KTF-040N from KOYO Thermo Systems Co.). The sample holder was filled with sample and placed at the center of the reactor. A simple thermocouple (NiCr-Constantan, HT 20 from Hakko Electric Machine Works Co.) was placed directly on top of the sample holder. The condenser and the two-neck round-bottom flask capacity 1×10^{-3} m^3 were assembled and ice was filled fully in the bath below the reactor. The sampling bag was connected with a borosilicate gas inlet adapter on the top of the condenser.

The principal experimental conditions of pyrolysis are represented in **Table 3.1**. Before the experiment started, the N_2 gas was supplied at 9.0×10^{-3} m^3 h^{-1} (at s.t.p.) to sweep the air out of furnace for at least 10 minutes. After that, the reactor was closed tightly and the furnace switch was turned on. The sample, which was at room temperature was heated, and it took approximately 0.5 hour to reach the specified pyrolysis temperature. After reaching the specified pyrolysis temperature, the system was maintained isothermally for the specified pyrolysis time. Then, the furnace was turned off and cooled down to room temperature. All of the gases flowing out from the other end of the reactor were sent to be condensed liquid in the two-neck round-bottom flask. The off-gas was started collecting at pyrolysis temperature approximately 400 K until the experiment finished using 1×10^{-3} m^3 gas sampling bag (GL Sciences Inc.).

The obtained solid sample was washed several times using 0.1 kmol m^{-3} NaOH to neutralize the solution until its pH of the washing solution became about 6−7. The washed sample was dried at 383 K for 24 h to obtain the palm kernel shell activated carbon (PKSAC). The PKSAC was stored in the desiccator for further experimental studies.

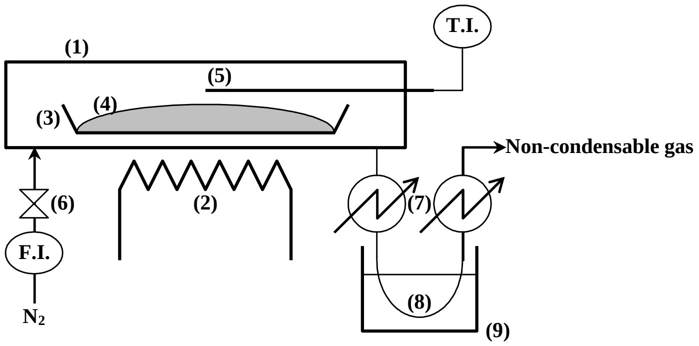

Figure 3.1 Schematic diagram of pyrolysis apparatus:
(1) tubular reactor (inner diameter 0.038 m, length 0.7 m); (2) electric tubular furnace; (3) sample holder (depth 0.015 m, width 0.03 m, length 0.4 m); (4) feed; (5) NiCr-Constantan thermocouple; (6) valves; (7) condensers; (8) liquid product trap; (9) iced bath (275277 K); F.I. flow indicator; T.I. temperature indicator (Othaman *et al.*, 2008)

Figure 3.2 Appearance of the pyrolysis apparatus

Table 3.1 Principal experimental conditions of pyrolysis

Feed	PKS w/ and w/o chemical treatment
Mass of feed [kg]	1.0×10^{-2}
Atmospheric gas	nitrogen
Flow rate of nitrogen [$m^3\ h^{-1}$]	9.0×10^{-3}
Temperature, T [K]	673−1073
Time, t [h]	1, 2

b) Analyses

Specific surface area and pore volume analyzer

The specific surface area and porosity properties of PKSAC were characterized by nitrogen adsorption–desorption using BELSORP-max: BEL JAPAN Co. Prior to the analysis, roughly 5.0×10^{-5} kg of PKSAC was degassed at 573 K for 6 h under vacuum conditions in order to clean the surface from impurities. Nitrogen adsorption isotherm was determined over a relative pressure range (P/P_o) of 0.01 to 0.99. The specific surface area of PKSAC, S_{BET}, was determined using the Brunauer–Emmett–Teller (BET) method, and the total pore volume (V_p) was obtained from the total amount of N_2 adsorbed at a relative pressure (P/P_o) of ~0.99. The micropore volume (V_{micro}) was calculated using the *t*-plot method, and the mesopore volume (V_{meso}) was obtained by subtracting the micropore volume from the total pore volume (Tanaka *et al*. 2012). **Figure 3.3** shows the picture of the instrument for specific surface area and porosity properties of PKSAC.

Figure 3.3 BELSORP-max: BEL JAPAN for specific surface area and porosity properties analysis of PKSAC

Fourier-transform infrared spectroscopy

The chemical property of PKSAC was characterized in term of surface functional groups. The chemical functional groups present on PKSAC surface were recorded using an infrared spectrometer IRAffinity-1 (Shimadzu, Japan) with Quest ATR accessory with a diamond crystal (Specac, USA). LabSolution IR software was used as an interface between the spectrometer and the control computer. The spectra were recorded in the 4000 – 400 cm^{-1} region using the spectral resolution of 4 cm^{-1} and 128 scans. Data were acquired with 40 scans at a resolution of 4 cm^{-1} and processed using the LabSolution IR software by Shimadzu. **Figure 3.4** shows the instrument for surface functional groups analysis of PKSAC.

Figure 3.4 Infrared spectrometer IRAffinity-1 (Shimadzu, Japan) for surface functional groups analysis of PKSAC

Elemental analyzer

The elemental composition of PKSAC was analyzed by an elemental analyzer (J-Science JM10) same as explained in Chapter 2.

pH meter

pH of condensable liquid was measured by pH meter (Horiba Scientific, F74). Before the measurement, the pH meter calibration was performed using standard buffer solutions of pH 4 and 7 (Horiba Ltd.). The analysis was repeated three times in each sample in order to obtain accurate result. **Figure 3.5** is the picture of the pH meter.

Figure 3.5 pH meter (Horiba Scientific, F74) for pH value measurement

Karl Fischer titrator

The water content in the condensable liquid was measured by Karl Fischer Instruments (758 KFD Titrino) from Metrohm company. The conditions of analysis are stated in **Table 3.2**. **Figure 3.6** is the picture of the device.

Table 3.2 Conditions for Karl Fischer Titrator (758 KFD Titrino, 739 Exchange unit, 703 Titration stand, Citizen display (iDP562-RS))

Titration chemical	Hydranal Composite 5
Dehydration solvent	Methanol
Injector	Micro syringe (10μL)
Input Unit	g

Figure 3.6 Karl Fischer Instruments (758 KFD Titrino) for water content analysis

Gas chromatograph

The chemical components in condensable liquid were analyzed by gas chromatograph (GC-2010 Shimadzu Company; Hicap-CBP1 column I.D. 0.00032 m×50 m). **Table 3.3** shows the working conditions for condensable liquids analysis. The samples were injected automatically by the autosampler (AOC-20i). The data were acquired and processed on a personal computer, using Shimadzu GC Solution software. The analysis was repeated three times in each sample. Before performing the actual analysis, calibration curves of each chemical component were made. 1-Propanol was used as a solvent. **Figure 3.7** shows the picture of the instrument for condensable liquid analysis

Table 3.3 Working conditions for gas chromatograph (GC-2010, Hicap-CBP1 column)

Carrier gas and flow rate [m^3 h^{-1}]	N_2, 0.0016
Detector gas and flow rate [m^3 h^{-1}]	Hydrogen, 0.0028
FID gas and flow rate [m^3 h^{-1}]	Air, 0.027
Injector temperature [K]	573
Detector temperature [K]	573
Column temperature [K]	343 →373
Column heating rate [K h^{-1}]	300
Split ratio (outlet : inlet column) [−]	1:50
Split flow rate [m^3 h^{-1}]	0.0025
Column flow rate [m^3 h^{-1}]	0.0001

Figure 3.7 Gas chromatograph (GC-2010) for chemical components analysis in condensable liquid

Off-gas from pyrolysis was analyzed by Tracera High-Sensitivity gas chromatograph (Shimadzu Company; Micropacked ST column I.D. 0.003 m×0.001 m). The working conditions for the analysis is described in **Table 3.4**. A 1.0×10^{-6} m^3 gas tight syringe (Hamilton, Reno, NV, USA) was used for all manual injections. The integration was performed with LabSolutions. The analysis was repeated three times in each sample. Before performing the actual analysis, calibration curves of six components hydrogen (H_2), oxygen (O_2), carbon dioxide (CO_2), nitrogen (N_2), carbon monoxide (CO), and methane (CH_4) were made. **Figure 3.8** shows the picture of the instrument for off-gas analysis.

Table 3.4 Working conditions for gas chromatograph (Tracera GC-2010 Plus A + BID-2010 Plus, Micropacked ST column)

Carrier gas and pressure [kPa]	He, 50
Injector temperature [K]	423
Detector temperature [K]	553
Column temperature [K]	308 →523→543
Purge flow rate [m^3 h^{-1}]	0.0042
Injection volume [m^3]	1.0×10^{-6}
Split ratio (outlet : inlet column) [−]	1:5

Figure 3.8 Gas chromatograph (Tracera GC-2010) for off-gas analysis

3.3 RESULTS AND DISCUSSION

3.3.1 Appearance of activated carbon and other products

The appearance of PKSAC produced from different chemical concentrations is shown in **Figure 3.9**. PKSAC had dark brown to black color depended on the chemical concentration. The higher the c_P, the darker the PKSAC. The size of PKSAC size was almost the same with the feed PKS.

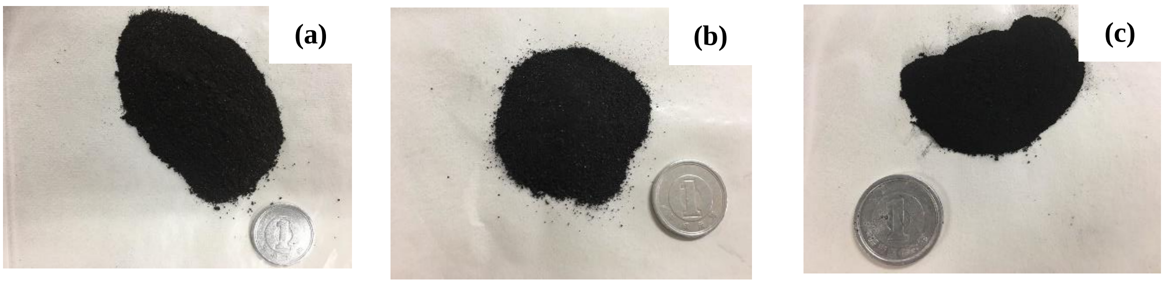

Figure 3.9 Appearance of PKSAC produced from different H_3PO_4 concentrations (a) c_P= 2 kmol m^{-3} (b) c_P= 4 kmol m^{-3} (c) c_P= 8 kmol m^{-3})

The appearance of condensable liquid is exhibited in **Figure 3.10**. The color of condensable liquid from pyrolysis of PKS with and without chemical treatment was different. Condensable liquid from pyrolysis of PKS without chemical treatment displayed opaque dark color with a strong odor whereas PKS with chemical treatment showed green color. The off-gas was colorless hence it could not be shown by picture.

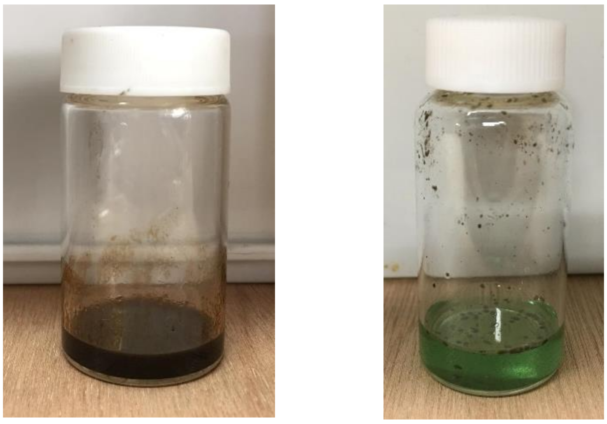

Figure 3.10 Appearance of condensable liquid (left: without chemical treatment right: with chemical treatment)

3.3.2 Yields of activated carbon and other products

The yield of PKSAC from the pyrolysis, Y_{PKSAC}, was defined as the mass ratio of PKSAC relative to the feed PKS. Y_{PKSAC} can be written as,

$$Y_{\mathrm{PKSAC}} = \frac{F_1}{F_0} \tag{3.1}$$

where F_0 and F_1 are the masses of PKS with or without chemical treatment feed for the pyrolysis and PKSAC obtained from the pyrolysis, respectively.

The yield of condensable liquid (L), Y_{L}, was defined as,

$$Y_{\mathrm{L}} = \frac{L_1}{F_0} \tag{3.2}$$

where L_1 is the mass of condensable liquid from the pyrolysis

The yield of the off-gas, Y_{OG}, was calculated by difference.

$$Y_{\mathrm{OG}} = 1 - (Y_{\mathrm{L}} + Y_{\mathrm{PKSAC}}) \tag{3.3}$$

a) Yield of palm kernel shell activated carbon

Figure 3.11 shows the effect of chemical concentration on yield of palm kernel shell activated carbon, Y_{PKSAC}. Y_{PKSAC} was around 0.5 with respective H_3PO_4 concentration, c_{P}. Y_{PKSAC} increased as c_{P} increased in the range at c_{P} 1 − 4 kmol m^{-3}. Thereafter, it decreased at $c_{\mathrm{P}} = 8$ kmol m^{-3}.

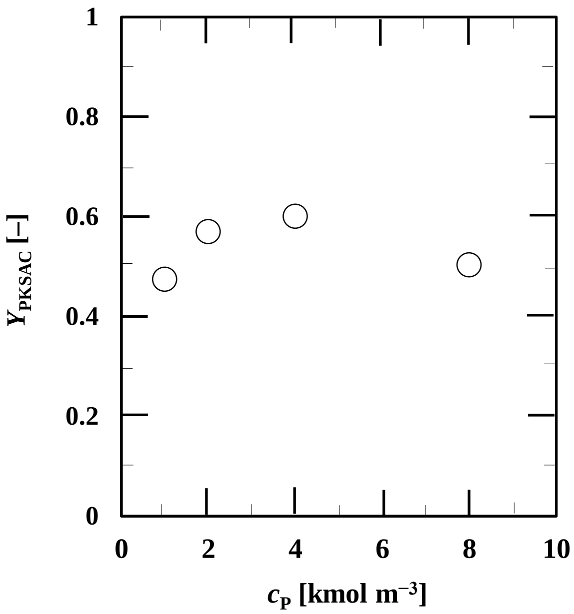

Figure 3.11 Effect of chemical concentration on the yield of palm kernel shell activated carbon

The effects of chemical treatment and pyrolysis operating conditions on Y_{PKSAC} are shown in **Figure 3.12**. It can be seen that Y_{PKSAC} decreased with an increase in pyrolysis temperature, T. The Y_{PKSAC} with chemical treatment was higher than that without chemical treatment at T in the range 673−873 K. Thereafter, they became almost similar at T = 1073 K. The chemical activating reagent caused the formation of a crosslinking structure, which resulted in a high Y_{PKSAC}. The concentration of H_3PO_4, c_P, and pyrolysis time, t, had little effect on Y_{PKSAC}. The Y_{PKSAC} of 0.8 was the maximum obtained in this work.

b) Yield of other products

Figure 3.13 and **3.14** show the yield of off-gas (Y_{OG}), and condensable liquid (Y_L) from pyrolysis, respectively. Y_{OG} increased with T in all runs. Y_{OG} from pyrolysis of PKS without chemical treatment gradually decreased with T and its Y_{OG} ranged from 0.25 to 0.30 on average. On the other hand, Y_{OG} from pyrolysis of PKS with chemical treatment were relatively low at T in the range 673−873 K. Thereafter they became high at T= 1073 K.

The Y_L from pyrolysis of PKS without chemical treatment was higher that of with chemical treatment, and it was almost constant with respective T. The Y_L reached the maximum points at around 873 K in all runs. Thereafter, Y_L decreased in the range of more than 873 K due to secondary reaction of the tar cracking which leads to more production of gases (Othaman *et al.*, 2008).

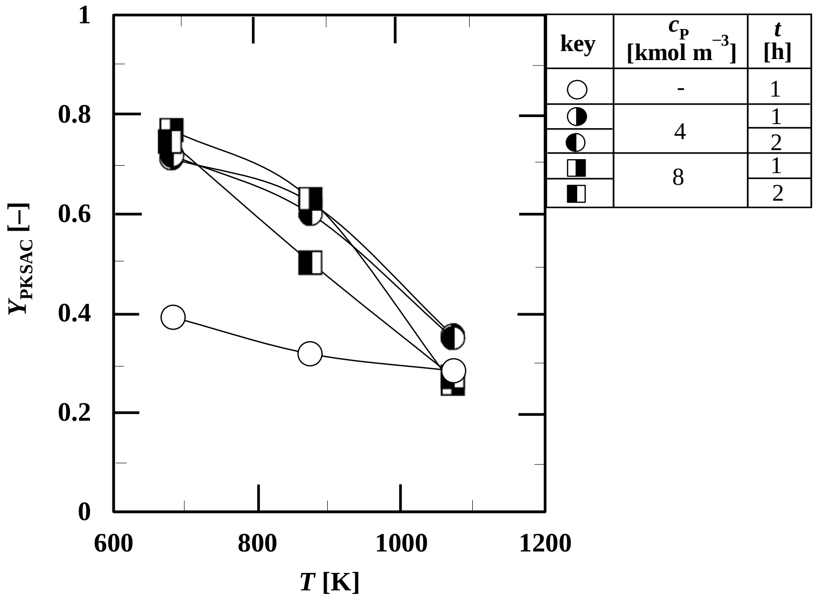

Figure 3.12 Effects of chemical treatment and pyrolysis operating conditions on the yield of palm kernel shell activated carbon

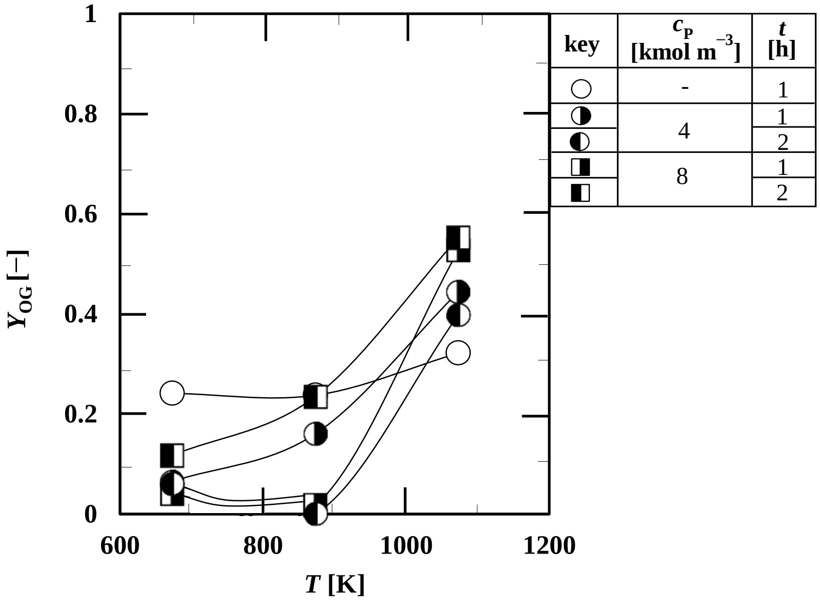

Figure 3.13 Effects of chemical treatment and pyrolysis operating conditions on the yield of off-gas

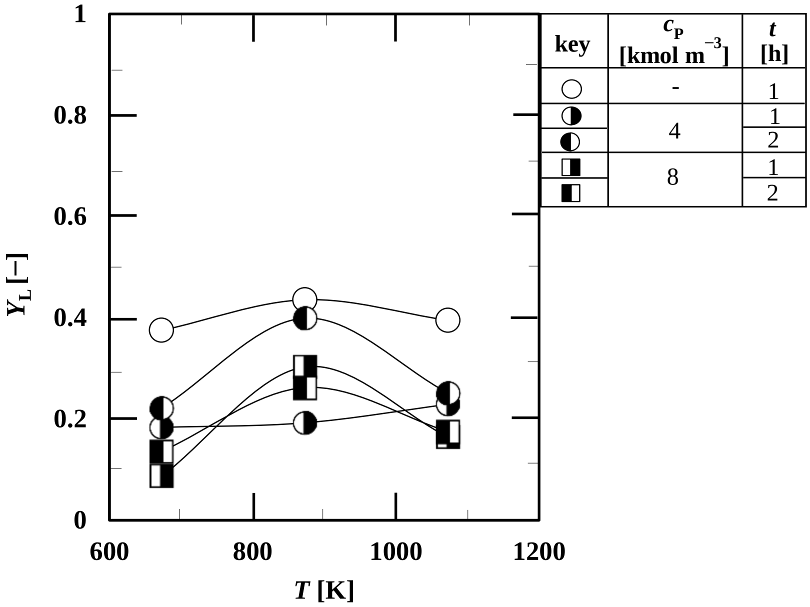

Figure 3.14 Effects of chemical treatment and pyrolysis operating conditions on the yield of condensable liquid

3.3.3 Characterization of activated carbon and other products

a) Characterization of palm kernel shell activated carbon

The effect of chemical concentration on PKSAC specific surface area, S_{BET}, and total pore volume, V_p, is exhibited in **Figure 3.15**. S_{BET} could be improved by the increasing of c_P. Similar trends have also been found through H_3PO_4 activation of other lignocellulosic material such as *Oreganum* stalks, Fox nut, and corncob (Sych *et al.*, 2010: Chen 2017, Bouchemal *et al.*, 2009). As S_{BET} of PKSAC prepared with $c_P = 1$ and 2 kmol m^{-3} was very small. PKS chemically treated with c_P 4 and 8 kmol m^{-3} were chosen for further study.

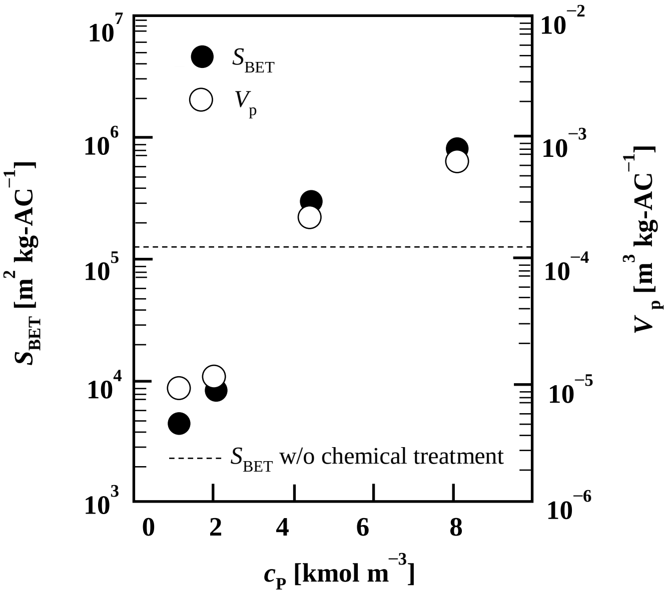

Figure 3.15 Effects of chemical concentrations on palm kernel shell activated carbon characteristics T= 873 K t= 2 h

The effects of chemical treatment and pyrolysis operating conditions on the specific surface area, S_{BET}, and total pore volume, V_p, of PKSACs are represented in **Figure 3.16**. Both S_{BET} and V_p show the same trend. The chemical treatment with H_3PO_4 enhanced S_{BET} and V_p at a lower pyrolysis temperature and time, and the larger the value of c_P, the greater the values of S_{BET} and V_p. The same findings were reported by various studies with different lignocellulosic materials with chemical treatment by H_3PO_4. The highest S_{BET} for operating pyrolysis temperatures ranged from 673 K to 773 K under t= 1 h from their studies (Chen 2017: Nicholas *et al.*, 2018).

The effect of pyrolysis time, t, on S_{BET} and V_p was insignificant. The chemical activating reagent, H_3PO_4, basically facilitated the development of a cross-linked structure such as phosphocarbonaceous structure and improved the pore structure, thereby enhancing S_{BET} and V_p (Yorgun and Yıldız, 2015). With chemical treatment, both S_{BET} and V_p of PKSAC decreased as T increased up to 873 K. Thereafter, it increased above 873 K. Below 873 K, there was considerable the formation of tars and other liquid products, which clogged up the pores and lowered S_{BET} and V_p. Above 873 K, the phosphorus species reacted with carbon and released gaseous phosphorus, and hence, S_{BET} and V_p increased with T (Chen, 2017). The same trend of AC surface area decreased in this T range was also found by Chen 2017, and Nicholas *et al.*, 2018.

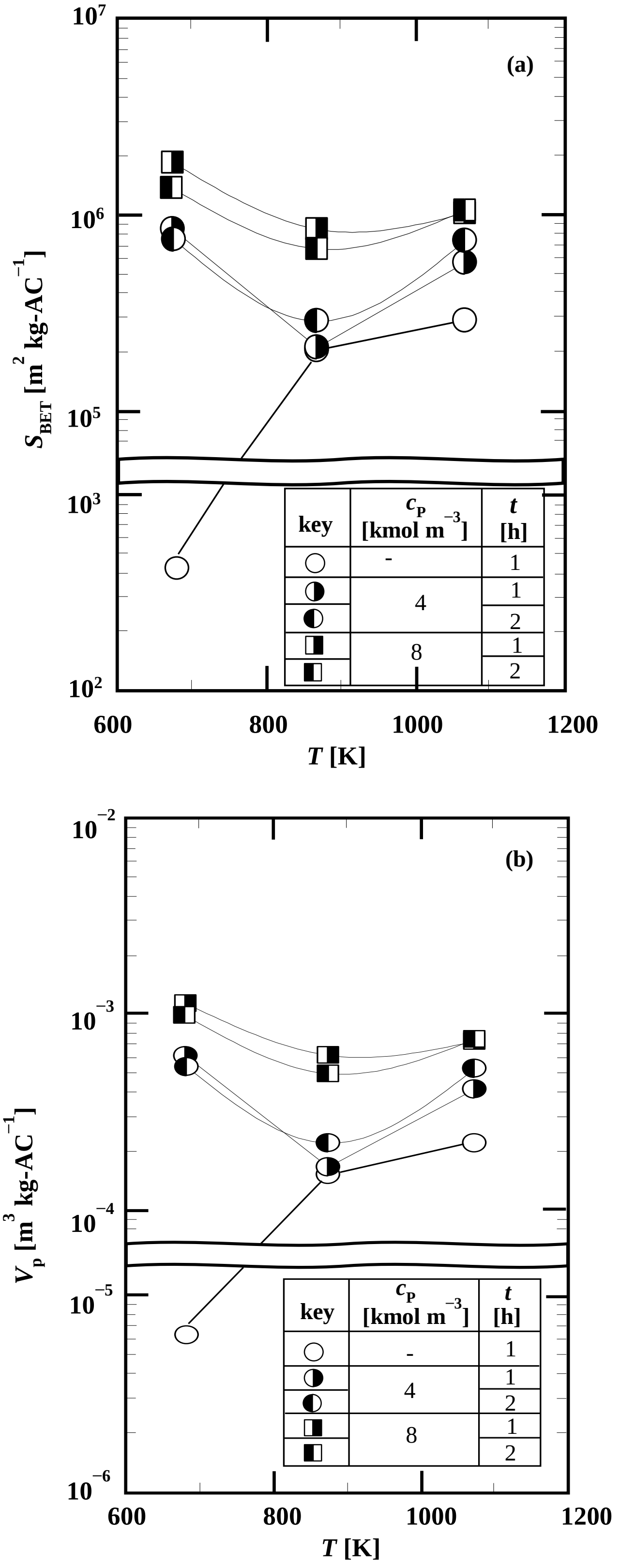

Figure 3.16 Effects of chemical treatment and pyrolysis operating conditions on the (a) specific surface area and (b) total pore volume of palm kernel shell activated carbons

Li *et al.*, 2015 reported the main reactions occurred during pyrolysis of lignocellulosic material with H_3PO_4 treatment under different temperature ranges as follows:

400–650 K (primary pyrolysis);

$$2H_3PO_4 \rightarrow H_4P_2O_7 + H_2O \quad \textbf{(3.4)}$$

$$3H\ _3PO_4 \rightarrow H_5P_3O_{10} + 2H_2O \quad \textbf{(3.5)}$$

$$n\ H_3PO_4 \rightarrow H_{n+2}P_nO_{3n+1} + (n\text{-}1)\ H_2O \quad \textbf{(3.6)}$$

650–900 K (secondary pyrolysis);

$$H_{n+2}P_nO_{3n+1} \rightarrow P_4O_{10} + H_2O \quad \textbf{(3.7)}$$

$$P_4O_{10} + C \rightarrow P_4O_6 + CO_2 \quad \textbf{(3.8)}$$

Above 900 K;

$$P_4O_{10} / P_4O_6 + CH_x \rightarrow PH_3 + CO_2/CO \quad \textbf{(3.9)}$$

The reactions 3.4–3.6 were mainly dehydration of phosphoric acid and the decomposition of some functional groups. From 650–900 K $H_{n+2}P_nO_{3n+1}$ was dehydrated and transformed into phosphorus pentoxide (P_4O_{10}). Then phosphorus trioxide (P_4O_{10}) reacted with C and formed new pores, enlarged the existing pores, and produced CO_2. Above 900K, P_4O_{10} and P_4O_6 reacted with CHx and generate phosphine (PH_3), CO_2, and CO.

However, the reactions that took place during the pyrolysis was quite complicated to describe. The above reactions are only the representatives of many reactions that might occur during the pyrolysis in this study.

Table 3.5 shows the comparison of specific surface area of activated carbon produced from different raw materials and palm kernel shell with orthophosphoric acid activation. The table indicates that AC could be produced from different raw materials under various pyrolysis temperatures and times. The S_{BET} and yield of AC from previous literatures was ranged between 800×10^3 to 1100×10^3 m^2 kg-AC^{-1}, and 0.40 to 0.50, respectively. These results were lower than the results obtained in this study. In addition, this study could produce the higher S_{BET} and yield with lower pyrolysis temperature compared to other AC, indicating that the present PKSAC production method is effective. Table 3.5 was a brief comparison, the comparison still lacked of some information such as the gas flow rate, the size of precursor, and the concentration of phosphoric acid used for AC production.

Table 3.5 Comparison of specific surface area of activated carbon produced from various raw materials and palm kernel shell with orthophosphoric acid activation

Raw material	**T [K]**	**t [h]**	**Yield [−]**	**S_{BET}×10^3 [m^2 kg-AC^{-1}]**	**Ref.**
Rice husk	773	1	-	1016	Li *et al.*, 2015
Coconut shell	973	40 mins	0.37	889	Wang *et al.*, 2013
Pecan shell	773	-	-	1130	Guo and Rockstraw, 2006
Birch wood	873	1	-	761	Budinova *et al.*, 2006
Grape seed	773	2	0.50	1139	Bahri *et al.*, 2012
Palm kernel shell	773	2	0.40	1135	Guo and Lau, 2003
Palm kernel shell	700	0.5	0.50	1109	Lim *et al.*, 2010
Palm kernel shell	673	1	0.77	1856	This study

Table 3.6 summarizes the physical properties of PKSACs and commercial AC (CAC) used in the adsorption study. The chemical treatment by H_3PO_4 could enhance micropore volume (V_{micro}) in PKSACs, and produced PKSACs were predominantly microporous. V_{micro} of the PKSACs increased with increase in c_P, whereas T and t decreased similar to that in the case of S_{BET}. Some produced PKSACs had larger S_{BET} than that of CAC.

Table 3.6 Physical properties of PKSACs and CAC used in the adsorption study

c_P [kmol m^{-3}]	**T [K]**	**t [h]**	**V_{meso}×10^{-3} [m^3 kg-AC^{-1}]**	**V_{micro}×10^{-3} [m^3 kg-AC^{-1}]**	**S_{BET}×10^3 [m^2 kg-AC^{-1}]**
w/o chemical treatment	873	1	0.017	0.139	235
4	1073	1	0.010	0.407	616
4	673	2	0.013	0.527	795
4	673	1	0.019	0.592	889
8	1073	2	0.015	0.724	1094
8	673	2	0.031	0.944	1403
8	673	1	0.041	1.078	1856
CAC			0.020	0.541	992

The Fourier-transform infrared spectroscopy (FT-IR) spectra of the PKSACs compared with PKS are shown in **Figure 3.17**. The surfaces of all the samples presented several chemical functional groups, and the number of functional groups depended on the chemical concentration and pyrolysis operating conditions. The FT-IR spectrum of PKS exhibited a number of absorption peaks, indicating the complex nature of the materials. The main surface functional groups obtained with PKS were carbonyl groups (C=O) such as ketone and quinone, ethers (C−O−C), and phenol (O−H), which are commonly found in lignocellulosic materials (Guo and Lau, 2003; Hamza *et al.*, 2016).

The spectra of the PKSACs were different from that of PKS; some bands remained while many bands disappeared due to the vaporization of organic matter at high *T*. PKSAC without chemical treatment showed C=C stretch in aromatics, C−O−C stretch vibrations in ethers, and C−OH out-of-the-plane in ethers (Guo and Lau, 2003). On the other hand, PKSACs with H_3PO_4 treatment showed the P=O group from polyphosphates, P^+-O^- in acid phosphate esters, and O−C stretching vibration in the P−O−C (aromatic) linkage (Wang *et al.*, 2011; Puziy *et al.*, 2002), indicating the incorporation of phosphates onto the carbon during pyrolysis. The chemical functional groups were broken when *T* increased, and with an increase in c_P, the intensity of phosphorus-containing groups also increased.

The results of elemental composition of PKSACs from various operating conditions are tabulated in **Table 3.7**. PKSAC without chemical treatment had higher C, N, and lower ash contents than that of PKSAC with chemical treatment. The high ash content was found in PKSAC with chemical due to the formation of polyphosphates derived from H_3PO_4 during the pyrolysis. The polyphosphates were difficult to remove during the washing and contributed to ash content (Quesada-Plata *et al.*, 2016). The carbon content increased with the increase in *T* and *t* maybe due to an increasing degree of aromaticity (Kumar and Jena, 2016).

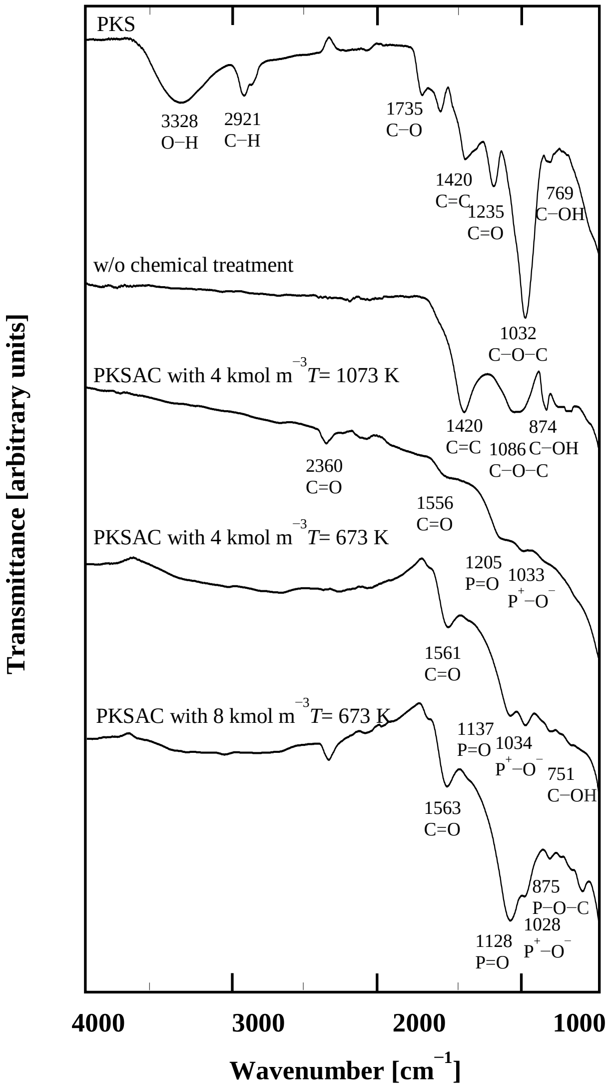

Figure 3.17 Fourier-transform infrared spectroscopy spectra of palm kernel shell and palm kernel shell activated carbons

Table 3.7 Elemental composition of PKSACs obtained from various operating conditions

PKSAC			**Elemental composition (in mass fraction)**				
c_P **[kmol m^{-3}]**	***T*** **[K]**	***t*** **[h]**	**C**	**H**	**N**	**O**	**Ash**
-	873	1	0.68	0.04	0.0074	0.19	0.08
-	1073	1	0.79	0.03	0.0074	0.099	0.08
4	873	1	0.48	0.03	0.0041	0.30	0.20
4	1073	1	0.53	0.03	0.0042	0.24	0.20
8	873	1	0.51	0.03	0.0038	0.27	0.19
8	1073	1	0.61	0.02	0.0057	0.12	0.24
8	673	2	0.70	0.03	0.0033	0.13	0.14

b) Characterization of other products

Characterization of off-gas

The components of five major off-gases from pyrolysis, H_2, O_2, CO_2, CO, and CH_4**,** were studied. The calculations to estimate the amount of component in off-gas can be found in Appendix A.2. **Figure 3.18** shows the evolution of off-gas flow rate versus sampling time. All of the target off-gases started generating at the early stage of sampling time. The composition of off-gases decreased as sampling time increased and off-gases almost finished generating at sampling time 1.5 h. Therefore, pyrolysis time one hour was enough to obtain a sufficient amount of off-gas for further utilization. The amount of off-gas generated from pyrolysis of PKS with chemical treatment was lower than PKS without chemical treatment.

The mass fraction of off-gas from pyrolysis of PKS without and with chemical treatment is displayed in **Figure 3.19**. The mass fraction of off-gas from pyrolysis of PKS without chemical treatment was almost constant with respective *T*. On the other hand, it was found that the amount of CH_4 was very low at T= 673 K from pyrolysis with PKS with chemical treatment. Thereafter the mass fraction of off-gas increased remarkably. The overall of flammable gases increased when *T* increased but the overall of non-flammable decreased.

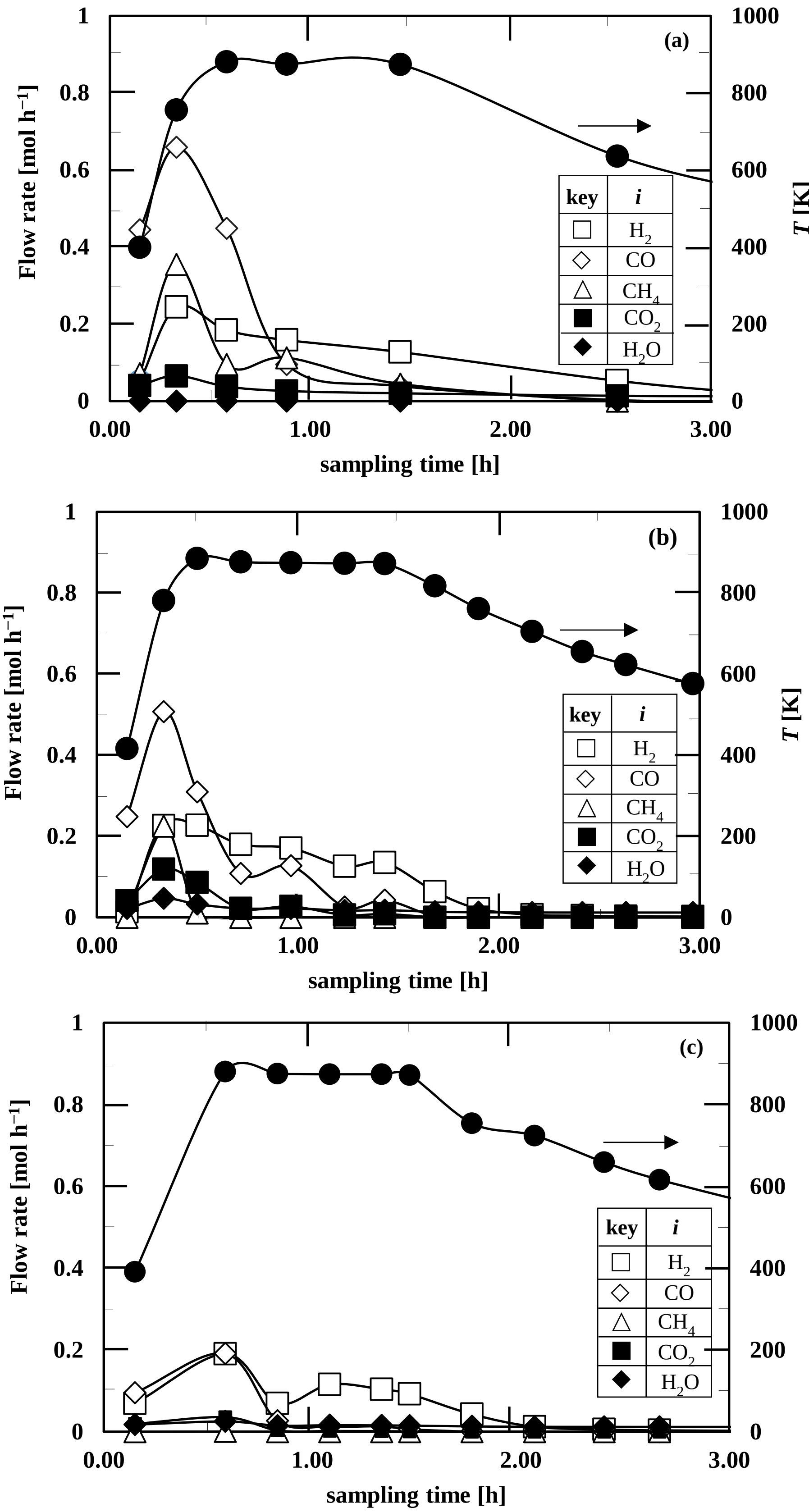

Figure 3.18 The evolution of off-gas flow rate versus sampling time *t*=1 h; *T* = 873 K (a) without chemical treatment (b) c_P= 4 kmol m^{-3} (c) c_P= 8 kmol m^{-3}

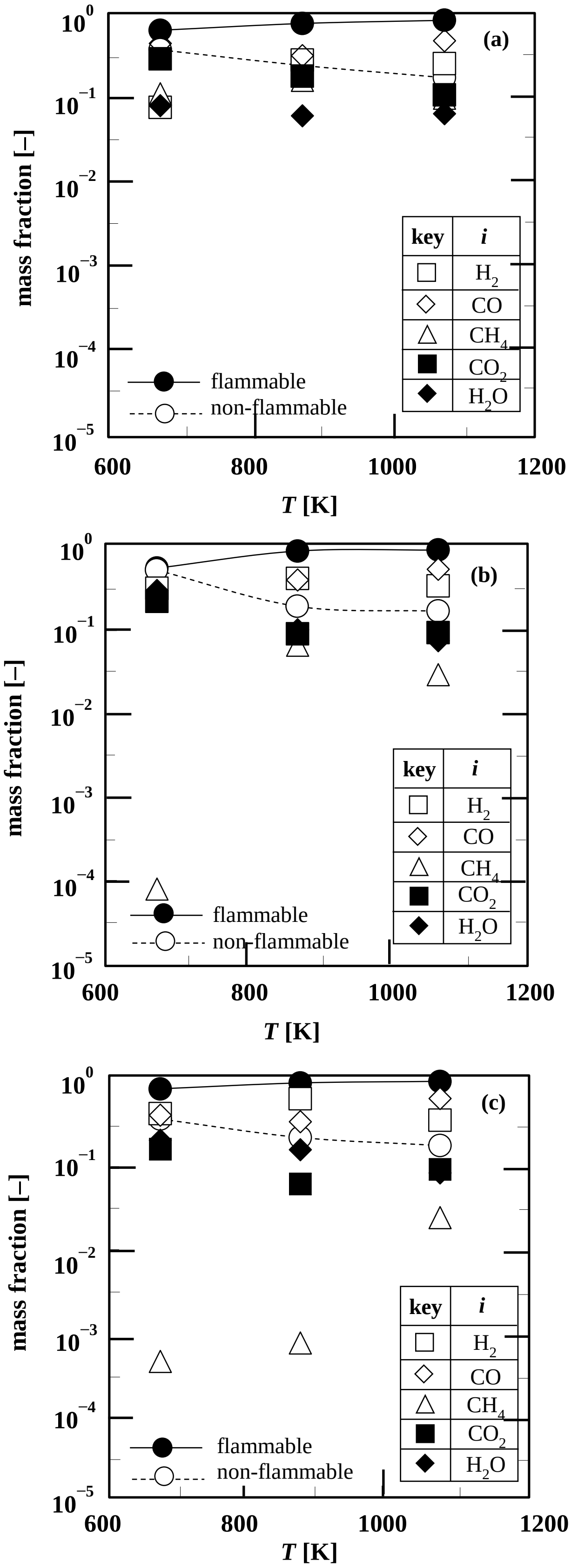

Figure 3.19 Mass fraction of off-gas components from pyrolysis at t=1 h (a) without chemical treatment (b) c_P= 4 kmol m^{-3} (c) c_P= 8 kmol m^{-3}

The heating value of the off-gas from pyrolysis of PKS without and with chemical treatment are shown in **Figure 3.20** and **3.21**, respectively. The heating value of off-gas was calculated using the enthalpy of combustion of the flammable gases as stated in **Table 3.8**. The heating value of the off-gas in all runs increased as T increased. The composition and heating value of off-gas from pyrolysis of PKS without chemical treatment was higher than that of PKS with chemical treatment.

Table 3.8 Enthalpy of combustion for flammable gas component in off-gas (Othaman *et al.*, 2008)

Component	**Enthalpy of combustion [kJ m^{-3}]**
H_2	- 10757
CO	- 12704
CH_4	- 35872

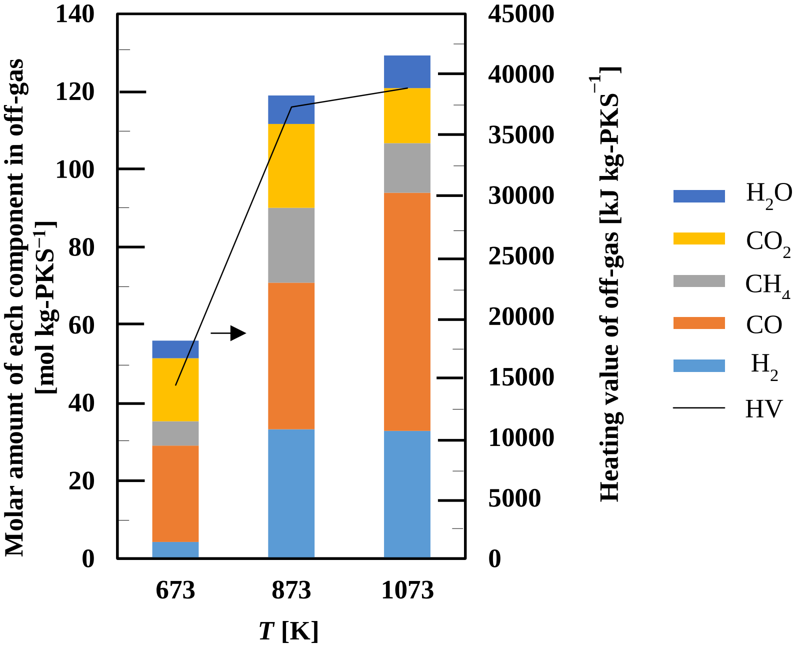

Figure 3.20 Molar amount of each component in off-gas from various pyrolysis temperatures of PKS and their heating values at t=1 h

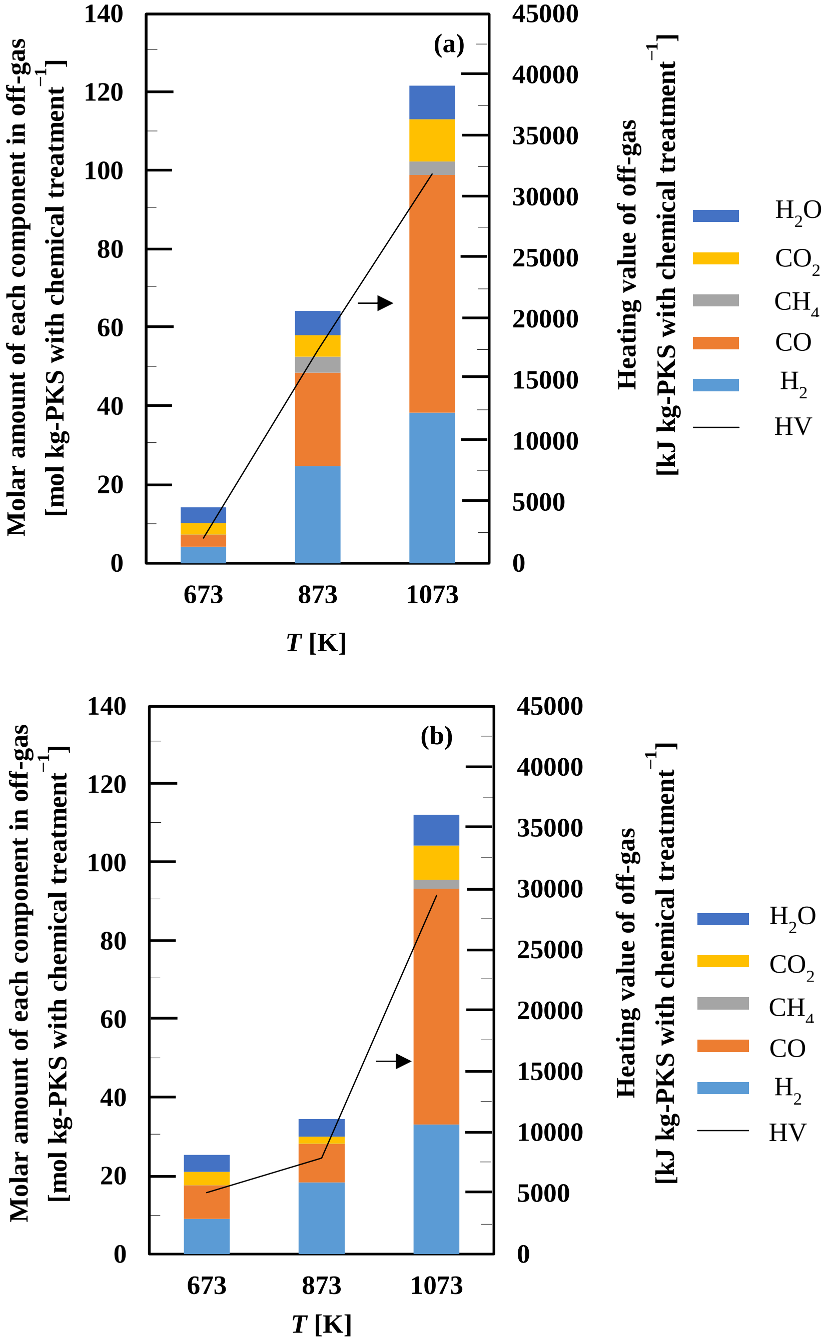

Figure 3.21 Molar amount of each component in off-gas from various pyrolysis temperatures of PKS with chemical treatment and their heating values at t=1 h (a) c_P= 4 kmol m^{-3} (b) c_P= 8 kmol m^{-3}

Characterization of condensable liquid

The pH of condensable liquid from pyrolysis of PKS without and with chemical treatment is shown in **Figure 3.22**. pH of condensable liquid in all runs were highly acidic and ranged from 1 to 2 on average. pH of condensable liquid from pyrolysis of PKS with chemical treatment was lower than that of PKS without chemical treatment and the pH decreased as *T* increased.

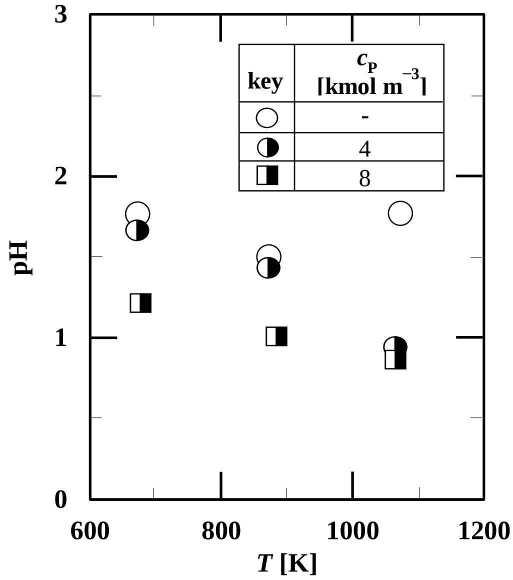

Figure 3.22 pH of condensable liquid from pyrolysis of PKS without and with chemical treatment at t=1 h

Figure 3.23 illustrates the mass fraction of components in condensable liquid from pyrolysis of PKS without and with chemical treatment. Water content in condensable liquid was in the range from 0.4 to 0.8. The water content of PKS with chemical treatment considered relatively high. Similar results were also reported by Hassan *et al.* (2009). Their study stated that the presence of dehydrating chemical reagents such as H_3PO_4, H_2SO_4, and NaOH enhanced the production of water. The studied chemical components in condensable liquid were methanol, acetone, acetic, phenol, and guaiacol. These chemicals have been reported as major chemical components that remained in condensable liquid from various studies (Uysal *et al.*, 2014: Lu *et al.*, 2018: Liu *et al.*, 2013). The major chemical components in condensable liquid from pyrolysis of PKS without chemical treatment were methanol, acetic acid, and phenol whereas in the case of PKS with chemical treatment were methanol and acetic acid. The decrease in phenol may be attributed to the promotion of char formation during lignin decomposition in the pyrolysis, resulting in the prevention of phenol formation (Liu *et al.*, 2013). The component of guaiacol was relatively low in all runs.

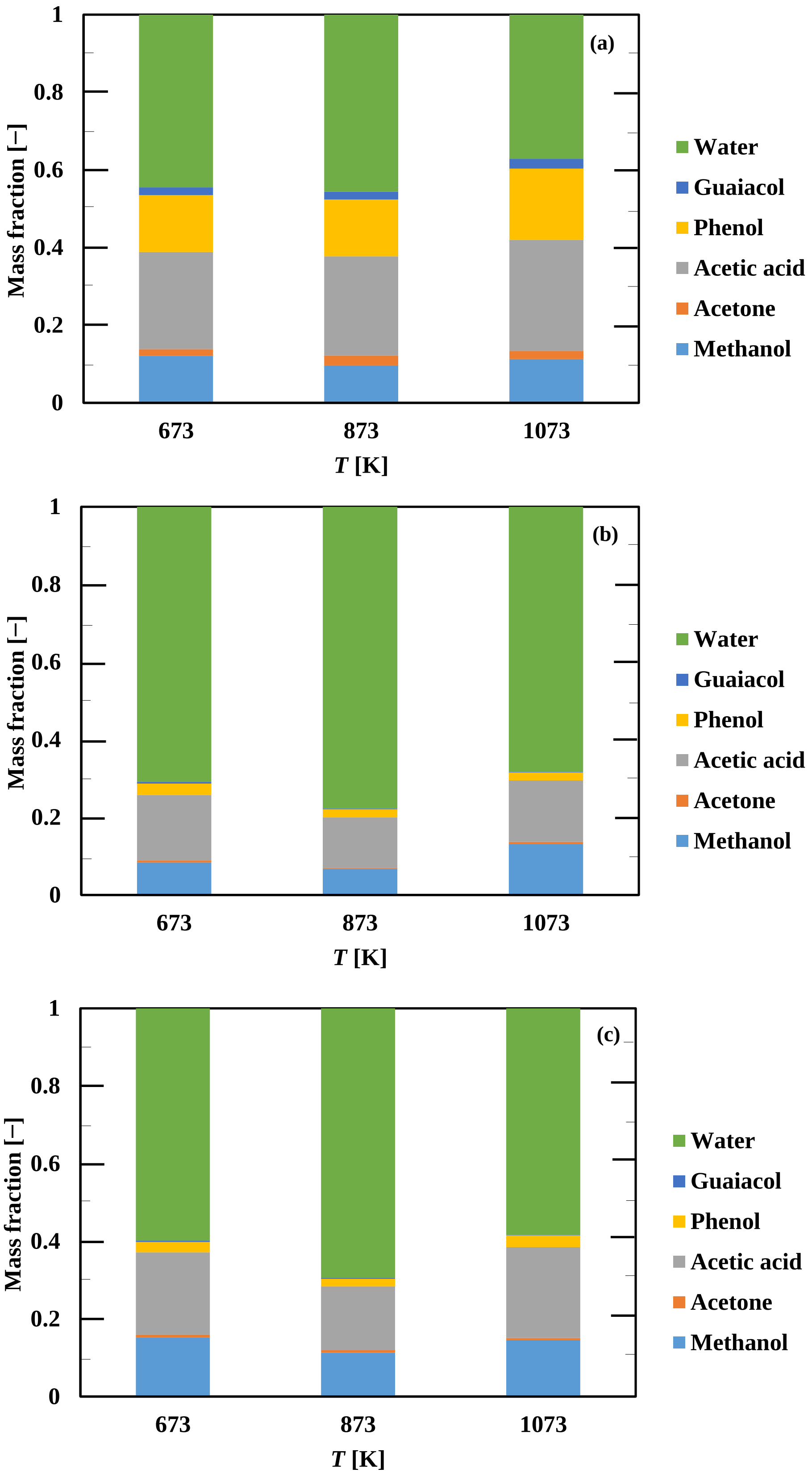

Figure 3.23 Components in condensable liquids from pyrolysis of PKS without and with chemical treatment at *t*=1 h (a) without chemical treatment (b) c_P= 4 kmol m^{-3} (c) c_P= 8 kmol m^{-3}

3.3.4 Elemental balance in pyrolysis

The elemental balances among the pyrolysis products are shown in **Figure 3.24**. The element compositions of PKSAC were obtained from CHN elemental analyzer, while those of condensable liquid were calculated from mass balance of carbon, hydrogen, and oxygen as shown in equation 3.4.

$$x_{i,PKS} = Y_{PKSAC} x_{i,PKSAC} + Y_{OG} x_{i,OG} + Y_L x_{i,L} \qquad \textbf{3.4}$$

where *i* stand for the element C, H and O. $x_{\mathrm{i,PKS}}$, $x_{\mathrm{i,PKSAC}}$, $x_{\mathrm{i,OG}}$, and $x_{\mathrm{i,L}}$ are the mass fraction of element *i* in PKS, PKSAC, off-gas, and condensable liquid, respectively. Y_{PKSAC}, Y_{OG}, and Y_{L} are the yields of PKSAC, off-gas, and condensable liquid, respectively. The mass fraction of element in each product changed with the pyrolysis temperature. The carbon content mainly remained in PKSAC while the oxygen content remained in off-gas and condensable liquid. The hydrogen content in all products were relatively low.

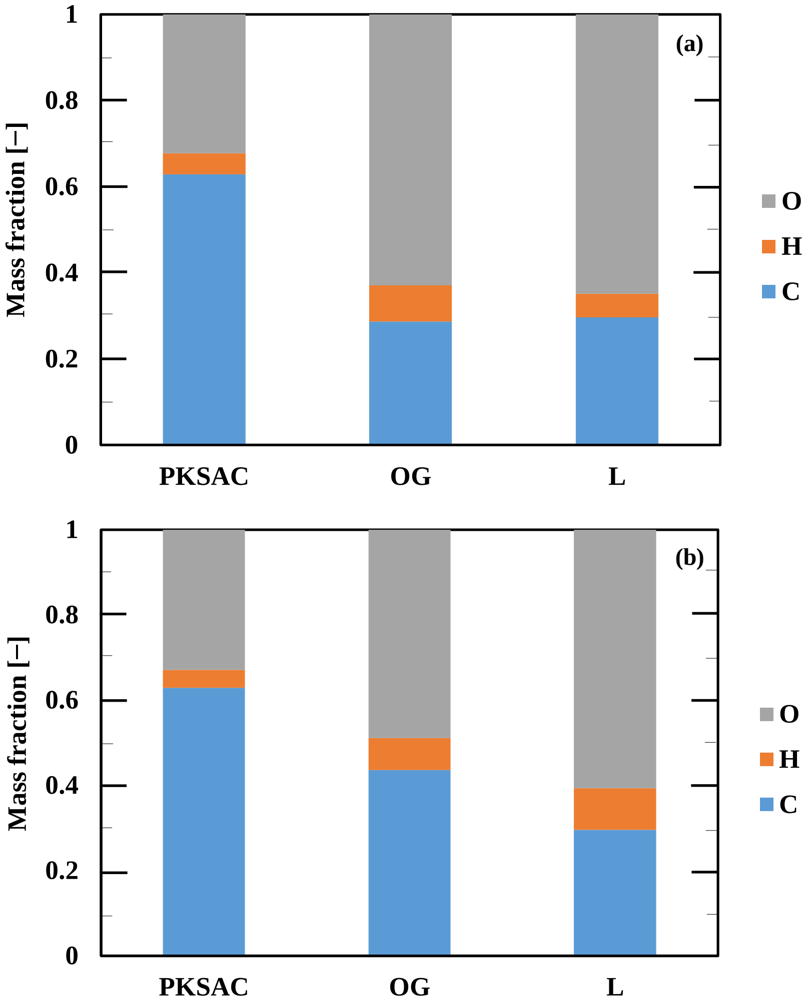

Figure 3.24 Elemental balances among pyrolysis products of PKS with chemical treatment at c_{P}= 8 kmol m^{-3} t=1 h (a) T= 673 K (b) T= 873 K

The carbon and oxygen balances among pyrolysis products under various pyrolysis temperature are shown in **Figure 3.25** and **3.26**, respectively. The carbon content in PKSAC decreased and the oxygen content in off-gas increased as pyrolysis temperature increased. The oxygen contents in PKSAC migrated to the condensable liquid and gaseous products in the form of oxygen-containing organic compounds, water, CO, and CO_2 (Barbanera and Muguerza, 2019).

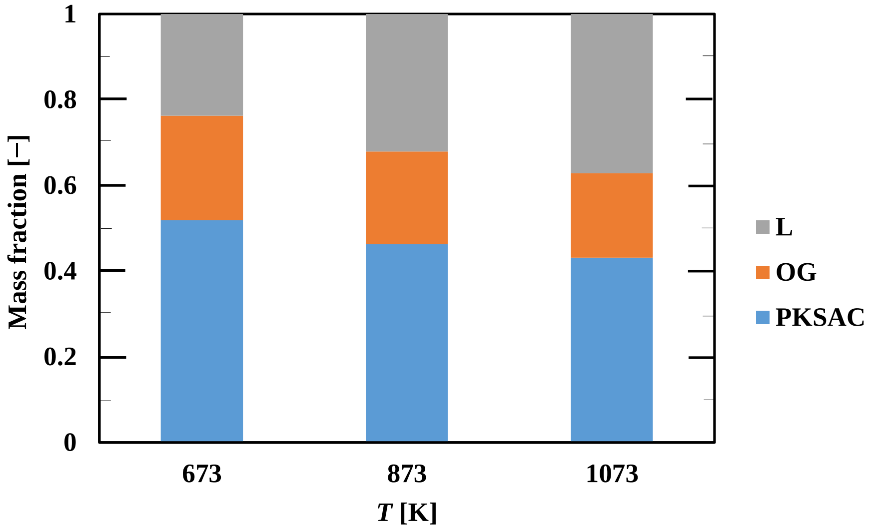

Figure 3.25 Carbon balance among pyrolysis products of PKS with chemical treatment at c_P= 8 kmol m^{-3} t=1 h

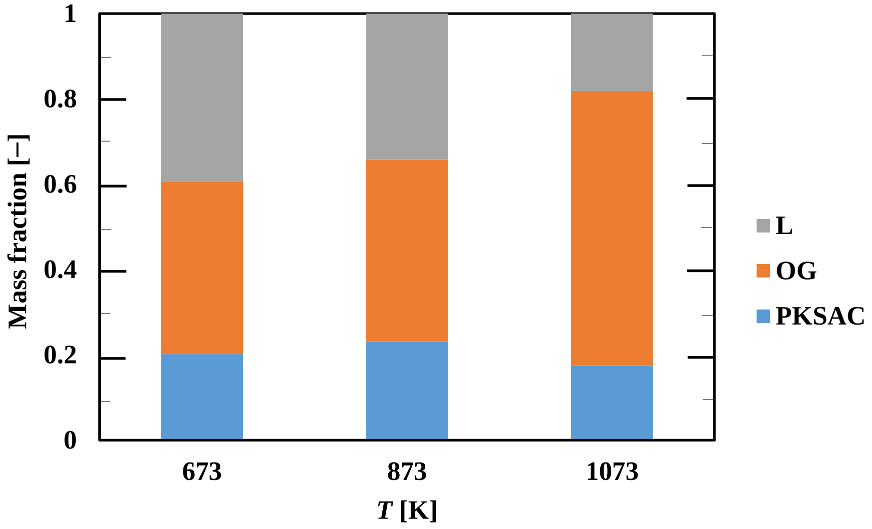

Figure 3.26 Oxygen balance among pyrolysis products of PKS with chemical treatment at c_P= 8 kmol m^{-3} t=1 h

3.4 CONCLUSIONS

Palm kernel shell activated carbon and other products were obtained from pyrolysis. The presence of orthophosphoric acid in palm kernel shell could improve yield of palm kernel shell activated carbon. The effect of pyrolysis temperature significantly affected yield of palm kernel shell activated carbon whereas the effects of orthophosphoric acid concentration and pyrolysis time were insignificant. The pyrolysis temperature also showed the effect on yield of other products. Produced palm kernel shell activated carbon had a relatively high micropore volume and specific surface area which were suitable to be used as an adsorbent. The surface functional groups of palm kernel shell activated carbon also changed by chemical treatment. The off-gas contained flammable and non-flammable gases and one hour of pyrolysis time was sufficient to obtain almost all of the off-gas. The condensable liquid contained chemical components such as acetic acid and methanol. The carbon content mainly remained in PKSAC while the oxygen content remained in off-gas and condensable liquid.

CHAPTER 4

EQUILIBRIUM ADSORPTION OF UNFAVORABLE COMPOUNDS IN PALM OIL MILL EFFLUENT USING PALM KERNEL SHELL ACTIVATED CARBON

4.1 INTRODUCTION

From the previous chapter, the palm kernel shell activated carbon had sufficient specific surface area which can be used as an adsorbent. Therefore, to evaluate the performance of palm kernel shell activated carbon for treating the unfavorable compounds in palm oil mill effluent, the adsorption of unfavorable compounds by palm kernel shell activated carbon was conducted. In this chapter, the palm kernel shell activated carbons produced from various operating conditions were applied for the adsorption of unfavorable compounds in model palm oil mill effluent. The parameters that affected adsorption performance were discussed respectively.

4.2 EXPERIMENTAL

4.2.1 Material

The adsorbents used in this chapter were palm kernel shell activated carbon (PKSAC) produced from different operating conditions in Chapter 3.

Phenol, *m*-cresol, *p*-cresol, and commercial activated carbon (CAC) in the analytical grade were purchased from FUJIFILM Wako Pure Chemical Corp. Lignin (CAS No.: 8068-05-1) was purchased from Sigma-Aldrich Co.

4.2.2 Adsorption procedure and principal conditions

a) Adsorption procedure

Phenolic compounds and lignin were chosen as representatives of unfavorable compounds in POME. These two compounds were major unfavorable compounds which are usually reported in POME characteristics by several studies (Khongkhaem *et al*., 2016; Tosu *et al*., 2015; Mellyanawaty *et al*., 2018). An aqueous solution of phenolic compounds and lignin was continually contacted with the PKSAC at constant temperature using a thermostatic shaking water bath (T-N22S, Thomas Kagaku. Co., Ltd.) for five days to equilibrate it. Then the solution and PKSAC were separated by filtration. The filtrate solution of phenolic compounds and lignin was analyzed by gas chromatograph with FID (Shimadzu GC-14B), and UV-Vis spectrometer (UV-1280, Shimadzu), respectively.

b) Principal conditions for batch equilibrium adsorption

The principal conditions of batch equilibrium adsorption of phenolic compounds and lignin are represented in **Table 4.1-4.3**. Phenolic compounds, namely, phenol, *m*-cresol and *p*-cresol were the representative hazardous compounds and lignin was a representative of colored material in POME. The concentration of adsorbate in feed solution was varied. The binary adsorption of phenolic compounds were also studied under mass fraction of 1:1.

Table 4.1 Principal conditions for single solute batch equilibrium adsorption of hazardous compounds

Feed (model POME)	Aqueous solution of phenol, *m*-cresol, and *p*-cresol
Concentration of adsorbate in feed solution, $C_{i,0}$ [kmol m^{-3}]	0.005−0.030
Adsorbent	PKSAC
Mass of adsorbent, S_0 [kg]	1.0×10^{-4}
Volume of feed, L_0 [m^3]	2.5×10^{-5}
Ratio of adsorbent mass to feed solution volume, S_0/L_0 [kg m^{-3}]	4
Time [h]	120
Temperature [K]	300

Table 4.2 Principal conditions for binary solutes batch equilibrium adsorption of hazardous compounds

Feed (Binary solutes)	Aqueous solution of two phenolic compounds (phenol and *p*-cresol, or phenol and *m*-cresol)
Concentration of adsorbate in feed solution, $C_{i,0}$ [kmol m^{-3}]	0.005−0.030
Adsorbent	PKSAC
Mass of adsorbent, S_0 [kg]	1.0×10^{-4}
Volume of feed, L_0 [m^3]	2.5×10^{-5}
Mass fraction of phenolic compound [–]	1
Ratio of adsorbent mass to feed solution volume, S_0/L_0 [kg m^{-3}]	4
Time [h]	120
Temperature [K]	300

Table 4.3 Principal conditions for single solute batch equilibrium adsorption of colored material

Feed (model POME)	Lignin
Concentration of adsorbate in feed solution, $C_{Lg,0}$ [kmol m^{-3}]	0.001−0.01
Adsorbent	PKSAC and CAC
Mass of adsorbent, S_0 [kg]	1.0×10^{-4}
Volume of feed, L_0 [m^3]	2.5×10^{-5}
Ratio of adsorbent mass to feed solution volume, S_0/L_0 [kg m^{-3}]	4
Time [h]	120
Temperature [K]	300

4.2.3 Analyses

a) Gas chromatograph

The concentration of phenolic compounds was analyzed using gas chromatography (GC-14B with FID, Shimadzu Co., Ltd.; ULBON HR-20M column I.D. 0.00053 m×30 m). A 1.0×10^{-6} m^3 syringe (Hamilton, Reno, NV, USA) was used for all manual injections. The data were acquired and processed on a personal computer, using Shimadzu GC Solution software. The analysis was repeated three times in each sample. 1-Propanol was used as a solvent. The working conditions for GC are tabulated in **Table 4.4. Figure 4.1** shows the picture of instrument for phenolic compounds analysis.

Table 4.4 Working conditions for gas chromatograph (GC-14B, ULBON HR-20M column)

Carrier gas and pressure [kPa]	Helium, 120
Make-up gas and pressure [kPa]	Helium, 50
Detector gas and pressure [kPa]	Hydrogen, 60
FID gas and pressure [kPa]	Air, 50
Injector temperature [K]	523
Detector temperature [K]	523
Column temperature [K]	363→473
Column heating rate [K h^{-1}]	300
Split ratio (outlet : inlet column) [−]	1:50
Split flow rate [m^3 h^{-1}]	0.0025
Column flow rate [m^3 h^{-1}]	0.00042
Purge flow rate [m^3 h^{-1}]	0.00018
Range [−]	1
Injection volume [m^3]	2.0×10^{-10}

Figure 4.1 Gas chromatograph (GC-14B) for phenolic compounds analysis

b) UV-Vis spectrometer

The concentration of lignin was analyzed using UV-Vis spectrometer (UV-1280, Shimadzu) with a detecting wavelength at 202 nm. The solution was diluted before performing the analysis. The dilution ratio was varied between 1:30 and 1:150. The filtrate solution of PKSAC contacted with DI water was used as a blank for baseline correction. **Figure 4.2** shows the picture of instrument for lignin analysis.

Figure 4.2 UV-Vis spectrometer (UV-1280, Shimadzu) for lignin analysis

4.3 RESULTS AND DISCUSSION

4.3.1 Basic relationships

Material balance relationship and two equations, namely, fractional removal, and Langmuir isotherm were employed in the adsorption study. The details of the material balance relationship and equations are described below.

The material balance relationship of compound *i* in the batch equilibrium adsorption,

$$L_0C_{i,0} + S_0q_{i,0} = LC_i + Sq_i \qquad \textbf{4.1}$$

was used to calculate q_i under the assumptions of $q_{i,0} = 0$, $L = L_0$, $S = S_0$,
where L_0, L, S_0, and S denote mass of the feed aqueous solution at initial, mass of the feed aqueous solution at equilibrium, and mass of adsorbent at the initial, mass of adsorbent at equilibrium, respectively. $C_{i,0}$ and q_i are concentration of compound *i* in feed aqueous solution at initial, and adsorbed amount of compound *i* at equilibrium on PKSAC, respectively.

The fractional removal of compound *i*, $R_{i,}$, was defined as,

$$R_i = \frac{L_0C_{i,0} - LC_i}{L_0C_{i,0}} \qquad \textbf{4.2}$$

Langmuir isotherm model was employed for single solute adsorption to predict the adsorption performance of PKSAC with unfavorable compounds in model POME. Langmuir isotherm equation can be written as:

$$q_i = \frac{q_i^{*}K_{L,i}C_i}{1 + K_{L,i}C_i} \qquad \textbf{4.3}$$

where q_i^* and $K_{L,i}$ are the saturated adsorbed amount of compound *i* and Langmuir parameter, respectively.

The Langmuir isotherm model for single solute adsorption is based on the following assumptions (Choy, *et al*., 2000):

1. All sites for adsorption are equally identical on a homogeneous, and adsorbed molecules do not interact.
2. All sites for adsorption are energetically equivalent and the energy of adsorption is equal for all sites.
3. When adsorbent is in a saturated condition, only a monolayer is formed. No more layers can form above the first layer.

In the case of binary solute system, q_i was represented by the extended Langmuir isotherm model with the same assumption as for single solute adsorption. The extended Langmuir isotherm model can be expressed as:

$$q_i = \frac{q_i^* K_{L,i} C_i}{1 + \sum K_{L,i} C_i} \qquad \textbf{4.4}$$

where the q^*_{i} and $K_{\mathrm{L,i}}$ are the saturated adsorbed amount and Langmuir parameter, respectively, obtained in single solute system (Choy, *et al*., 2000). Therefore, in binary solute system, equation 4.4 written for solute 1 and 2 becomes:

$$q_{i,1} = \frac{q_{i,1}^* K_{L,1} C_{i,1}}{1 + K_{L,1} C_{i,1} + K_{L,2} C_{i,2}} \qquad \textbf{4.5}$$

$$q_{i,2} = \frac{q_{i,2}^* K_{L,2} C_{i,2}}{1 + K_{L,1} C_{i,1} + K_{L,2} C_{i,2}} \qquad \textbf{4.6}$$

where $q_{i,1}$ and $q_{i,2}$ are the adsorption amount of solute 1 and 2 at the equilibrium, respectively. The extended Langmuir equation can be used when $q_{i,1} \neq q_{i,2}$.

4.3.2 Fractional removals of unfavorable compounds in model palm oil mill effluent

Figure 4.3 show the fractional removals of phenolic compounds, R_i, with PKSACs produced from different operating conditions calculated by Eq. 4.2. The PKSACs could adsorb and remove phenolic compounds in the model POME successfully. R_i decreased with the increasing initial concentration of phenolic compounds, $C_{i,0}$. R_i was from 0.2 to higher than 0.9 at maximum in the range of this work. Adsorption of phenol by PKSACs with chemical treatment was higher than that of PKSAC without chemical treatment.

Figure 4.4 show the fractional removals of lignin, R_{Lg}, with PKSACs. The PKSACs could adsorb and remove lignin in the model POME successfully same as in the case of phenolic compounds. R_{Lg} decreased as the initial concentration of lignin, $C_{\mathrm{Lg},0}$, increased. R_{Lg} of 0.5 was the maximum obtained in the concentration range considered in this work. R_{Lg} of PKSAC without chemical treatment was almost zero. Furthermore, it can be seen that R_{Lg} by PKSACs was lower than that of phenolic compounds. The decrease in R_{Lg} could be due to the larger molecular weight of lignin. In this study, the lignin molecular weight was assumed to be 0.51 kg mol^{-1} (ChemicalBook Inc.) which was approximately five times larger than that of phenolic compounds.

The comparison of change in color intensity of lignin solution before adsorption and at equilibrium is shown in **Figure 4.5**. The color change could not be observed in this study with the small mass of PKSAC (Figure 4.5b). However, when the mass of PKSAC increased, the color intensity of lignin reduced and the solution became clear (Figure 4.5c and 4.5d). Therefore, produced PKSACs could remove lignin and be an effective adsorbent for decolorization of POME.

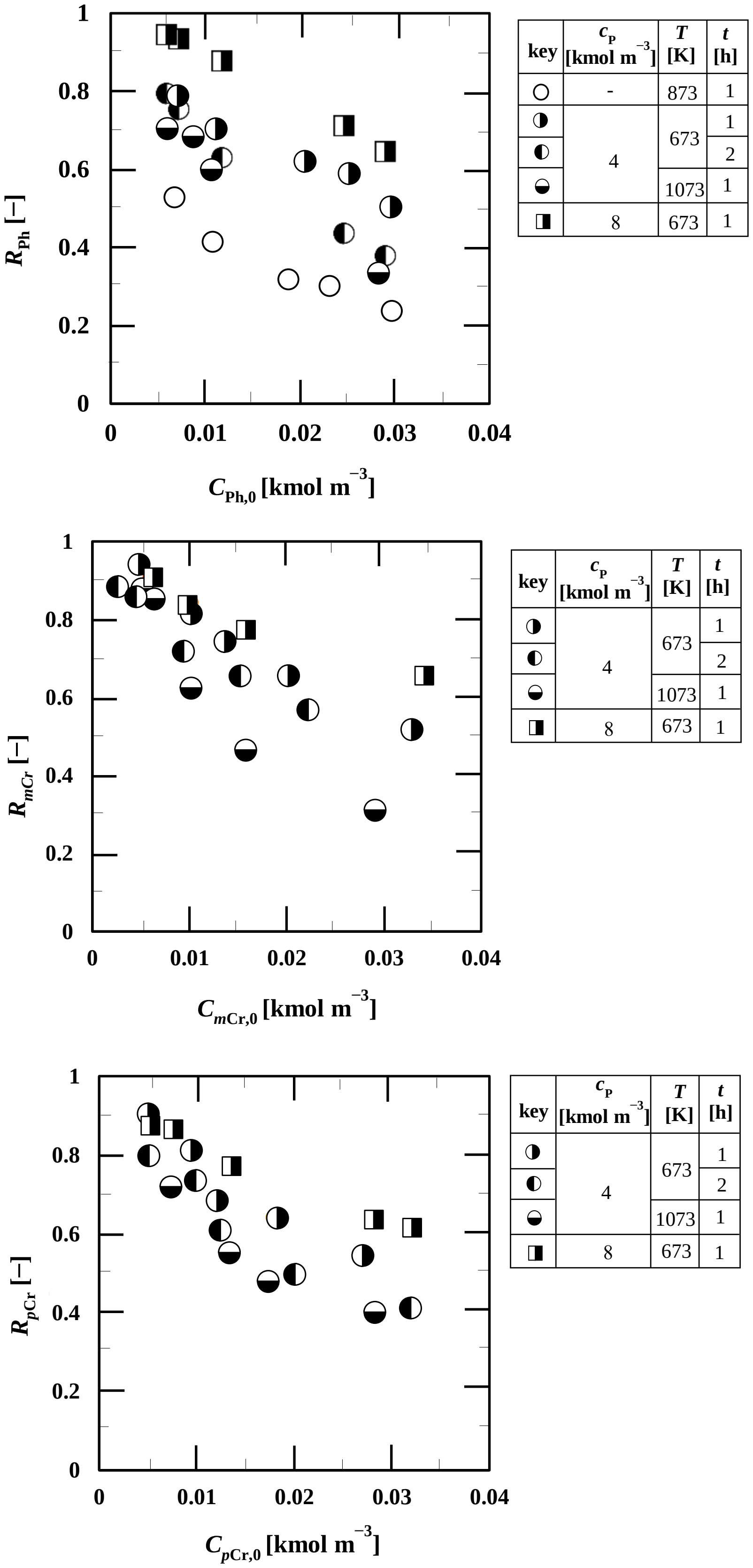

Figure 4.3 Fractional removals of phenolic compounds on palm kernel shell activated carbons

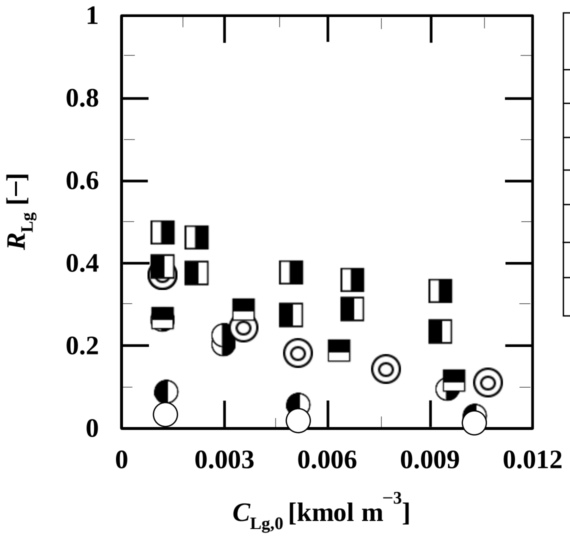

key	c_P [kmol m^{-3}]	T [K]	t [h]
○	-	873	1
◑	4	673	1
◐			2
◨	8	673	1
◧			2
⬒		1073	2
◎	commercial AC		

Figure 4.4 Fractional removals of lignin on palm kernel shell activated carbons

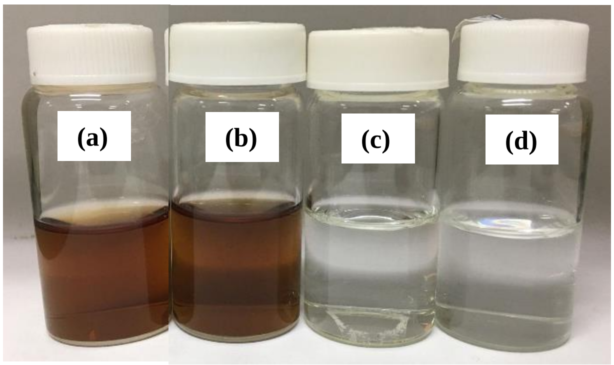

	c_P [kmol m^{-3}]	T [K]	t [h]	S_{BET} ×10^3 [m^2 kg-AC^{-1}]
b	8	673	1	1856
c				
d	8	673	2	1403

Figure 4.5 Comparison of change in color intensity (a) lignin solution before adsorption at $C_{Lg,0}$ = 0.001 kmol m^{-3}; (b) lignin solution at equilibrium with 0.0001 kg of PKSAC; (c) and (d) lignin solution at equilibrium 0.0013 kg of PKSAC

4.3.3 Adsorption isotherms of unfavorable compounds in model palm oil mill effluent

The adsorption isotherms of phenolic compounds calculated by Eq. 4.3 on PKSACs are shown in **Figure 4.6**. The adsorption of phenolic compounds with PKSACs followed the Langmuir model. The adsorbed amount of phenolic conpounds, q_i, increased with an increase in the concentration of phenolic compounds at equilibrium, C_i. The q_{Ph} of PKSACs with chemical treatment was higher than that of PKSAC without chemical treatment. q_i increased as H_3PO_4 concentration, c_P, increased or pyrolysis temperature, T, decreased.

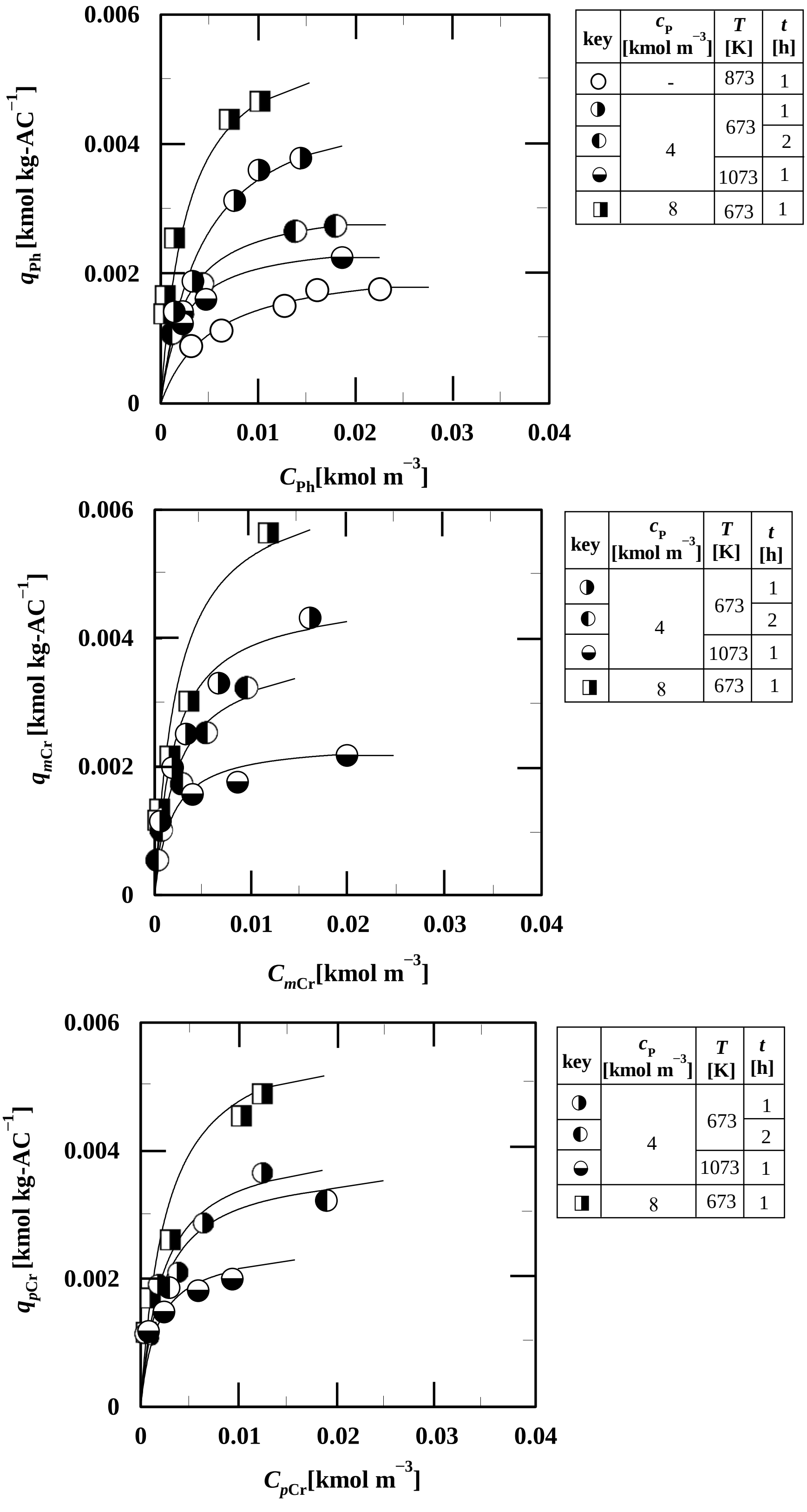

Figure 4.6 Adsorption isotherms of phenolic compounds on palm kernel shell activated carbons

The adsorption isotherms of lignin on PKSACs are shown in **Figure 4.7**. The obtained adsorbed amount of lignin, q_{Lg}, gave a good fit for the Langmuir adsorption isotherm. There was an increase in q_{Lg} as the increment of concentration of lignin in liquid at equilibrium, C_{Lg}, in the model POME.

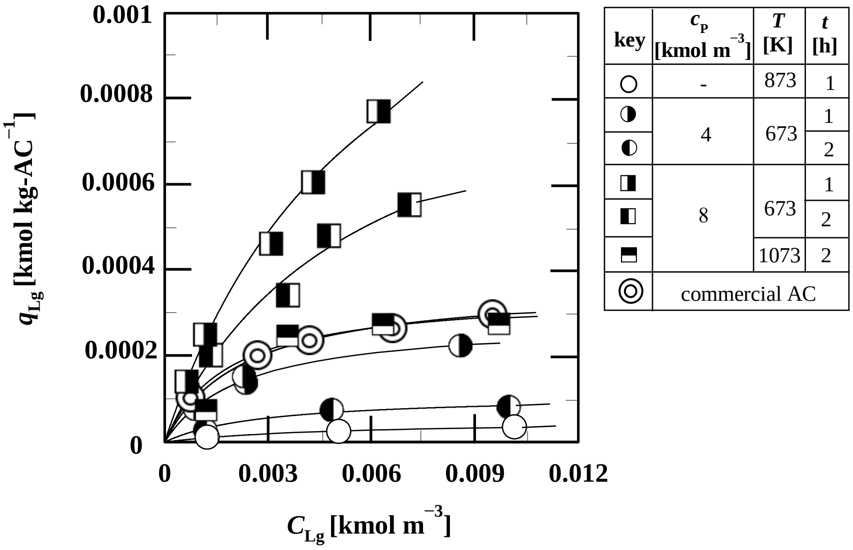

key	c_{P} [kmol m^{-3}]	T [K]	t [h]
○	-	873	1
◑	4	673	1
◐			2
◨	8	673	1
◧			2
⬒		1073	2
◎	commercial AC		

Figure 4.7 Adsorption isotherms of lignin on palm kernel shell activated carbons

Table 4.5 summarizes Langmuir parameters for adsorption isotherms of unfavorable compounds determined from Eq. 4.3. The saturated adsorbed amount, q_i*, of phenolic compounds and lignin increased as c_{p} increased but decreased as T and t increased. The chemical activation increased both q_{Ph}^* and $K_{\mathrm{L,Ph}}$. q_{Ph}^* of *m*Cr and *p*Cr was higher than that of Ph in some runs. PKSACs could adsorb lignin greater than CAC, showing that PKSAC is a feasible adsorbent in terms of the environmental and economical aspects.

Since the adsorption performance by PKSACs produced at t= 1 h showed good results, only PKSACs produced at t= 1 h were selected for adsorption in the binary solute system. **Figure 4.8** represents the adsorption isotherms of phenolic compounds in single and binary solutes systems. The PKSACs could adsorb the phenolic compounds in binary solutes system. The q_i in binary solutes system increased as c_{p} but decreased with the increment of T same as in the case of single solute system. The q_i of each phenolic compound in binary solutes system was lower than in single solute system due to the effect of co-existing solute in the system. It was assumed that phenol and cresol shared in the same adsorption site in the binary solute system as q_i^* of them were close with each other and their molecular structures were similar.

Figure 4.9 represents the comparison of adsorption amounts calculated by Eq. 4.4 and experimental results. Eq. 4.4 could roughly predicted the q_{pCr} and q_{mCr}, but $q_{\mathrm{Ph,calc}}$ was higher than $q_{\mathrm{Ph,exp}}$.

Table 4.5 Langmuir parameters for adsorption isotherms of unfavorable compounds in single solute system

Adsorbate ***i***	c_P **[kmol m^{-3}]**	***T*** **[K]**	***t*** **[h]**	**Langmuir parameters**	
				q_i^* **[kmol kg-AC^{-1}]**	$K_{L,i}$ **[m^3 kmol^{-1}]**
Ph	-	873	1	0.0022	190
Lg				0.00005	203
Ph	4	1073	1	0.0025	444
*m*Cr				0.0024	578
*p*Cr				0.0025	593
Ph	4	673	2	0.0031	398
*m*Cr				0.0038	453
*p*Cr				0.0038	435
Lg				0.0001	354
Ph	4	673	1	0.0049	235
*m*Cr				0.0047	494
*p*Cr				0.0041	447
Lg				0.0003	442
Lg	8	1073	2	0.0004	433
Lg	8	673	2	0.0010	183
Ph	8	673	1	0.0059	370
*m*Cr				0.0065	430
*p*Cr				0.0060	390
Lg				0.0015	165
Lg		CAC		0.0004	535

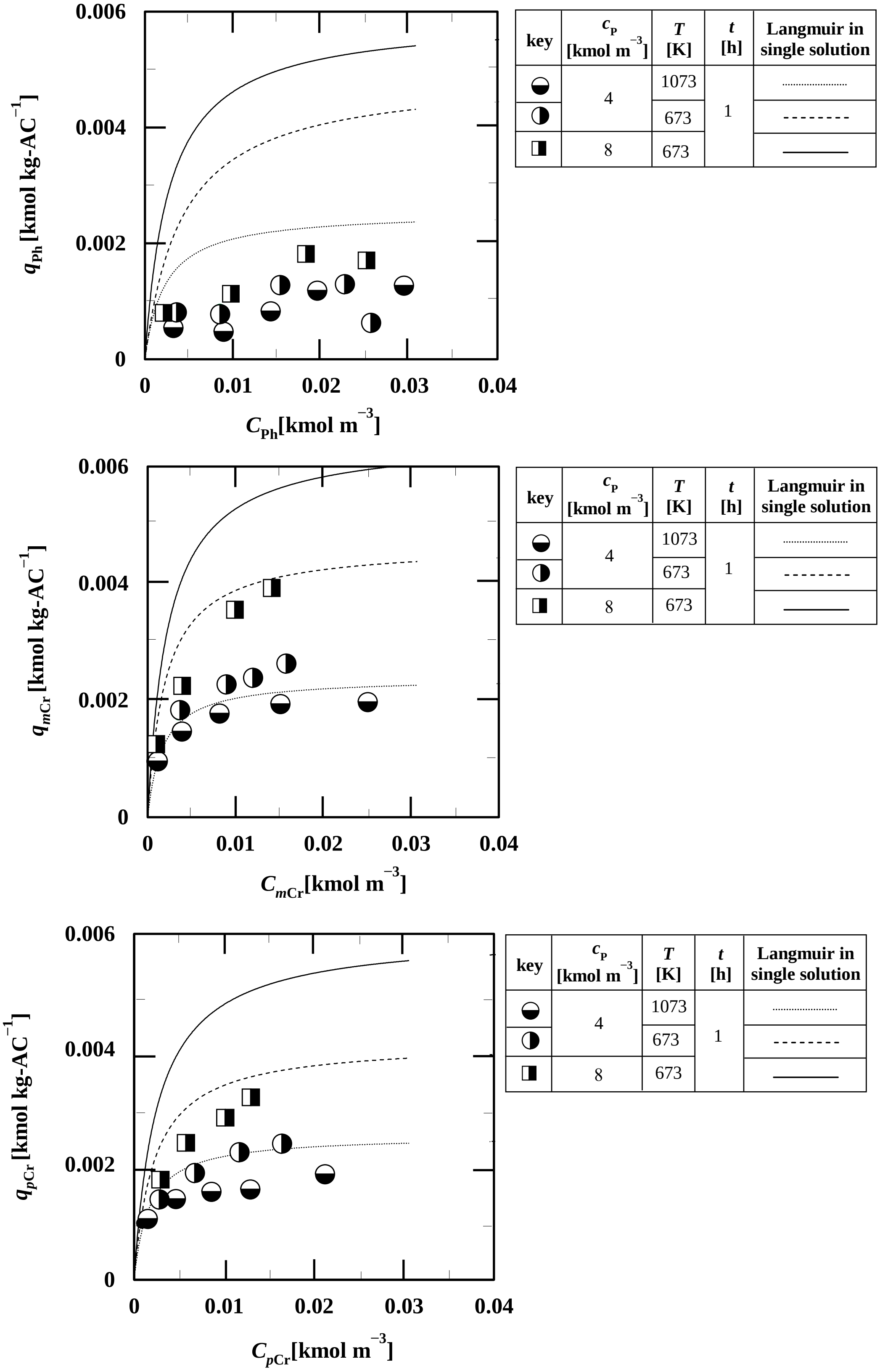

Figure 4.8 Adsorption isotherms of phenolic compounds on palm kernel shell activated carbons in single and binary solute system

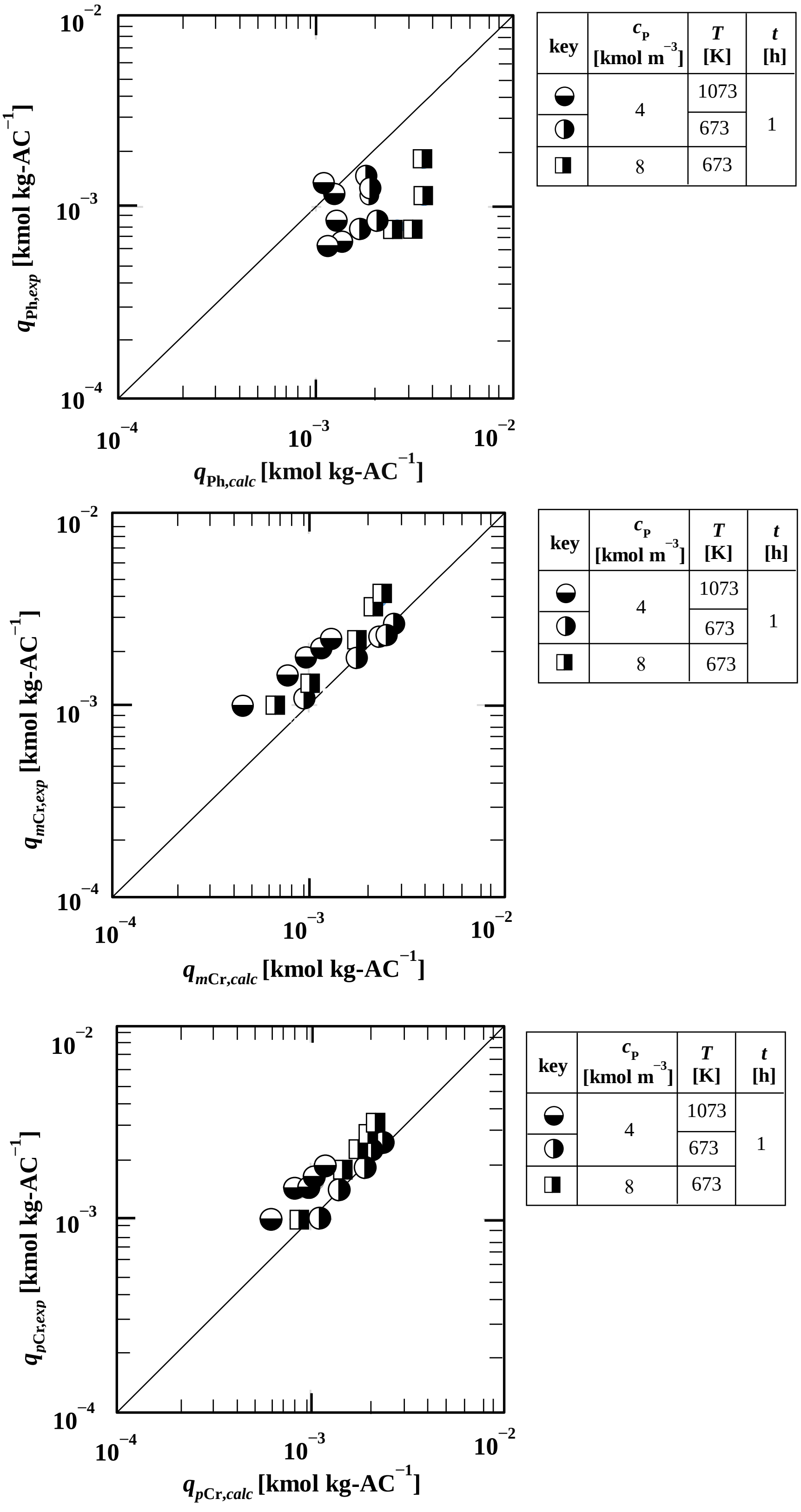

Figure 4.9 Comparison of adsorption amounts calculated and experimental results by extended Langmuir isotherm model

A comparison of phenol adsorption performance of activated carbon produced from different raw materials with orthophosphoric acid activation is shown in **Table 4.6**. The adsorption performance of phenol by PKSAC was higher than other prepared AC due to the higher in S_{BET}. The pyrolysis temperature and time used in this study were also lower and shorter than other AC listed in Table 4.6.

Table 4.7 compares lignin adsorption performance of different adsorbents. Lignin removal by adsorption is still rarely reported in the previous literatures. Table 4.7 indicates that different types of adsorbents could be used for lignin adsorption and the adsorption performance of lignin depended on the S_{BET}. As this study could produce a relatively high S_{BET} compared to other adsorbents, the adsorption performance of lignin by PKSAC was highest.

Table 4.6 Comparison of phenol adsorption performance of activated carbon produced from different raw materials with orthophosphoric acid activation

Raw material	T **[K]**	t **[h]**	$S_{\mathrm{BET}}\times10^3$ **[$\mathrm{m^2\ kg\text{-}AC^{-1}}$]**	q_i^* **[kmol kg-AC^{-1}]**	**Ref.**
Olive stone	680	2.5	1040	0.000625	Bohli *et al.*, 2013
Apricot stone	673	-	1370	0.0013	Daifullah *et al.*, 1994
Eucalyptus	698	2	1460	0.0024	Gonzalez-Serrano *et al.*, 2004
Kraft lignin	773	2	940	0.0011	Fierro *et al.*, 2004
Coffee ground	873	45 mins	640	0.00003	Namane *et al.*, 2005
Commercial AC		-	950	0.00004	
palm kernel shell	673	1	1856	0.0059	This study

Table 4.7 Comparison of lignin adsorption performance of different adsorbents

Adsorbent	$S_{\mathrm{BET}}\times10^3$ **[$\mathrm{m^2\ kg\text{-}AC^{-1}}$]**	q_i^* **[kmol kg-AC^{-1}]**	**Ref.**
Fly ash	28.6	0.00002	Andersson *et al.*, 2011
Activated charcoal	840	0.0005	
Commercial AC	992	0.0004	This study
PKSAC	1856	0.0015	This study

4.3.4 Correlation of adsorption performance with palm kernel shell properties

Figure 4.10 shows the relationship between q_i^* and S_{BET}. The q_i^* showed a good correlation with S_{BET}. The q_i^* increased with the increase in S_{BET}, thereby indicating the critical role played by S_{BET} in phenolic compounds and lignin adsorption. q_{Lg}^* increased steeply due to the effect of molecular size distribution of lignin. Lignin is a heterogeneous molecule and has wide molecular size distribution (Mazar *et al.*, 2021: Oasmaa *et al.*, 2003). Hence the higher the S_{BET}, the more the lignin molecule could be adsorbed. As mentioned in chapter 3, the chemical activation by H_3PO_4 effectively increased the S_{BET} of the PKSAC even at a relatively low pyrolysis temperature and short pyrolysis time. These resulted in the effective removal of phenolic compounds and lignin from the POME. Even though several chemical functional groups on PKSAC surface were found, the effect of these chemical functional groups toward the adsorption was still unclear in this study.

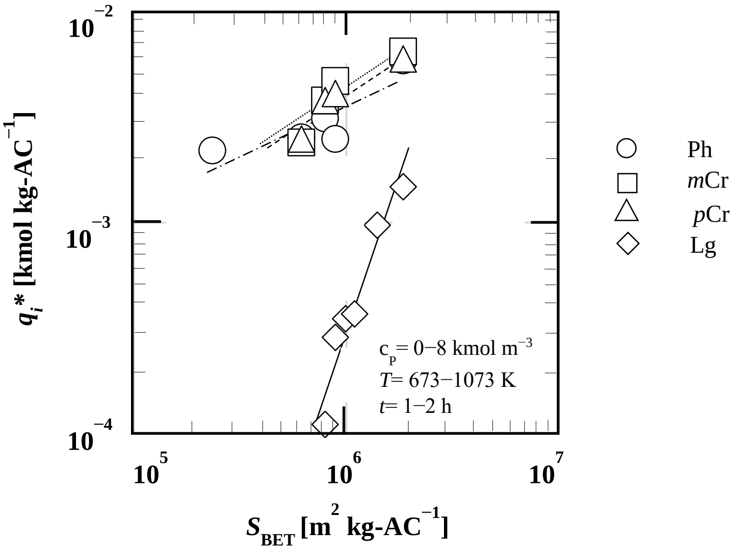

Figure 4.10 Saturated adsorption amounts of unfavorable compounds against specific surface area of palm kernel shell activated carbons

4.4 CONCLUSIONS

Palm kernel shell activated carbons produced from various operating conditions could successfully adsorb and remove unfavorable compounds, namely, phenolic compounds and lignin in model palm oil mill effluent. The adsorption of phenolic compounds and lignin followed Langmuir model. The adsorption performance of phenolic compounds was higher than lignin. Produced palm kernel shell activated carbons showed better adsorption performance than commercial activated carbon and could decolorize lignin in some runs. The saturated adsorbed amount of unfavorable compounds increased as orthophosphoric acid concentration increased but decreased as pyrolysis temperature and time increased. The specific surface area of palm kernel shell activated carbon was found to significantly affect the phenolic compounds and lignin adsorption performance.

CHAPTER 5

APPLICATION OF EFFLUENT TREATMENT USING PALM KERNEL SHELL ACTIVATED CARBON IN PALM OIL MILL PROCESS

5.1 INTRODUCTION

The objective of this chapter is to apply the effluent treatment using palm kernel shell activated carbon into the current palm oil mill process in Thailand by introducing proposed process. Firstly, the proposed process was designed suitably and introduced into the current process to make the proposed process become reliable and practicable as possible. Following this, the material and energy balances in the proposed process were calculated based on the experimental results obtained from chapter 3 and 4 and discussed accordingly. Subsequently, the feasibility of using palm kernel shell activated carbon and other products from pyrolysis in the proposed process was investigated and discussed in detail.

5.2 OUTLINE OF PROPOSED PROCESS

The diagram of the proposed process for application in Thailand’s palm oil mill industry is shown in **Figure 5.1**. The proposed process is an additional process that aims to apply the effluent treatment using palm kernel shell activated carbon. The PKS obtained from palm oil production process is chemically treated with orthophosphoric acid in the chemical treatment operation. Then, PKS with chemical treatment is heated by pyrolysis operation to obtain PKSAC, off-gas, and condensable liquid. PKSAC is used as the adsorbent to treat unfavorable compounds in POME treatment. Off-gas is used as an energy source for additional operations in the palm oil mill process and condensable liquid could be used as a raw materials for other chemical processes.

5.3 CALCULATION

The systems are assumed at steady-state, that is, that all properties of the system are invariant with time. Therefore, the rate of mass transfer (energy transfer) into the system must equal to the rate of mass transfer (energy transfer) out of the system.

The symbols used in the proposed process are defined as follows:

Material or energy flow rate, *F* or *E*
$F_{k,j}$: Flow of material *k* from process *j* [kg]
$F_{k,s}$: Flow of material *k* from operation *s* [kg]
$E_{r,s}$: The energy recovery *r* from operation *s* [kJ]

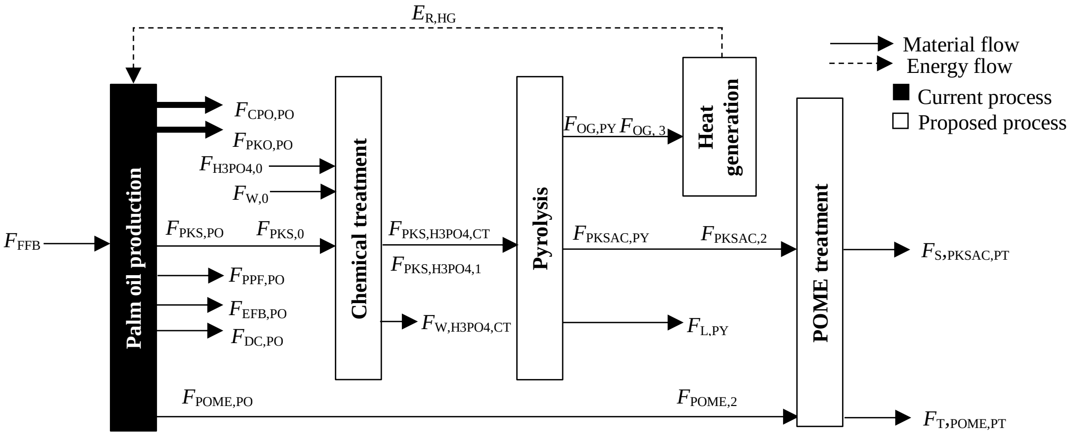

Figure 5.1 Proposed process for application in palm oil mill process

Material, *k*

FFB: fresh fruit brunch, CPO: crude palm oil, PKO: palm kernel oil, PKS: palm kernel shell, PPF: palm press fiber, EFB: empty fruit brunch, DC: decanter cake, POME: palm oil mil effluent, H_3PO_4: orthophosphoric acid, W: water, PKS,H_3PO_4: PKS with chemical treatment, W, H_3PO_4: residue of H_3PO_4 solution, PKSAC: palm kernel shell activated carbon, OG: off-gas, L: condensable liquid, S,PKSAC: Spent PKSAC, T,POME: treated POME

Process, *j*

PO: palm oil production

Operation, *s*

CT: chemical treatment, PY: pyrolysis, PT: palm oil mill effluent treatment, HG: heat generation. Besides those, the numbering was given for the proposed process as below:

0: inlet of chemical treatment

1: inlet of pyrolysis

2: inlet of palm oil mill effluent treatment

3: inlet of heat generation

Energy, *r*

R: Energy recovery

The details of material feeds, products and calculations in each operation are described below.

Chemical treatment

$F_{PKS,0}=0.015\times F_{PKS,PO}$

$F_{PKS,H3PO4,CT}=0.15(F_{H3PO4,0}+F_{W,0}+F_{PKS,0})$

The chemical treatment operation consists of chemical treatment of PKS, filtration, and drying. In this operation, 4 and 8 kmol m^{-3} of orthophosphoric acid, water, and PKS are used. The amount of PKS was fixed. According to the material balance shows in Figure 1.9, POME, and PKS are generated 0.34 kg, and 0.06 kg from 1 kg of fresh fruit bunch, respectively. However, the palm oil mill is unable to use all of the generated PKS for the pyrolysis. It is estimated that 0.50 of the PKS is consumed by palm oil mill boilers as its primary fuel, and 0.25 of the PKS by other industries (Dit, 2007). Therefore, this study assumed that 0.25 of the PKS or 0.015 kg is available for the chemical treatment operation. The amount of PKS with chemical treatment was calculated based on experimental results and it was 0.15 of the amount of feed materials for chemical treatment.

Pyrolysis

$F_{PKS,H3PO4,CT}= F_{PKS,H3PO4,1}$
$F_{PKSAC,PY}= F_{PKS,H3PO4,1}\times Y_{PKSAC}$

$F_{L,PY} = F_{PKS,H3PO4,1}\times Y_{L}$

$F_{OG,PY} = F_{PKS,H3PO4,1}\times Y_{OG}$

The PKS with chemical treatment obtained from chemical treatment operation is then pyrolyzed under various pyrolysis temperatures and pyrolysis time 1 hour. The amount of nitrogen gas is neglected because nitrogen gas is an inert gas. Y_{PKSAC}, $Y_{OG,}$ and Y_{L} were the yield of products based on experimental results from chapter 3.

The required energy for pyrolysis (Q) was calculated from the difference in feed (PKS with chemical treatment) and products (PKSAC, off-gas, and condensable liquid) enthalpy as shown in equation 5.1 and 5.2.

$$Q = \Delta H_{f,products} - \Delta H_{f,feed} \qquad \textbf{5.1}$$

$$= \left(M_{PKSAC}\Delta H_{f,PKSAC} + M_{OG}\Delta H_{f,OG} + M_{L}\Delta H_{f,L}\right) - \left(M_{PKS,H3PO4}\Delta H_{f,PKS,H3PO4}\right)$$
$$+\int_{298}^{T_{out}} (M_{PKSAC}C_{p,PSKAC} + M_{OG}C_{p,OG} + M_{L}C_{p,L})dT - \int_{298}^{T_{in}} (M_{PKS,H3PO4}C_{p,PKS,H3PO4})dT \qquad \textbf{5.2}$$

where Q, $\Delta H_{f,\mathrm{feed}}$, $\Delta H_{f,\mathrm{products}}$, M, and C_p denote the total required energy, enthalpy formation of feed, enthalpy formation of product, mass of feed or product, and heat capacity of feed or product, respectively. The enthalpy of formation and heat capacity of all corresponding substances are summarized in **Table 5.1** and **5.2**. The standard heat capacity was employed in this study.

Table 5.1 Standard enthalpy of formation of substances at 298.15 K (Othaman *et al.*, 2008)

Substances (phase)	**Heat capacity [kJ kg^{-1}K^{-1}]**	**Enthalpy of formation [kJ kg^{-1}]**
Methanol (g)	1.38	-6262.8
Acetic Acid (g)	1.11	-7198.2
Acetone (g)	1.29	-3753.4
Phenol (g)	1.10 [300 K] 2.26 [800 K]	-1495.4
Cellulose (s)	1.00 − 1.21	-5915.4
Orthophosphoric acid (s)	1.48	-13106.7

Table 5.2 Standard enthalpy of formation of the gas components and carbon at various pyrolysis temperatures (Othaman *et al.*, 2008)

Substances (phase)	**Enthalpy of formation [kJ kg^{-1}] at**		
	673 [K]	873 [K]	1073 [K]
H_2 (g)	5432.19	8367.98	11357.2
CO (g)	-3546.28	-3319.98	-3084.35
CH_4 (g)	-3597.45	-2831.58	-1952.06
CO_2 (g)	-8568.38	-8337.31	-8092.37
H_2O (g)	-12690.8	-12264.5	-11810.2
C (s)	434.8603	757.8915	1113.525

Palm oil mill effluent treatment

$F_{\mathrm{PKSAC,PY}}=F_{\mathrm{PKSAC,2}}$

$F_{\mathrm{POME,PO}}=F_{\mathrm{POME,2}}$

$F_{\mathrm{PKSAC,2}}= F_{\mathrm{S,PKSAC,PT}}$

$F_{\mathrm{POME,2}}= F_{\mathrm{T,POME,PT}}$

POME is treated with PKSAC. The amount of POME in this operation was taken from the amount of POME reported by previous study. This operation assumed that the amount of POME and PKSAC at output was unchanged with the input, and there was no energy change of the output and the input.

Heat generation

$F_{OG,PY}=F_{OG,3}$

Off-gas from pyrolysis is used as an energy source for additional operation in palm oil mill process. The amount of off-gas was coming from pyrolysis at respective pyrolysis temperature. The energy recovery from off-gas was calculated based on the total heating value of flammable gas.

The summary of the calculation for each operation in proposed process is shown in **Figure 5.2**.

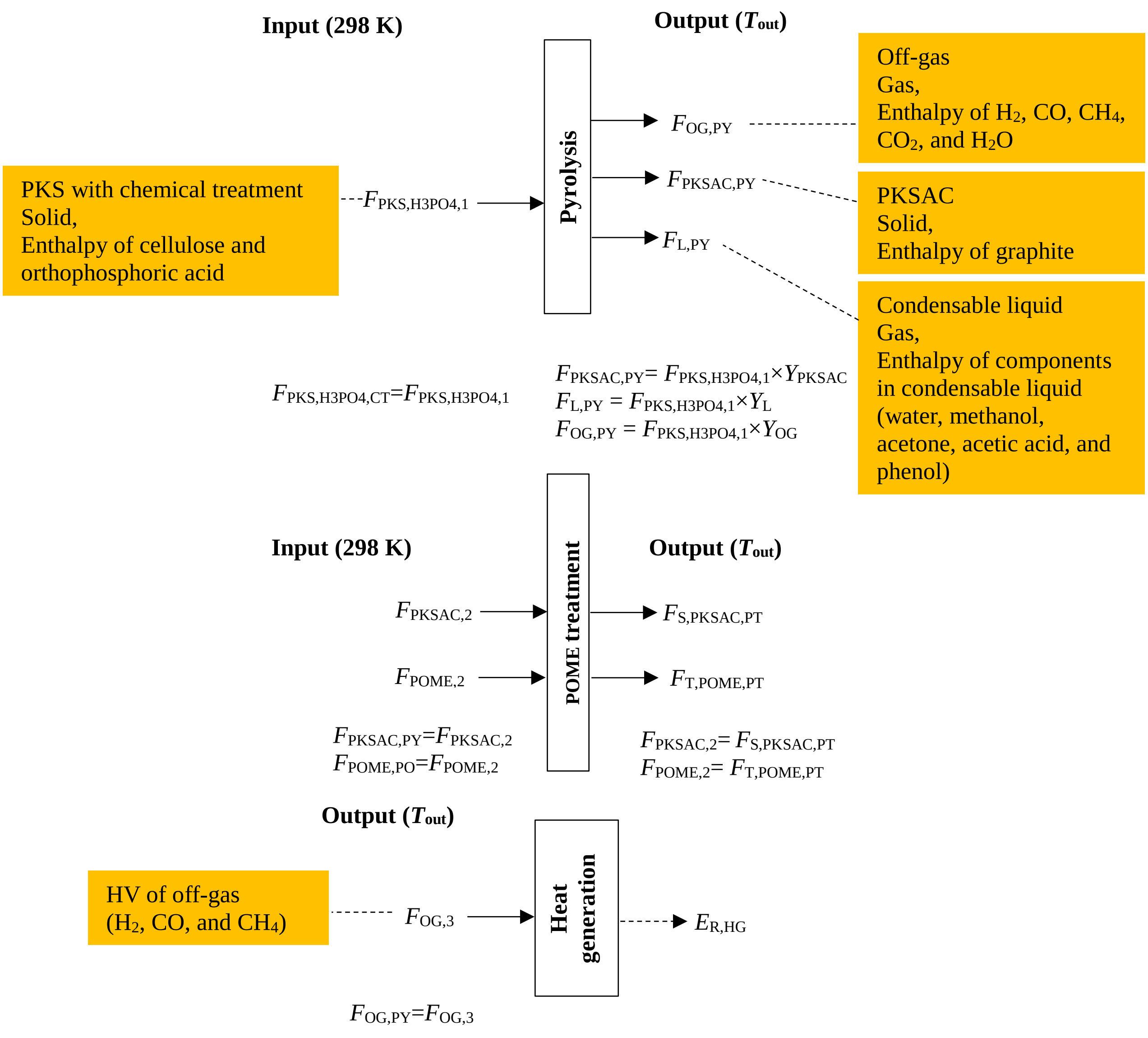

Figure 5.2 Calculation for each operation in proposed process

5.4 RESULTS AND DISCUSSION

5.4.1 Material balances of unfavorable compounds in palm oil mill effluent

The material balances of unfavorable compounds in palm oil mill effluent was estimated from the comparison between the capacity of PKSAC to adsorb unfavorable compounds $((F_{\mathrm{PKS,H3PO4,1}}Y_{\mathrm{PKSAC}}q_i^*)/F_{\mathrm{FFB}})$ and the generated amount of unfavorable compounds in POME $((F_{\mathrm{POME,2}}/\rho_{\mathrm{POME}})C_{i,\mathrm{POME}})/F_{\mathrm{FFB}})$. The concentrations of unfavorable compounds in POME, $C_{i,\mathrm{POME}}$, were taken from POME characteristic reported by previous literatures (Mohammed and Chong, 2014: Neoh *et al.,* 2013: Khongkhaem *et al.,*2016). The saturated adsorbed amounts of unfavorable compounds, q_i^*, were obtained from chapter 4 and the density of POME (ρ_{POME}) was assumed to be same as that of water (10^3 kg m^{-3}). The diagonal line means that the capacity of PKSAC to adsorb unfavorable compounds is equal to the generated amount of unfavorable compounds in POME. **Figure 5.3** shows the comparision between the capacity of PKSAC to adsorb unfavorable compounds and the generated amount of unfavorable compounds in POME. The result clearly indicated that the capacity of PKSAC to adsorb unfavorable compounds in POME was higher than the amount of unfavorable compounds discharged in POME. Consequently, the amount of PKSAC was enough to remove unfavorable compounds in POME and the treatment of POME with produced PKSAC would be a feasible method. Although the color change in the lignin adsorption study could not be clearly observed, the treated POME should be discharged into environmental water to dilute after treatment. Therefore, it is unnecessary to completely remove colored material in POME. The study and result presented here was simple. For a future study, the actual concentration of the unfavorable compounds in palm oil mill effluent and the kinetic study should be taken into account.

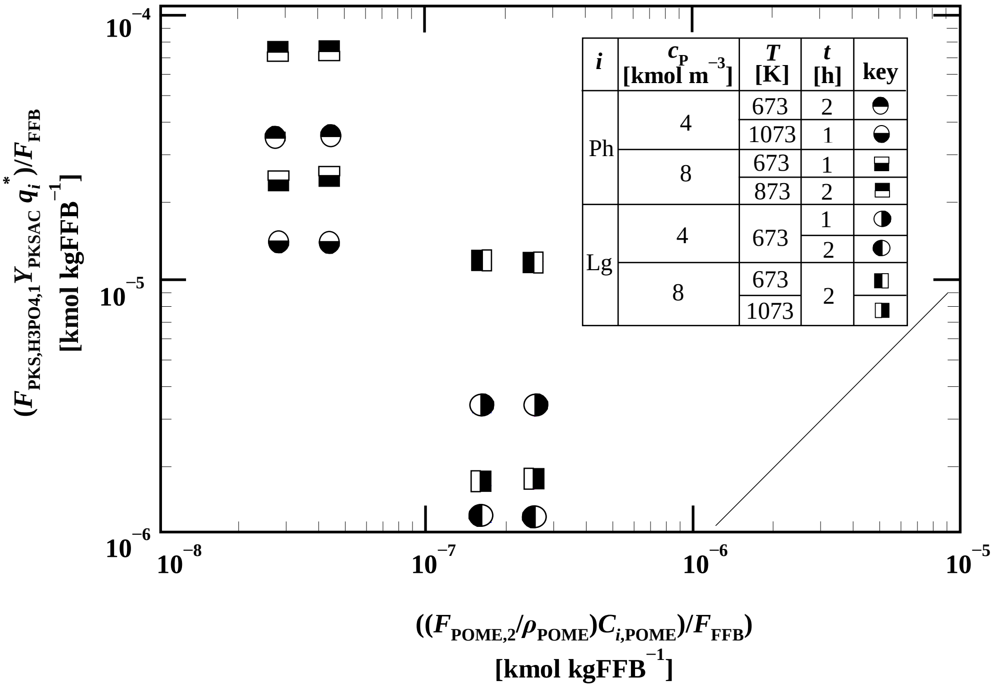

Figure 5.3 Relationship between capacity of palm kernel shell activated carbon and generated amount of unfavorable compound in palm oil mill effluent

5.4.2 Utilization of other products from pyrolysis than activated carbon

a) Utilization of off-gas

The energy balances from pyrolysis in the proposed process are shown in **Figure 5.4**. The enthalpy of feeds was almost constant over studied pyrolysis temperature range. The required energy for the pyrolysis decreased with the pyrolysis temperature increase, while the energy recovery from off-gas increased. As proposed in the proposed process, the energy recovered from off-gas is to be used to recover the required energy for the pyrolysis. If energy recovery from off-gas was higher than the required energy, then the off-gas could fully recover the required energy. The proposed process could be run at pyrolysis temperature in the range of 673−873 K. Although the energy recovery from off-gas was lower than the required energy in some runs, the additional choice to obtain more energy is to burn the spent PKSAC and utilize the off-gas from burning. At high pyrolysis temperature (*T*= 1073 K), the energy recovery from off-gas was much higher than the required energy. Therefore, the off-gas needs to be discharged. The study did not consider the quality of energy. For future study, the quality of energy should be taken into account to make the research become more practical.

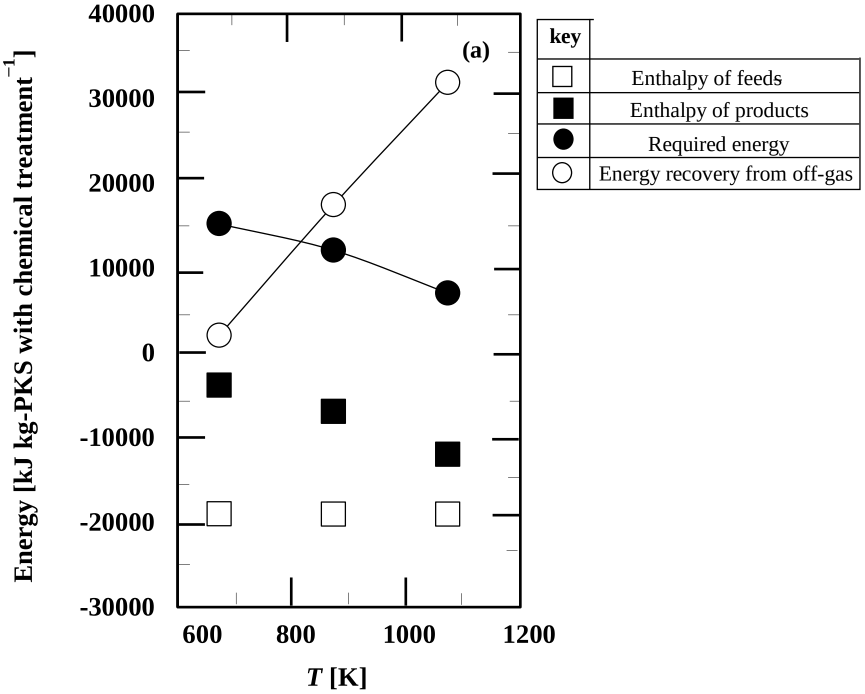

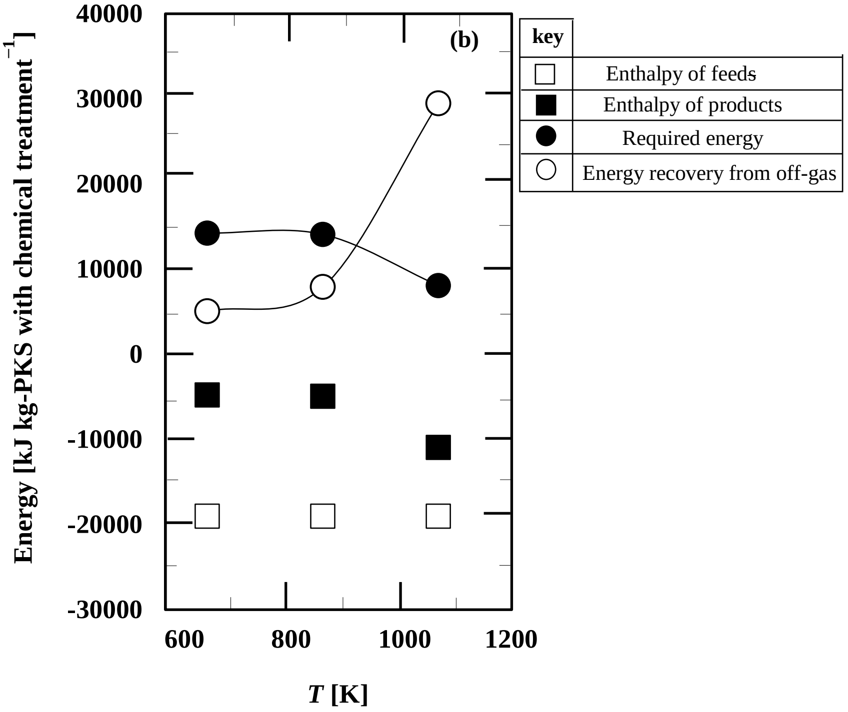

Figure 5.4 Energy balances from pyrolysis the proposed process (a) c_P= 4 kmol m^{-3} (b) c_P= 8 kmol m^{-3} at *t*= 1 h

b) Utilization of condensable liquid

Table 5.3 lists the properties of chemical components in the condensable liquid and their utilization (Engineeringtoolbox). As mentioned in chapter 3, the condensable liquid from pyrolysis of PKS with chemical treatment contained some chemical components such as acetic acid and methanol which can be further utilized. Table 5.3 shows that the chemical components in condensable liquid could be raw materials for other industries such as chemical and food industries. To evaluate the feasibility of using condensable liquid in the proposed process, the effective separation method under the consideration of cost and feasibility still needs to be studied.

Table 5.3 Properties of chemicals in condensable liquid and their utilization

Component	Chemical formula	Heat of combustion [kJ kg^{-1}]	Utilization
Methanol	CH_3OH	22650	-precursor to other commodity chemicals (formaldehyde, acetic acid)
Acetic acid	$C_2H_4O_2$	14550	-precursor to chemical compounds production -food additive (vinegar)
Phenol	C_6H_6O	32450	-precursors for plastics - antiseptic
Acetone	C_3H_6O	30810	- solvent for plastics and synthetic fibers

5.5 CONCLUSIONS

The outline of the proposed process for applying the effluent treatment using palm kernel shell activated carbon into the current palm oil mill process in Thailand was introduced. The proposed process consists of four new operations: chemical treatment, pyrolysis, palm oil mill effluent treatment, and heat generation. The products obtained from pyrolysis could be applied in the process by three ways. Palm kernel shell activated carbon could be used as an adsorbent to treat unfavorable compounds in palm oil mill effluent treatment. Off-gas could be used as an energy source for additional operations in the current process. The chemical compounds contained in the condensable liquid might be utilized as raw materials for other chemical processes. Based on the process feasibility study, palm kernel shell activated carbon was an effective adsorbent to remove the unfavorable compounds in palm oil mill effluent treatment and the amount of palm kernel shell activated carbon was sufficient. The off-gas could be used for heat generation. Chemical components contained in condensable liquid could be raw materials for other industries.

CHAPTER 6

GENERAL CONCLUSIONS

The palm oil mill industry is one of the major agro-industries in Thailand. Thailand is currently the world's third-largest palm oil producer. The industry has been growing rapidly together with the concern of environmental issues from the liquid waste generated from palm oil production. The main objective of this thesis is to treat the effluent by adsorption using activated carbon produced from palm kernel shell in palm oil mill process in Thailand.

Firstly, palm kernel shell from Thailand was characterized by proximate, ultimate, and thermogravimetric analyses. The high carbon and low ash contents in palm kernel shell indicated that palm kernel shell is a favorable precursor to prepare palm kernel shell activated carbon. The pyrolysis of palm kernel shell should be done at temperature above 500 K. The presence of chemical activating reagent, orthophosphoric acid, could hinder thermal decomposition in palm kernel shell in the high temperature, indicating the potential to produce a high yield of palm kernel shell activated carbon.

Secondly, the palm kernel shell which was chemically treated with orthophosphoric acid was pyrolyzed to produce palm kernel shell activated carbon and other products (off-gas and condensable liquid). The presence of orthophosphoric acid in palm kernel shell could improve yield of palm kernel shell activated carbon. The effect of pyrolysis temperature significantly affected yield of palm kernel shell activated carbon whereas the effects of orthophosphoric acid concentration and pyrolysis time were insignificant. The pyrolysis temperature also showed the effect on yield of other products. Produced palm kernel shell activated carbon had a relatively high micropore volume and specific surface area which were suitable to be used as an adsorbent. The surface functional groups of palm kernel shell activated carbon also changed by chemical treatment. The off-gas contained flammable and non-flammable gases and one hour of pyrolysis time was sufficient to obtain almost all of the off-gas. The condensable liquid contained chemical components such as acetic acid and methanol. The carbon content mainly remained in PKSAC while the oxygen content remained in off-gas and condensable liquid.

Then, the produced palm kernel shell activated carbons were applied for the adsorption of unfavorable compounds in model palm oil mill effluent. Palm kernel shell activated carbons produced from various operating conditions could successfully adsorb and remove unfavorable compounds, namely, phenolic compounds and lignin in model palm oil mill effluent. The adsorption of phenolic compounds and lignin followed Langmuir model. The adsorption performance of phenolic compounds was higher than lignin. Produced palm kernel shell activated carbons showed better adsorption performance than commercial activated carbon and could decolorize lignin in some runs. The saturated adsorbed amount of unfavorable compounds increased as orthophosphoric acid concentration increased but decreased as pyrolysis temperature and time increased. The specific surface area of palm kernel shell activated carbon was found to significantly affect the phenolic compounds and lignin adsorption performance.

Lastly, the outline of the proposed process for applying the effluent treatment using palm kernel shell activated carbon into the current palm oil mill process in Thailand was introduced. The proposed process consists of four new operations: chemical treatment, pyrolysis, palm oil mill effluent treatment, and heat generation. The products obtained from pyrolysis could be applied in the process by three ways. Palm kernel shell activated carbon could be used as an adsorbent to treat unfavorable compounds in palm oil mill effluent treatment. Off-gas could be used as an energy source for additional operations in the current process. The chemical compounds contained in the condensable liquid might be utilized as raw materials for other chemical processes. Based on the process feasibility study, palm kernel shell activated carbon was an effective adsorbent to remove the unfavorable compounds in palm oil mill effluent treatment and the amount of palm kernel shell activated carbon was sufficient. The off-gas could be used for heat generation. Chemical components contained in condensable liquid could be raw materials for other industries.

Based on the above findings, palm oil mill effluent treatment using palm kernel shell activated carbon was proposed for the application in Thailand’s palm oil mill process.

APPENDIX

A.1 CALIBRATION IN GAS CHROMATOGRAPHY

phenol

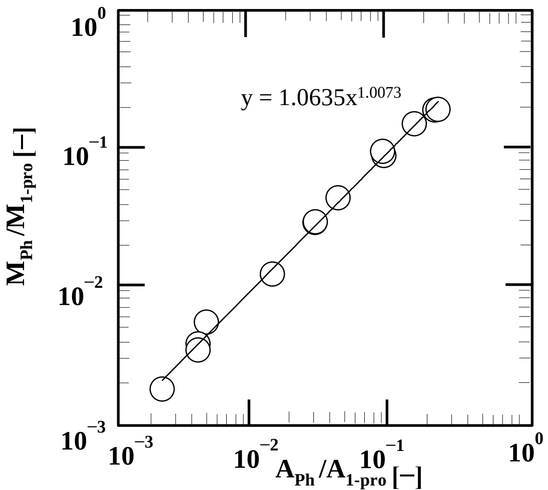

***m*-cresol**

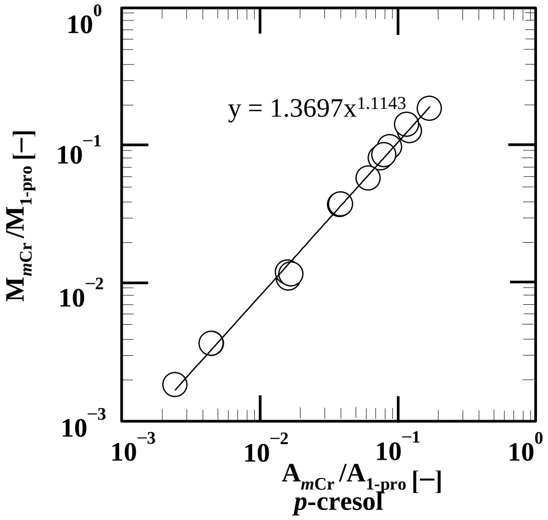

***p*-cresol**

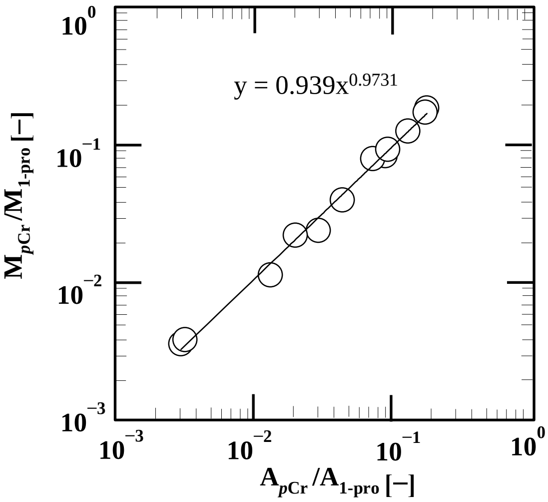

Figure A1 Calibration curves of phenolic compounds

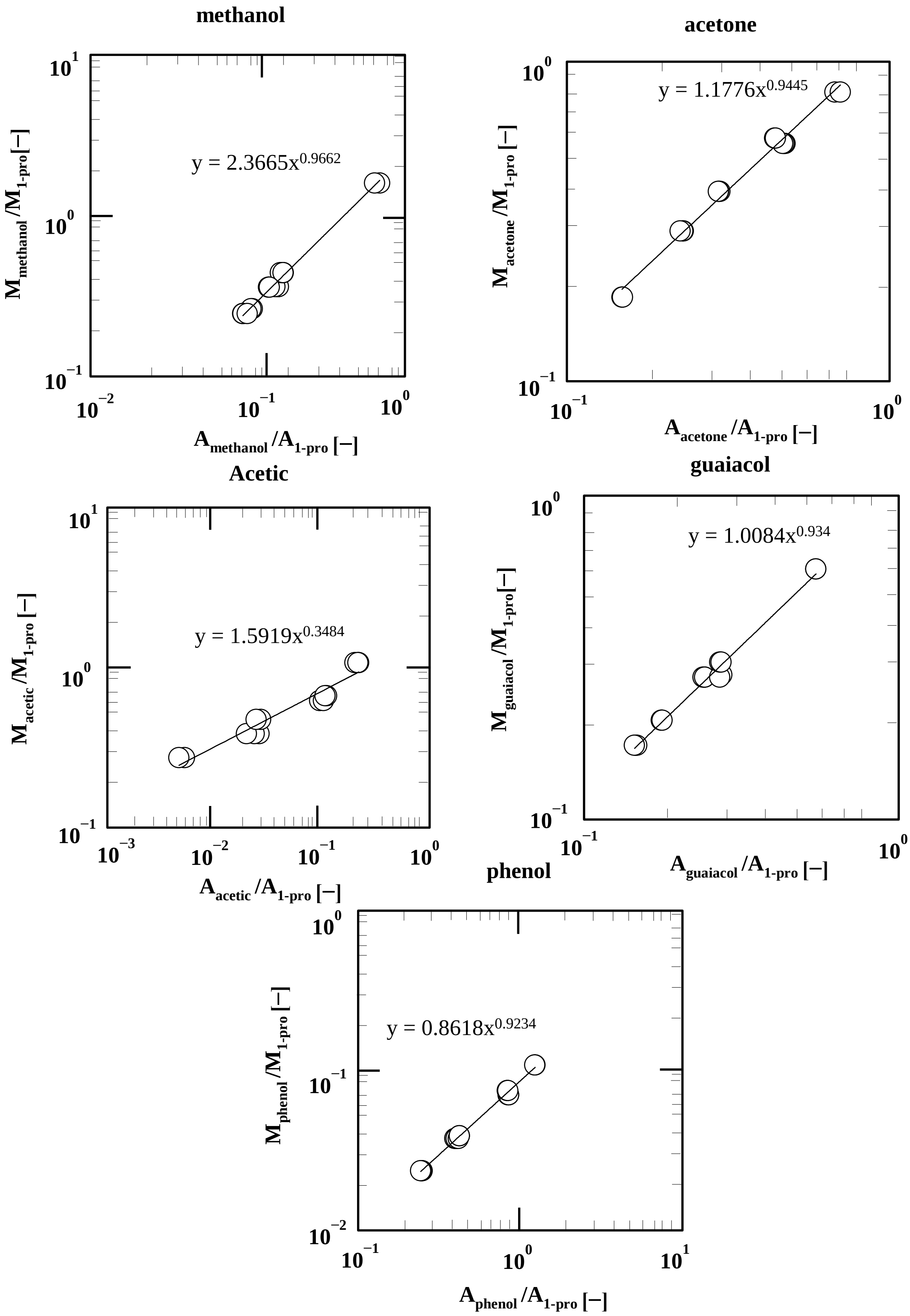

Figure A2 Calibration curves of chemical components in condensable liquid from pyrolysis

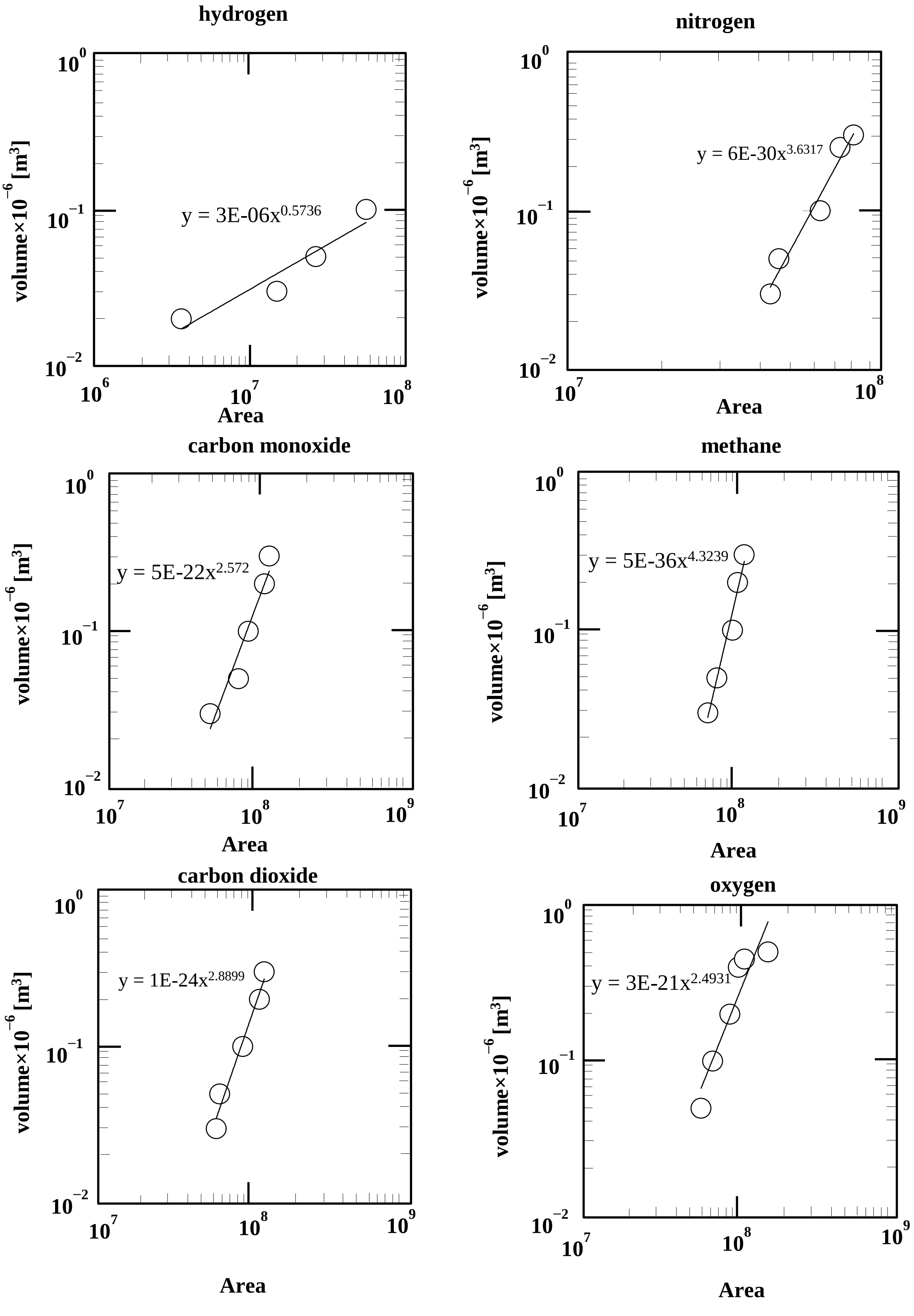

Figure A3 Calibration curves of gaseous products from pyrolysis

A.2 ESTIMATION OF COMPOSITION IN GASEOUS PRODUCT FROM PALM KERNEL SHELL PYROLYSIS

Mass faction of component in off-gas was calculated from chromatogram. In order to calculate the mass of off-gas, amount in mol was calculated using below equation as N_2 gas was used as tracer:

$$f_i = f_{N_2} \times x_i \div (x_{N_2} - \frac{0.79}{0.21} x_{O_2}) \qquad \text{(A2-1)}$$

where f_i and f_{N_2} are volume flow rates of component *i* and N_2 gas (0.009 m^3 h^{-1}), respectively. x_i, x_{N2} and x_{O2} is the mass fraction of component *i* , N_2, and O_2 in off-gas as calculated from the chromatogram, respectively.

Volume flow rate was deduced to mole flow rate in mol h^{-1}, f_i' , by,

$$f_i' = f_i \times (\frac{273.15}{0.0024 \times 299.15}) \qquad \text{(A2-2)}$$

In eq. A2-2, the value of 299.15 K is the room temperature, thus $\frac{0.0224 \times 299.15}{273.15}$ m^3 h^{-1} was based on the amount of N_2 in 1 mol ideal gas at room temperature.

The mass fraction of steam could not be measured by chromatograph, so it was calculated by the saturated vapor pressure at output pyrolysis temperature from the following equation,

$$x_{H_2O} = \frac{P_{H_2O}}{P_{all}} \qquad \text{(A2-3)}$$

where x_{H_2O} is the mass fraction of steam and P_{H_2O} is the vapor pressure at 296 K from the vapor pressure of all components, P_{all} , in Pa. The mol flow rate of steam was also calculated by eq. A2-1 and A2-2.

The total mol of off-gas could be determined from summation of mol of components in off-gas. The mol of each component was calculated by integrating the flow rate of each component in off-gas with time to obtain the off-gas,

$$M_i = \sum (\frac{f'_{i,n} + f'_{i,n+1}}{2}) \times (t_{n+1} - t_n) \qquad \text{(A2-4)}$$

where M_i is the mol of component *i* in off-gas, $f'_{i,n}$ is the mol flow rate of nth order of component *i* in off gas in mol h^{-1}, and t_n is the time at nth order in h.

ACKNOWLEDGEMENTS

First of all, I would like to express my appreciation and gratitude toward my PhD supervisor, Associate Prof. Egashira Ryuichi, for his tremendous support, guidance, suggestion, and providing me the opportunity to do research in his laboratory. Great thanks are also extended to Asst. Prof. Habaki Hiroaki for his support and supervision. Without them, it is impossible to finish this work.

I am very thankful to my committee members, Prof. Nakasaki, Associate Prof. Takahashi, Associate Prof. Mori, and Associate Prof. Yoshimura, for their valuable comments, guidance, immense knowledge and advice to make this research meaningful.

A special thanks to Prof. Komatsu Takayu for permitting me to operate the surface area analyzer instrument as well as Yamamoto san, technician from open research facilities for life science and technology, for guiding me how to operate gas chromatograph.

I want to extend my sincere appreciation to JICA Innovative Asia scholarship for providing me the financial support to study PhD degree in such a wonderful country as Japan. Without this scholarship, I would not be able to follow my dream here.

Thanks are also given to Asian Palm Oil Co., Ltd. for providing me the precious opportunity to visit palm oil mill industry and provide me the palm kernel shell.

I also wish to make a special note of thanks to my lab mates for their assistance personally, academically, and mentally throughout my study: Mr. Enrico, Mr. Li, Mr. Abe, Ms. Hana, Ms. Tan, Mr. Kurihara, Mr. Mizono, Ms. Zhang and many more. Thanks many of my peers in Japan for their encouragement and excellent times together both outside and inside the university.

Finally, I would like to thank my family and friends back in Thailand who have provided endless support and encouraged me to study in Japan. I also would like to thank Keen for his understanding and giving me advices and strengths to be the best version of myself. Without their support, I would not be here fighting for my dreams today.

NOMENCLATURE

C_p = heat capacity [kJ kg^{-1}K^{-1}]
c_P = concentration of H_3PO_4 in treatment solution [kmol m^{-3}]
C_i = concentration of component i in liquid at equilibrium [kmol m^{-3}]
$C_{i,0}$ = concentration of component i in liquid at initial [kmol m^{-3}]
$C_{i,\mathrm{POME}}$ = concentration of component i in palm oil mill effluent [kmol m^{-3}]
$E_{r,s}$ = The energy recovery r from operation s [kJ]
$F_{k,j}$ = Flow of material k from process j [kg]
$F_{k,s}$ = Flow of material k from operation s [kg]
F_0 = mass of palm kernel shell without or with chemical treatment [kg]
F_1 = mass of palm kernel activated carbon [kg]
H_i = enthalpy formation of substance i
$K_{\mathrm{L},\,i}$ = Langmuir parameter of component i [m^3 kmol^{-1}]
L = volume of liquid at equilibrium [m^3]
L_0 = volume of liquid at initial [m^3]
L_1 = mass of condensable liquid from the pyrolysis [kg]
M = mass of feed or product [kg]
Q = total required energy [kJ kg^{-1}]
S = mass of adsorbent at equilibrium [kg]
S_0 = mass of adsorbent at the initial [kg]
q_i = adsorbed amount of component i at equilibrium on AC [kmol kg-AC^{-1}]
q_i^* = saturated adsorbed amount of component i on AC [kmol kg-AC^{-1}]
$q_{i,0}$ = adsorbed amount of component i at initial on AC [kmol kg-AC^{-1}]
S_{BET} = specific surface area of AC [m^2 kg-AC^{-1}]
T = pyrolysis temperature [K]
t = pyrolysis treatment time [h]
V_{meso} = mesopore volume of AC [m^3 kg-AC^{-1}]
V_{micro} = micropore volume of AC [m^3 kg-AC^{-1}]
V_{p} = total pore volume of AC [m^3 kg-AC^{-1}]
R_i = fractional removal of component i [−]
x_{i} = mass fraction of element i [−]
Y_L = yield of condensable liquid from pyrolysis [−]
Y_{PKSAC} = yield of palm kernel activated carbon from pyrolysis [−]
Y_{OG} = yield of off-gas from pyrolysis [−]

<Greek>
ρ_{POME} = density of palm oil mill effluent [kg m^{-3}]

<Subscript>
0 = inlet of chemical treatment
1 = inlet of pyrolysis
2 = inlet of palm oil mill effluent treatment
3 = inlet of heat generation
BET = Brunauer–Emmett–Teller
CPO = crude palm oil
CT = chemical treatment

DC = decanter cake
EFB = empty fruit brunch
FFB = fresh fruit bunch
HG = heat generation
j = process
k = material
L = liquid
L = Langmuir
Lg = lignin
*m*Cr = m-cresol
meso = mesopore
micro = micropore
OG = off-gas
p = orthophosphoric acid
*p*Cr = p-cresol
Ph = phenol
PKO = palm kernel oil
PKS = palm kernel shell
PKS,H_3PO_4 = palm kernel shell with chemical treatment
PKSAC = palm kernel shell activated carbon
PO = palm oil production
POME = palm oil mill effluent
PPF = palm press fiber
PT = palm oil mill effluent treatment
PY = pyrolysis
r = energy recovery
s = operation
W = water
W,H_3PO_4 = residue of orthophosphoric acid solution

LITERATURE CITED

Abnisa, F., W. M. A. W. Daud, W. N. W. Husin and J. N. Sahu, “Utilization possibilities of palm shell as a source of biomass energy in Malaysia by producing bio-oil in pyrolysis process,” *Biomass and Bioenergy*, **35**, 1863–1872 (2011)

Andersson, K. I., M. Eriksson and M. Norgren, “Removal of lignin from wastewater generated by mechanical pulping using activated charcoal and fly ash: Adsorption isotherms and thermodynamics,” *Ind. Eng. Chem. Res.*, **50**, 7722–7732 (2011)

Baharuddin, A. S., L. S. Hock, M. Zulkhairi and N. A. A. Rahman, “Effects of palm oil mill effluent (POME) anaerobic sludge from 500 m^3 of closed anaerobic methane digested tank on pressed-shredded empty fruit bunch (EFB) composting process,” *African J. Biotechnol.*, **9**, 2427–2436 (2010)

Bahri, M. Al, L. Calvo, M. A. Gilarranz and J. J. Rodriguez, “Activated carbon from grape seeds upon chemical activation with phosphoric acid: Application to the adsorption of diuron from water,” *Chem. Eng. J.*, **203**, 348–356 (2012)

Baker, H. M. and R. Ghanem, “Evaluation of treated natural zeolite for the removal of o-chlorophenol from aqueous solution,” *Desalination*, **249**, 1265–1272 (2009)

Barbanera, M. and I. F. Muguerza, “Effect of the temperature on the spent coffee grounds torrefaction process in a continuous pilot-scale reactor,” *Fuel*, **262**, (2020)

Bedia, J., M. Peñas-Garzón, A. Gómez-Avilés, J. J. Rodriguez and C. Belver, “Review on Activated Carbons by Chemical Activation with $FeCl_3$,” *C — J. Carbon Res.*, **6**, (2020)

Bello, M. M., M. M. Nourouzi, L. C. Abdullah, T. S. Y. Choong, Y. S. Koay and S. Keshani, “POME is treated for removal of color from biologically treated POME in fixed bed column: Applying wavelet neural network (WNN),” *J. Hazard. Mater.*, **262**, 106–113 (2013)

Bohli, T., N Fiol, I Villaescusa and A Ouedern, “Adsorption on Activated Carbon from Olive Stones: Kinetics and Equilibrium of Phenol Removal from Aqueous Solution,” *J. Chem. Eng. Process Technol.*, **4**, 3–7 (2013)

Boontham, W., H. Habaki, and R. Egashira; “Removal of Phenol from Oil Mill Effluent Using Activated Carbon Prepared from Kernel Shell in Thailand's Palm Industry," *J. Chem. Eng. Japan*, **53**, 682–688 (2020)

Bouchemal, N., M. Belhachemi, Z. Merzougui and F. Addoun, “The effect of temperature and impregnation ratio on the active carbon porosity,” *Desalin. Water Treat.*, **10**, 115–120 (2010)

Budinova, T., E. Ekinci, F. Yardim, A. Grimm, E. Björnbom, V. Minkova and M. Goranova, “Characterization and application of activated carbon produced by H_3PO_4 and water vapor activation,” *Fuel Process. Technol.*, **87**, 899–905 (2006)

Canales Flores, R. A., F. Prieto and E. M. Otazo, “Physico-Chemical Characterization of Agricultural Residues as Precursors for Activated Carbon Preparation Short Title : Precursors for activated carbon preparation,” December, 2017

Chaouati, N., A. Soualah and M. Chater, “Adsorption of phenol from aqueous solution onto zeolites y modified by silylation,” *Comptes Rendus Chim.*, **16**, 222–228 2013)

ChemicalBook Inc.; “LIGNIN, ALKALI”, (online) https://www.chemicalbook.com/ChemicalProductProperty_EN_CB9772728 (20 November 2020)

Chen, J.; “Activated Carbon Fiber and Textiles,” *Act. Carbon Fiber Text.*, (2017)

Choy, K. K. H., J. F. Porter and G. McKay, “Langmuir isotherm models applied to the multicomponent sorption of acid dyes from effluent onto activated carbon,” *J. Chem. Eng. Data*, **45**, 575–584 (2000)

Daifullah, A. A. M. and B. S. Girgis, “Removal of some substituted phenols by activated carbon obtained from agricultural waste,” *Water Res.*, **32**, 1169–1177 (1998)

Department of Industry Works. 2006. Management Information Systems (MIS) Guide line for Eco-efficiency, Palm Oil Industry. Available on: http://www2.diw.go.th/PIC /download/ Guidelines/mis/MISGuidelines_PalmOilIndustry.pdf

Dit, M; "Palm Kernel Shell (PKS) is More Than Biomass for Alternative Fuel After 2005," *Proceedings of Chemistry and technology conference* (2007)

Engineeringtoolbox; "Heat of combustion", (online) https://www.engineeringtoolbox.com/standard-heat-of-combustion-energy-content-d_1987 (28 November 2020)

Fierro, V., V. Torné-Fernández, D. Montané and A. Celzard, "Adsorption of phenol onto activated carbons having different textural and surface properties," *Microporous Mesoporous Mater.*, **111**, 276–284 (2008)

Gonzalez-Serrano, E., T. Cordero, J. Rodriguez-Mirasol, L. Cotoruelo and J. J. Rodriguez, "Removal of water pollutants with activated carbons prepared from H_3PO_4 activation of lignin from kraft black liquors," *Water Res.*, **38**, 3043–3050 (2004)

Guo, J. and A. C. Lua, "Textural and chemical properties of adsorbent prepared from palm shell by phosphoric acid activation," *Mater. Chem. Phys.*, **80**, 114–119 (2003)

Guo, Y. and D. A. Rockstraw, "Physicochemical properties of carbons prepared from pecan shell by phosphoric acid activation," *Bioresour. Technol.*, **98**, 1513–1521 (2007)

Hamza, U. D., N. S. Nasri, N. A. S. Amin, J. Mohammed and H. M. Zain, "Characteristics of oil palm shell biochar and activated carbon prepared at different carbonization times," *Desalin. Water Treat.*, **57**, 7999–8006 (2016)

Hassan, E. B. M., P. H. Steele and L. Ingram, "Characterization of fast pyrolysis bio-oils produced from pretreated pine wood," *Appl. Biochem. Biotechnol.*, **154**, 182–192 (2009)

Hernndez-Montoya, V., J. Garca-Servin and J. Ivn, "Thermal Treatments and Activation Procedures Used in the Preparation of Activated Carbons," *Lignocellul. Precursors Used Synth. Act. Carbon - Charact. Tech. Appl. Wastewater Treat.*, (2012)

Kaman, S. P. D., I. A. W. Tan and L. L. P. Lim, "Palm oil mill effluent treatment using coconut shell - Based activated carbon: Adsorption equilibrium and isotherm," *MATEC Web Conf.*, **87**, 1–6 (2016)

Kerdsuwan, S. and K. Laohalidano, "Renewable Energy from Palm Oil Empty Fruit Bunch," *Renew. Energy - Trends Appl.*, (2011)

Khomphet, T., T. Eksomtramage and S. Duangpan, "Genetic variation of improved oil palm tenera hybrid populations using morphological and SSR markers," *Songklanakarin J. Sci. Technol.*, **40**, 1329–1335 (2018)

Khongkhaem, P., O. Suttinun, A. Intasiri, O. Pinyakong and E. Luepromchai, "Degradation of Phenolic Compounds in Palm Oil Mill Effluent by Silica-Immobilized Bacteria in Internal Loop Airlift Bioreactors," *Clean - Soil, Air, Water*, **44**, 383–392 (2016)

Kietkwanboot, A., S. Chaiprapat, R. Müller and O. Suttinun, "Biodegradation of phenolic compounds present in palm oil mill effluent as single and mixed substrates by Trametes hirsuta AK04," *J. Environ. Sci. Heal. - Part A Toxic/Hazardous Subst. Environ. Eng.*, **55**, 989–1002 (2020)

Kumar, A. and H. M. Jena, "Preparation and characterization of high surface area activated carbon from Fox nut (*Euryale ferox*) shell by chemical activation with H_3PO_4," *Results Phys.*, **6**, 651–658 (2016)

Li, A., H. Wu, Q. Zhang, G. Zhang, C. Long, Z. Fei, F. Liu and J. Chen, "Thermodynamic study of adsorption of phenolic compounds from aqueous solution by a water-compatible hypercrosslinked polymeric adsorbent," *Chinese J. Polym. Sci. English Ed.*, **22**, 259–267, (2004)

Li, W., K. Yang, J. Peng, L. Zhang, S. Guo and H. Xia; "Effects of carbonization temperatures on characteristics of porosity in coconut shell chars and activated carbons derived from carbonized coconut shell chars" *Ind. Crops. Prod.*, **28**, 190–198 (2008)

Li, Y., X. Zhang, R. Yang, G. Li and C. Hu, "The role of H_3PO_4 in the preparation of activated carbon from NaOH-treated rice husk residue," *RSC Adv.*, **5**, 32626–32636 (2015)

Lim, W. C., C. Srinivasakannan and N. Balasubramanian, "Activation of palm shells by phosphoric acid impregnation for high yielding activated carbon," *J. Anal. Appl. Pyrolysis*, **88**, 181–186 (2010)

Liu, J. L., J. C. Jiang and H. T. Huang, “Selective pyrolysis behaviors of willow catalyzed via phosphoric acid,” *Adv. Mater. Res.*, **724–725**, 413–418 (2013)

Lu, Q., Z. Zhang, X. Wang, H. Guo, M. Cui and Y. Yang, “Catalytic Fast Pyrolysis of Biomass Impregnated with Potassium Phosphate in a Hydrogen Atmosphere for the Production of Phenol and Activated Carbon,” *Front. Chem.*, **6**, 1–10 (2018)

Ma, Z., D. Chen, J. Gu, B. Bao and Q. Zhang, “Determination of pyrolysis characteristics and kinetics of palm kernel shell using TGA-FTIR and model-free integral methods,” *Energy Convers. Manag.*, **89**, 251–259 (2015)

Mazar, A., N. Jemaa, W. W. A. Dajani, M. Marinova and M. Perrier; “Optimization of Lignin Recovery from the Pre-Hydrolysate of Kraft-Based Dissolving Pulp Production Processes,” *Appl. Sci.*, **11**, 1–20 (2021)

Mellyanawaty, M., F. M. A. Chusna, H. Sudibyo, N. Nurjanah and W. Budhijanto, “Influence of Nutrient Impregnated into Zeolite Addition on Anaerobic Digestion of Palm Oil Mill Effluent (POME),” *IOP Conf. Ser. Mater. Sci. Eng.*, **316**, (2018)

Mohamed, E. F., C. Andriantsiferana, A. M. Wilhelm and H. Delmas, “Competitive adsorption of phenolic compounds from aqueous solution using sludge-based activated carbon,” *Environ. Technol.*, **32**, 1325–1336 (2011)

Mohammed, R. R. and M. F. Chong, “Treatment and decolorization of biologically treated Palm Oil Mill Effluent (POME) using banana peel as novel biosorbent,” *J. Environ. Manage.*, **132**, 237–249 (2014)

Mohtashami, S. A., N. Asasian Kolur, T. Kaghazchi, R. Asadi-Kesheh and M. Soleimani, “Optimization of sugarcane bagasse activation to achieve adsorbent with high affinity towards phenol,” *Turkish J. Chem.*, **42**, 1720–1735 (2018)

Namane, A., A. Mekarzia, K. Benrachedi, N. Belhaneche-Bensemra and A. Hellal, “Determination of the adsorption capacity of activated carbon made from coffee grounds by chemical activation with $ZnCl_2$ and H_3PO_4,” *J. Hazard. Mater.*, **119**, 189–194 (2005)

Neoh, C. H., C. Y. Lam, C. K. Lim, A. Yahya and Z. Ibrahim, “Decolorization of palm oil mill effluent using growing cultures of Curvularia clavata,” *Environ. Sci. Pollut. Res.*, **21**, 4397–4408 (2014)

Nicholas, A., M. Hussein, Z. Zainal and T. Khadiran, “Palm Kernel Shell Activated Carbon as an Inorganic Framework for Shape-Stabilized Phase Change Material,” *Nanomaterials*, **8**, (2018)

Oasmaa, A., E. Kuoppala and Y. Solantausta; “Fast Pyrolysis of Forestry Residue. 2. Physicochemical Composition of Product Liquid,” *Energy Fuels.*, **17**, 433–443 (2003)

Ohimain, E. I. and S. C. Izah, “A review of biogas production from palm oil mill effluents using different configurations of bioreactors,” *Renew. Sustain. Energy Rev.*, **70**, 242–253 (2017)

Othaman, R., K. G. Lim, S. Konishi, M. Sato, N. Shi and R. Egashira, “Thermal Treatment of Wood Residues and Effective Utilization of Its Products to Improve Rubberwood Manufacturing Process,” *J. Chem. Eng. Japan*, **41**, 1149–1158 (2008)

Pereira, R.G., C. M. Veloso, N. M. da Silva, L. F. de Sousa, R. C. F. Bonomo, A. O. de Souza, M. O. da Guarda Souza, and R. d. C. I. Fontan; “Preparation of activated carbons from cocoa shells and siriguela seeds using H_3PO_4 and $ZnCl_2$ as activating agents for BSA and α-lactalbumin adsorption” *Fuel Process. Technol.*, **126**, 476–486 (2014)

Phonepaseuth, P., V. Rakkiatsakul, B. Kachenchart, O. Suttinun and E. Luepromchai, “Phenolic compounds removal by grasses and soil bacteria after land application of treated palm oil mill effluent: A pot study,” *Environ. Eng. Res.*, **24**, 127–136 (2019)

Prasertsan, P. and H. Binmaeil, “Treatment of palm oil mill effluent by thermotolerant polymer-producing fungi,” *J. Water Environ. Technol.*, **16**, 127–137 (2018)

Puziy, A. M., O. I. Poddubnaya, A. Martínez Alonso, F. Suárez García and J. M. D. Tascón; “Synthetic carbons activated with phosphoric acid I. Surface chemistry and ion binding properties,” *Carbon*, **40**, 1493–1505 (2002)

Quesada-Plata, F., R. Ruiz-Rosas, E. Morallón and D. Cazorla-Amorós, “Activated Carbons Prepared through H_3PO_4-Assisted Hydrothermal Carbonisation from Biomass Wastes: Porous Texture and Electrochemical Performance,” *Chempluschem*, **81**, 1349–1359 (2016)

Rana, S., L. Singh, Z. Wahid and H. Liu, “A Recent Overview of Palm Oil Mill Effluent Management via Bioreactor Configurations,” *Curr. Pollut. Reports*, **3**, 254–267 (2017)

Roostaei, N. and F. H. Tezel, “Removal of phenol from aqueous solutions by adsorption,” *J. Environ. Manage.*, **70**, 157–164 (2004)

Rupani, P. F, R. P. Singh, M. H. Ibrahim and N. Esa, “Review of Current Palm Oil Mill Effluent (POME) Treatment Methods: Vermicomposting as a Sustainable Practice,” *World Appl. Sci. J.*, **10**, 1190–1201 (2010)

Sheil, D., A. Casson, E. Meijaard, M. Noordwijk, J. Gaskell, J. Sunderland-Groves, K. Wertz, and M. Kanninen., *The impacts and opportunities of oil palm in Southeast Asia: What do we know and what do we need to know?*, (2009)

Soni, H. and P. Padmaja, “Palm shell based activated carbon for removal of bisphenol A: An equilibrium, kinetic and thermodynamic study,” *J. Porous Mater.*, **21**, 275–284 (2014)

Sowcharoensuk, C. Thailand industry outlook 2020–22. Thailand: Krungsri Research. (2020)

Sych, N. V., S. I. Trofymenko, O. I. Poddubnaya, M. M. Tsyba, V. I. Sapsay, D. O. Klymchuk and A. M. Puziy, “Porous structure and surface chemistry of phosphoric acid activated carbon from corncob,” *Appl. Surf. Sci.*, **261**, 75–82 (2012)

Tanaka, H., I. Toda, H. Maruyama, H. Ono, S. Ohshio, H. Akasaka, Y. Tanaka, S. Himeno, T. Kokubu and H. Saitoh, “Effect of cooling rate of KOH activation process on activated carbons,” *Trans. Mater. Res. Soc. Japan*, **37**, 57–60 (2012)

Tosu, P., E. Luepromchai and O. Suttinun, “Activation and immobilization of phenol-degrading bacteria on oil palm residues for enhancing phenols degradation in treated palm oil mill effluent,” *Environ. Eng. Res.*, **20**, 141–148 (2015)

Uysal, T., G. Duman, Y. Onal, I. Yasa and J. Yanik, “Production of activated carbon and fungicidal oil from peach stone by two-stage process,” *J. Anal. Appl. Pyrolysis*, **108**, 47–55 (2014)

Wang, X., D. Li, W. Li, J. Peng, H. Xia, L. Zhang, S. Guo and G. Chen, “Optimization of mesoporous activated carbon from coconut shells by chemical activation with phosphoric acid,” *BioResources*, **8**, 6184–6195 (2013)

Wang, Z., E. Nie, J. Li, Y. Zhao, X. Luo and Z. Zheng, “Carbons prepared from Spartina alterniflora and its anaerobically digested residue by H_3PO_4 activation: Characterization and adsorption of cadmium from aqueous solutions,” *J. Hazard. Mater.*, **188**, 29–36 (2011)

Wikipedia; “Activated carbon”, (online) https://en.wikipedia.org/wiki/Activated_carbon (14 November 2020)

Wikipedia; “Palm oil”, (online) https://en.wikipedia.org/wiki/Palm_oil (14 November 2020)

Yorgun, S. and D. Yildiz, “Preparation and characterization of activated carbons from Paulownia wood by chemical activation with H_3PO_4,” *J. Taiwan Inst. Chem. Eng.*, **53**, 122–131 (2015)